MAGNETOM Flash

The Magazine of MR

Issue no. 2/2007
CMR Edition
Not for distribution in the USA

SIEMENS
medical

Cardiovascular Magnetic Resonance

Delayed Enhancement Imaging in Coronary Artery Disease
Page 14

Differentiation of Cardiomyopathies
Page 22

Myocardial Stress Perfusion Imaging
Page 34

Contains a CD with SCMR Recommended Protocols
Page 107

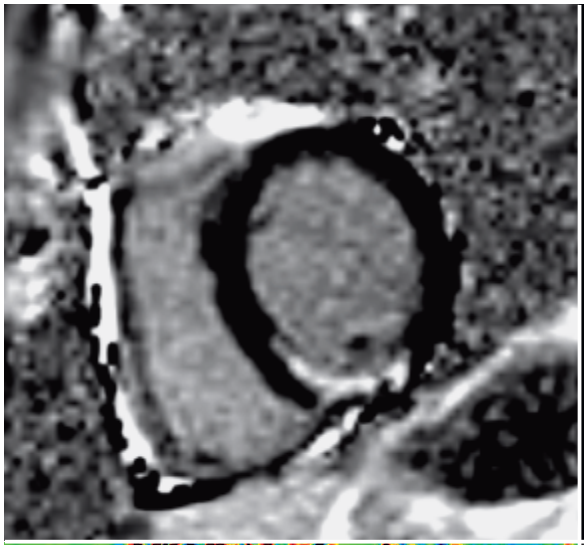

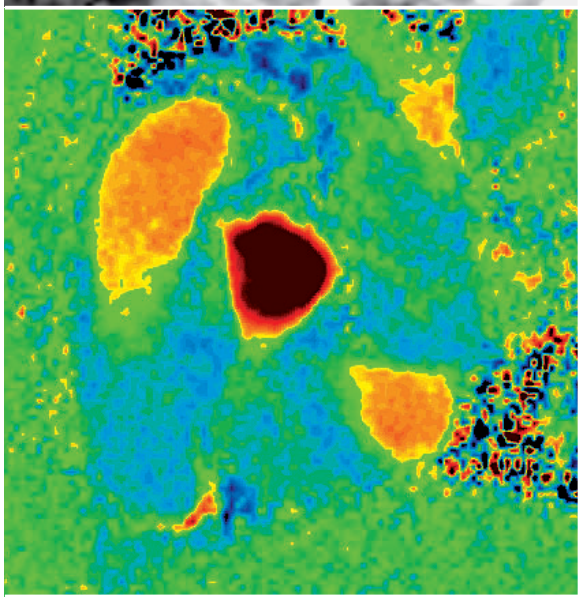

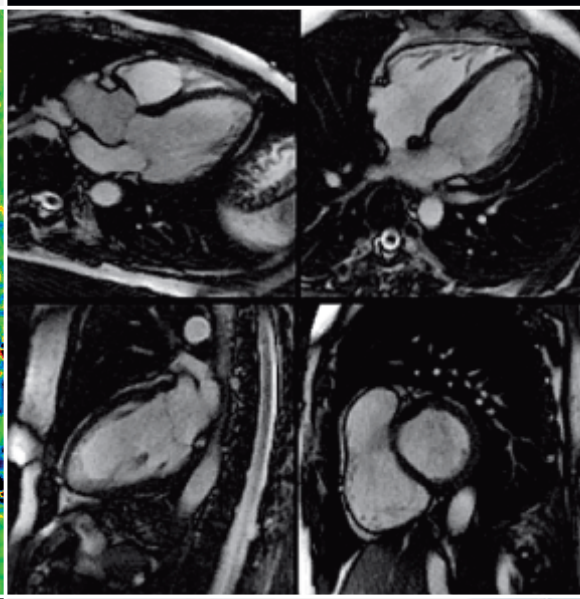

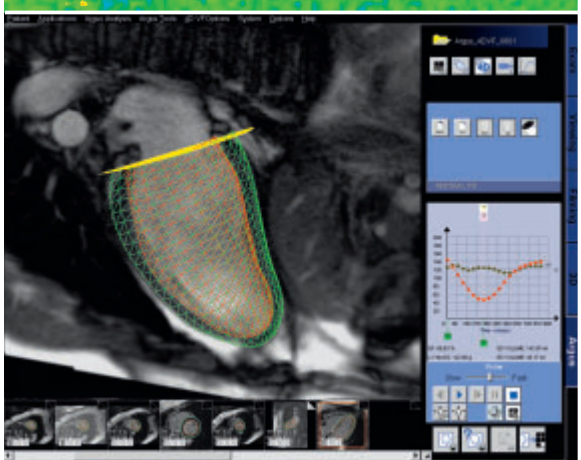

Okan Ekinci, M.D.
Segment Manager,
Cardiovascular MRI

Dear MAGNETOM user,

From vision to clinical practice, Cardiovascular MRI (CMR) emerges as a fully-established technique for routine cardiac imaging. In handling anatomy, function, morphology, tissue characterization, myocardial perfusion, angiography or molecular MRI, there is simply no other single modality in cardiology or radiology to offer as much insight into the heart as CMR.

Today, CMR allows us to detect multiple cardiac diseases such as myocardial infarct or cardiomyopathies more easily and to understand them much better. Indeed, recent studies show that CMR even helps to identify patients at risk of, for example, sudden cardiac death in DCM or HOCM.

This extension of capabilities, however, requires a deep knowledge about the role and use of CMR in clinical routine. From courses and symposia to user meetings, Siemens has consistently supported a broad range of educational activities to enable more institutions to perform CMR. And we are proud that this new issue of MAGNETOM Flash is totally dedicated to the field of CMR from a clinical perspective by authors who are opinion leaders in their respective fields.

The magazine also comes with two valuable bonuses:

Firstly, a CD presenting a comprehensive guide to performing a CMR exam (90+ pages) in accordance with SCMR recommendations, as well as ready-to-use (downloadable) CMR protocols for the most frequent indications. We are very appreciative of the cooperation of the SCMR in this regard.

Secondly, a poster depicting the common imaging planes, types of sequences frequently used in CMR and typical patterns of delayed enhancement imaging, not to mention many other features to offer you an extremely useful and accessible overview of CMR.

We hope you will enjoy and find value in this edition of MAGNETOM Flash.

Your feedback is very welcome.

Please mail any questions or comments to okan.ekinci@siemens.com

Okan Ekinci, MD
Guest Editor
Segment Manager, Cardiovascular MRI
Head, Application Marketing Center
Siemens Medical Solutions
MR Marketing

Contact

okan.ekinci@siemens.com

The Editorial Team

We appreciate your comments.
Please contact us at magnetomworld.med@siemens.com

A. Nejat Bengi, M.D.
Editor in Chief

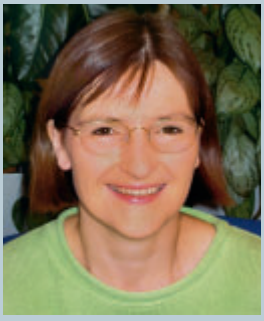

Antje Hellwich
Associate Editor

Dagmar Thomsik-Schröpfer,
Ph.D., MR Marketing-Products,
Erlangen, Germany

Cécile Mohr, Ph.D.
Head of Market Segment
Management, Erlangen

Heike Weh,
Clinical Data Manager,
Erlangen, Germany

Bernhard Baden,
Clinical Data Manager,
Erlangen, Germany

Peter Kreisler, Ph.D.
Collaborations & Applications,
Erlangen, Germany

Milind Dhamankar, M.D.
Director, MR Product
Marketing, Malvern, USA

Kathleen Giannini,
US Installed Base Manager,
Malvern, PA, USA

Gary R. McNeal, MS (BME)
Advanced Application Specialist,
Cardiovascular MR Imaging
Hoffman Estates, USA

Dr. Sunil Kumar S.L.
Senior Manager Applications,
Canada

Tony Enright, Ph.D.
Asia Pacific Collaborations,
Australia

Content

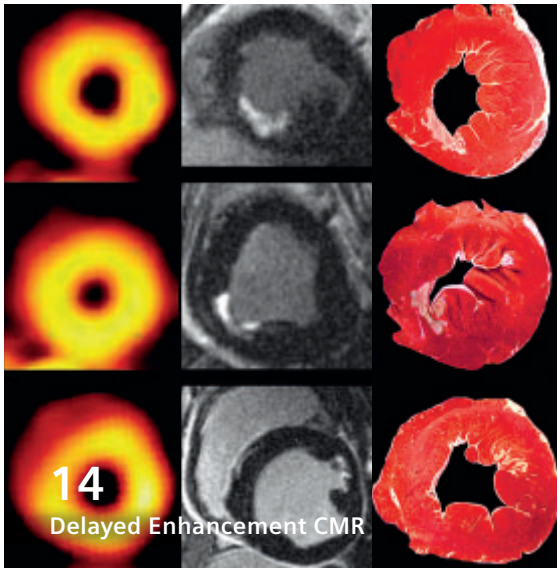

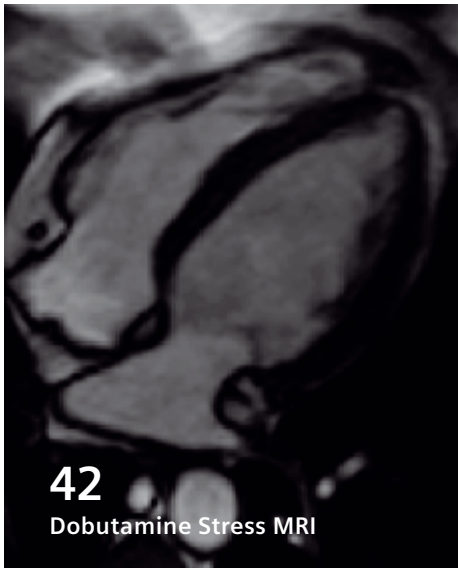

Cardiovascular MRI

Due to the increased interest in Cardiovascular MRI we dedicated this issue of MAGNETOM Flash to CMR. Experienced users, opinion leaders in their respective field, provide the key knowledge necessary to understand the role of CMR exams in today's clinical routine.

Clinical Cardiovascular MRI

6 CMR Assessment of Global Ventricular Function (Ekinci)

14 CMR Delayed Enhancement Imaging in Coronary Artery Disease (Klem)

22 Differentiation of Cardiomyopathies by Use of CMR (O'Hanlon, Pennell, Schulz-Menger et al.)

34 Stress-MRI: Adenosine Stress Perfusion MRI for Myocardial Ischemia Detection (Arai)

42 Stress-MRI: High-Dose Dobutamine Stress MRI for Myocardial Ischemia Detection (Jochims)

50 CMR for the Assessment of Valvular Disease (Cowan, Young et al.)

56 Evaluation of Cardiac Masses by CMR (Bruder et al.)

61 Clinical Application of 3D/4D MR Angiography in Cardiovascular Diseases (Barkhausen et al.)

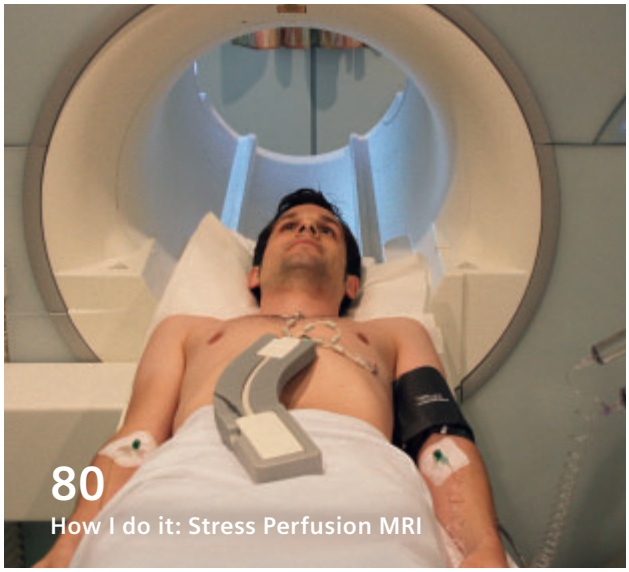

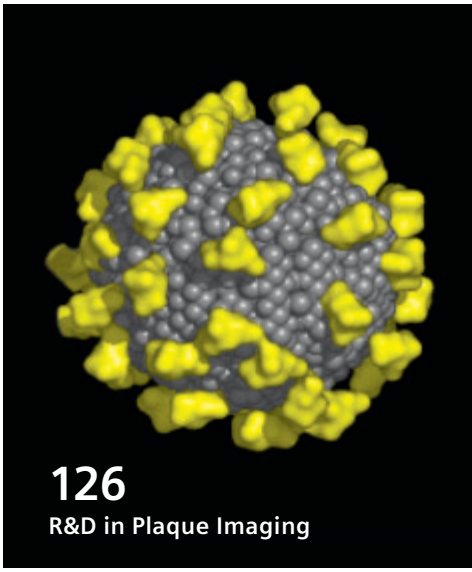

68 MR Imaging of Congenital Heart Disease (Muthurangu, Hansen, Taylor)

74 MR Imaging in the Electrophysiology Laboratory (Oakes, Marrouche et al.)

Cardiovascular MRI → How I do it

80 Workflow Optimization for CMR Adenosine Stress Perfusion in Clinical Routine (Recke et al.)

86 CMR Imaging of Myocardial Amyloidosis Using Late Contrast Enhanced (LCE) Imaging: Challenges and Potential Solutions (Voros et al.)

89 Flow measurements: Basics and the Application to the Main Pulmonary Artery (Abolmaali)

Education / Life

94 Guidelines for Credentialling in CMR (endorsed by the SCMR)

98 Training Sites / Courses for CMR

102 CMR Site Accreditation Process

107 SCMR Accredited Protocols & Comprehensive CMR Exam Guide (on CD)

108 Abbreviations

Technology & Trends

110 Dark Blood Delayed Enhancement Imaging: New Developments in the Imaging of Myocardial Viability (Rehwald)

118 The Promise of Molecular MRI in Cardiovascular Imaging (Sosnovik)

126 Nano_AG: Development of New Contrast Agents for the Detection of Vulnerable Plaques (Schnorr et al.)

129 Radiofrequency Coil Innovation in Cardiovascular MRI (Schmitt, Sosnovik et al.)

The information presented in MAGNETOM Flash is for illustration only and is not intended to be relied upon by the reader for instruction as to the practice of medicine. Any health care practitioner reading this information is reminded that they must use their own learning, training and expertise in dealing with their individual patients. This material does not substitute for that duty and is not intended by Siemens Medical Solutions to be used for any purpose in that regard. The drugs and doses mentioned in MAGNETOM Flash are consistent with the approval labeling for uses and/or indications of the drug. The treating physician bears the sole responsibility for the diagnosis and treatment of patients, including drugs and doses prescribed in connection with such use. The Operating Instructions must always be strictly followed when operating the MR System. The source for the technical data is the corresponding data sheets.

Not for distribution in the US.

CMR Assessment of Global Ventricular Function and Mass: Greater Efficiency and Diagnostic Accuracy with Argus 4D VF and Inline VF

Okan Ekinci, M.D.

Siemens Medical Solutions, Erlangen, Germany

CMR is considered the gold standard for accurate assessment of left and right ventricular function.

Both cardiac volumes and ejection fraction have important prognostic and therapeutic implications in cardiology, hence the accuracy of the data can significantly affect the appropriateness of certain diagnostic or therapeutic approaches in an individual patient, e.g. when considering the implantation of an Implantable Cardioverter Defibrillator (ICD) in a heart failure patient with an ejection fraction (EF) below 35%.
As a widely available and validated method, transthoracic echocardiography is used most frequently for left ventricular function assessment. But in today's medicine, multiple diagnostic tools are available for ventricular function (VF) assessment including nuclear techniques, CT and CMR. However, ejection fraction and volume measurements by these techniques are not completely interchangeable due to the different type of data entered into analysis. Normal values for CMR assessed ventricular function and mass are shown in tables 1A–C. In echocardiography there are various approaches for LV EF assessment:

M-mode echo with Teichholz correction (Fig. 1):

End-diastolic volume = $[7/(2{,}4+EDD)] \times EDD^3$
End-systolic volume = $[7/(2{,}4+ESD)] \times ESD^3$

(EDD = end-diastolic diameter,
ESD = end-systolic diameter)

1

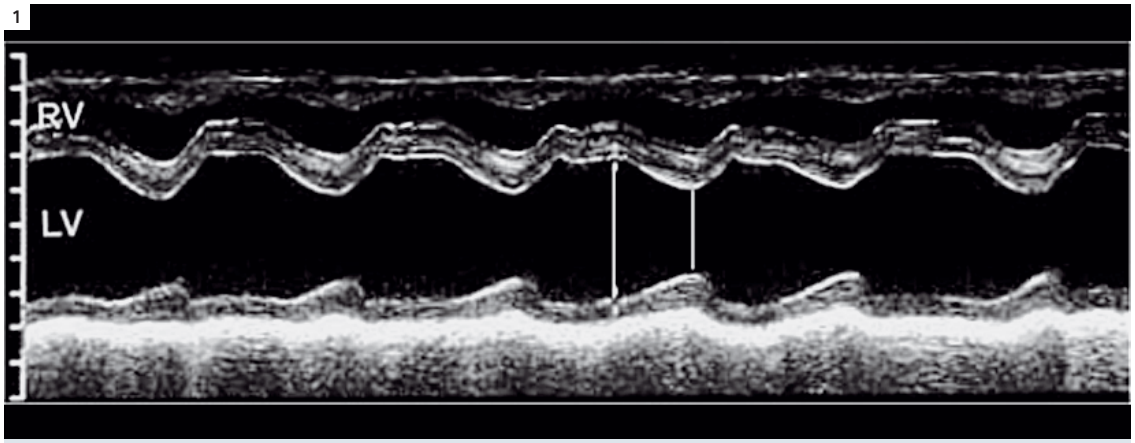

1 M-mode echocardiogram of the left ventricle. The long line shows the end-diastolic position; the short line shows the end-systolic position. The length of the lines reflects the LV diameter at end-diastole (EDD) and end-systole (ESD), respectively and can be used for LV function assessment.

Table 1A: CMR Assessed Left Ventricular (LV) Function Indexed by Body Surface Area (BSA)

Parameter	Mean ± SD		*p*
	Men	Women	
LVEDVI (mL/m²)	73.9 ± 14.7	64.5 ± 10.8	< 0.0001
LVESVI (mL/m²)	24.5 ± 8.8	18.2 ± 5.1	< 0.0001
LVSVI (mL/m²)	49.4 ± 9.9	46.3 ± 8.4	0.1457
LVEFI (%/m²)	35.5 ± 5.9	42.9 ± 5.6	< 0.0001
LVMI (g/m²)	85.1 ± 15.2	66.9 ± 10.9	< 0.0001
CI (mL/min/m²)	2.9 ± 0.6	2.9 ± 0.6	< 0.1675

Table 1B: CMR Assessed Left Ventricular (LV) Volumes and Mass

Parameter	Mean ± SD		*p*
	Men	Women	
LVEDV (mL)	142.2 ± 34.0	109.2 ± 22.5	< 0.0001
LVESV (mL)	47.4 ± 19.4	30.9 ± 9.5	< 0.0001
LVSV (mL)	94.8 ± 21.3	78.2 ± 17.0	< 0.0001
LVEF (%)	67.2 ± 7.2	71.8 ± 5.6	< 0.0001
LV mass (g)	163.8 ± 35.8	113.6 ± 24.2	< 0.0001
CO (mL/min)	5.6 ± 1.2	4.9 ± 1.1	< 0.0001

Table 1C: CMR Assessed Left Ventricular (LV) Function by Ethnicity

Parameter	White (mean ± SD)	*p*			AA (mean ± SD)	*p*		Hispanics (mean ± SD)	*p*	Asian (mean ± SD)
		AA	Hispanics	Asian		Hispanics	Asian		Asian	
LVEDV (mL)	148.0 ± 30.5	NS	NS	< 0.05	153.6 ± 30.9	NS	< 0.05	147.3 ± 26.7	< 0.05	116.5 ± 18.4
LVESV (mL)	50.1 ± 14.7	NS	NS	< 0.05	54.9 ± 16.5	NS	< 0.05	50.3 ± 13.6	< 0.05	36.5 ± 7.0
LVSV (mL)	97.9 ± 21.4	NS	NS	< 0.05	98.7 ± 20.9	NS	< 0.05	97.1 ± 18.2	< 0.05	80.0 ± 14.9
LVEF (%)	66.3 ± 6.4	NS	NS	NS	64.5 ± 6.9	NS	< 0.05	66.2 ± 6.2	NS	68.5 ± 4.4
LV mass (g)	170.0 ± 32.1	NS	NS	< 0.05	181.6 ± 35.8	< 0.05	< 0.05	163.8 ± 25.7	< 0.05	129.1 ± 20.0
CO (L/m²)	5.7 ± 1.4	NS	NS	< 0.05	5.81 ± 30.9	NS	< 0.05	5.7 ± 1.1	< 0.05	4.8 ± 1.0
LVEDVI (mL/m²)	74.5 ± 14.0	NS	NS	< 0.05	74.8 ± 12.1	NS	< 0.05	77.4 ± 13.0	< 0.05	68.3 ± 7.4
LVESVI (mL/m²)	25.2 ± 7.1	NS	NS	< 0.05	26.7 ± 7.4	NS	< 0.05	26.4 ± 7.1	< 0.05	21.4 ± 3.4
LVSVI (mL/m²)	49.3 ± 10.1	NS	NS	NS	48.1 ± 8.5	NS	NS	51.0 ± 8.8	NS	46.9 ± 6.7
LVMI (g/m²)	85.6 ± 14.7	NS	NS	< 0.05	38.8 ± 16.8	NS	< 0.05	85.9 ± 11.3	< 0.05	75.7 ± 8.2
CI (L/min/m²)	2.9 ± 0.6	NS	NS	NS	2.8 ± 0.6	NS	NS	3.0 ± 0.6	NS	2.8 ± 0.5

Table 1A–C: Normal values for MRI-assessed left ventricular function indexed by BSA **(A)**, for left ventricular volumes and mass by gender **(B)**, and left ventricular function by ethnicity **(C)**. Note – White = white Americans, AA = Africans, Asia = Asian-Americans, NS = not statistically significant, ESVI = end-systolic volume index, EDV = end-diastolic volume, ESV = end-systolic volume, SV = stroke volume, EF = ejection fraction, CO = cardiac output, EDVI = end-diastolic volume index, ESVI = end-systolic volume index, SVI = stroke volume index, MI = mass index, CI = cardiac index. P values based on on Dunnett's two-tailed t test, with the Asian-American group used as the control group
[Source: Cardiovascular Function in Multi-Ethnic Study of Atherosclerosis (MESA): Normal Values by Age, Sex, and Ethnicity. Natori S, Lai S, Finn P et al. AJR 2006;186:S357–S365.]

Single-plane area-length method (Fig. 2):

$$V = \pi/6 \times LD^2$$

(L = length of the ventricle,
D = diameter of the ventricle)

Biplane modified Simpson rule (BSR, Fig. 3A, B):

$$V=(\pi/4) \times (LVL/n) \sum_{i=1}^{n} DiX \times DiY$$

(V = volume,
LVL = length of LV,
n = number of slices,
DiX = diameter in plane X and slice *i*,
DiY = diameter in plane Y and slice *i*)

LV mass can be calculated in echocardiography by the corrected ASE simplified cubed equation:

$$LVM\ (grams) = 0.8\ [1.05\ [(LVID + IVST + PWT)^3 - (LVID)^3]]$$

(LVID = left ventricular internal dimension,
IVST = interventricular septum thickness,
and PWT = posterior wall thickness, 1.05 g/ml is the specific mass of myocardial tissue)
Due to the geometric assumptions in all of these techniques with regard to the left ventricular shape, the accuracy of LV EF assessment using 2D

2

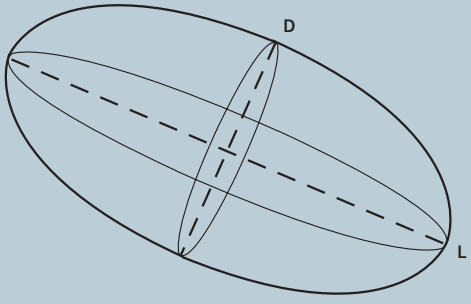

2 The ellipsoid model is used to make geometric assumptions for the left ventricular function calculation according to the single-plane area-length method (D = diameter of LV, L = length of LV).

3A

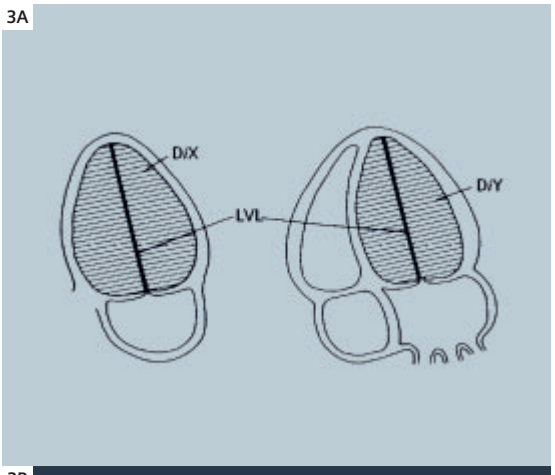

3B

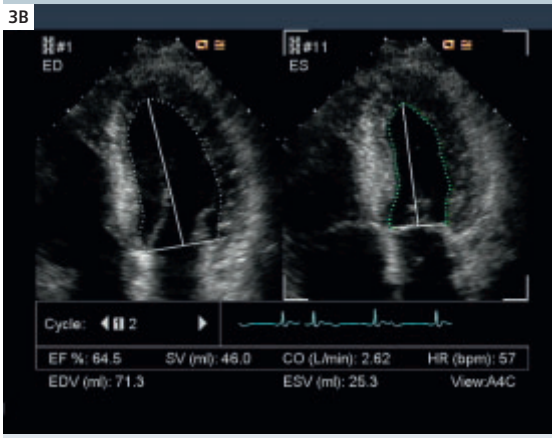

3 Illustration of the application of the biplane modified Simpson rule for LV function analysis to 2- and 4-chamber view images in echocardiography **(A)**. Endocardial contours are needed to be drawn in end-diastole and end-systole to calculate volume data for both phases **(B)**. (V = volume, LVL = length of LV, n = number of slices, DiX = diameter in plane X and slice i, DiY = diameter in plane Y and slice i).

echo is low, especially in patients with regional left ventricular wall motion abnormalities (Kuroda T et al., Echocardiography, 1994).
Although 3D echocardiography shows much higher correlation to CMR it has not yet replaced 2D VF assessment in cardiology (Table 2, Krenning BJ et al. Cardiovasc. Ultrasound, 2003 and Qi X et al., Echocardiography, 2007). Cardiovascular magnetic resonance is the preferred technique for volume and ejection fraction estimation in heart failure patients, because of its 3D approach for non-symmetric ventricles and superior image quality (Bellenger NG et al., Eur Heart J, 2000) which leads also to less user dependency and higher reproducibility. Due to the difficulties in appropriate

Table 2: Volume and function measurement by 3D Echo reconstruction in comparison with CMR

Author/ref.	Object	N	r.	SE	Mean Diff. ± SD
Gopal et al.	LV-EDV	15	0.92	7ml	
	LV-ESV	–	0.81	4ml	
Iwase et al.	LV-EDV	30	0.93	–	-17 ± 23ml
	LV-ESV	–	0.96	–	-4 ± 18ml
	LV-EF	–	0.85	–	-2 ± 6%
Buck et al.	LV-EDV	23	0.97	14.7ml	-10.7 ± 14.5ml
	LV-ESV	–	0.97	12.4ml	-3.4 ± 12.9ml
	LV-EF	–	0.74	5.6%	-2.5 ± 6.7%
Altmann et al.	LV-EDV	12	0.98	8.7ml	-14.2 ± 8.3ml
	LV-ESV	–	0.98	5.6ml	-3.4 ± 5.5ml
	LV-EF	–	0.85	5.3%	-4.4 ± 5.3%
Nosir et al.	LV-EDV	46	0.98	–	-1.4 ± 13.5ml
	LV-ESV	–	0.98	–	-1.5 ± 10.5ml
	LV-EF	–	0.98	–	0.2 ± 2.5%
Kim et al.	LV-EDV	18	–	–	6.4 ± 20ml
	LV-ESV	–	–	–	0.0 ± 13.3ml
	LV-EF	–	–	–	1.4 ± 3.5%
Kim et al.	LV-EDV	10	–	–	-3.1 ± 4.9ml
	LV-ESV	–	–	–	-1.4 ± 2.2ml
	LV-EF	–	–	–	0.5 ± 1.8%
Poutanen et al.	LV-EDV	0.80	–	–	4.0 ± 19.6ml
	LV-ESV	0.88	–	–	0.4 ± 13.0ml
	LV-EF	0.20	–	–	1.7 ± 15.1%
Mannaerts et al.	LV-EDV	17	0.74	–	-13.5 ± 13.5%
	LV-ESV	–	0.88	–	-17.7 ± 23.9%
	LV-EF	–	0.89	–	-1.8 ± 5.8%
Krenning et al.	LV-EDV	15	0.98	13.4ml	-22.7 ± 13.6ml
	LV-ESV	–	0.99	8.7ml	-12.6 ± 9.9ml
	LV-EF	–	0,97		

Table 2: Volume and function measurement by 3D Echo (reconstruction) in comparison with CMR. (N = number of subjects; LV = left ventricle; r = correlation coefficient; SE = standard error or regression; Diff. = difference; SD = standard deviation; EDV = end-diastolic volume; ESV = end-systolic volume; EF = ejection fraction). *[Mod. from: Krenning BJ, Voormolen MM, Roelandt JRTC. Assessment of left ventricular function by three-dimensional echocardiography. Cardiovasc Ultrasound. 2003;1:12].*

visualization of the right ventricle in transthoracic echocardiography this holds true even more for the assessment of right ventricular function.
MRI is considered also as the ideal method for the determination of LV mass for the same reasons, although transthoracic echo with second harmonic imaging and contrast echocardiographic techniques or 3D echo showed comparable accuracy (Bezante GP et al., Heart, 2005 & Mooney MG et al. Int J Card Imaging, 2000). However, most of the echocardiographic formulas overestimate LV mass, when compared to CMR (Scharhag et al. Z Kardiol, 2003).

Argus Function® allows for a comprehensive evaluation of right and left ventricular function.

CMR for quantification of ventricular function and mass

There are several ways for the acquisition of MR images for LV/RV function and mass assessment. TrueFISP (SSFP) sequences provide high spatial resolution and a high contrast between the dark myocardium and the bright blood-pool and therefore are preferred for this purpose: a stack of short-axis cine images (with a slice thickness of 8–12 mm) by which both ventricles can be covered without a gap in 1–2 breathholds.
Preferably, retrospectively ECG-gated sequences should be used to cover the whole R-R interval. Nevertheless, prospectively gated sequences can also be used, without losing accuracy. In a 2-breathhold acquisition, usually 4–6 slices with a gap of 100% from slice to slice are acquired during the first breathhold. Ideally, the acquisition can be planned on 4-chamber and 2-chamber plane. The most basal slice should cover the mitral valve plane in diastole and the stack should be parallel to the mitral valve plane in both orientations. For the second acquisition, the complete stack is shifted with the "gap filling +/-" functionality towards the apex. Using this 2-breathhold approach, a high spatial and temporal resolution can be ensured. The use of integrated Parallel Imaging Techniques – iPAT (e.g. GRAPPA) – can help to accelerate the acquisition or to increase the resolution even further, so that a single breathhold approach can be applied routinely.

With the new Argus 4D VF, LV EF analysis can be performed in less than a minute.

Tools for ventricular function and mass assessment

In cardiovascular MRI, Argus Function® has been used as a comprehensive tool for ventricular function and mass assessment by Siemens users for many years with continuous improvements in the functionalities over time.
The workflow is simple: When loading the acquired images into Argus Function, the images get sorted vertically according to the slice position, from base to apex, and horizontally according to the point in the cardiac cycle from the beginning of the systole to the end-diastole (Fig. 4). After zooming in on the region-of-interest (LV/RV), the endocardial and epicardial contours of LV and RV can be drawn manually or rather semi- or fully automatically on the first image. The contours can be propagated horizontally and vertically to the rest of the images for a fast analysis. Contour changes, e.g. for in- or excluding papillary muscles, can be applied manually with various tools.
The resulting section provides the typical volumetric and functional data for LV and RV including parameters such as EDV, ESV, SV, CO and filling rates. The calculation is done using the modified Simpson's rule. When both endo- and epicardial contours are drawn, ventricular mass and regional wall thickening can be calculated. Argus Function provides tabular and graphical, color-coded display of the results in parameter maps (e.g., in parameterized bull's-eye plots with a sector based model) or graphs (e.g., volume-time curve). The customizable layout of the Movie Viewer allows for single movie display or a simultaneous display of up to 8 movies, which is helpful especially in the setting of dobutamine stress MRI. AVI files can be generated and exported easily. Contrast and brightness windowing of the images can be done at any time during the analysis.
All results including the graphs and summary tables can be integrated in a DICOM structured report and stored to database. Data can be exported as ASCII files when needed.

New tools for LV function and mass assessment using CMR

Argus 4D VF®

In left ventricular analysis, the correct selection of the basal slice is of importance for highly accurate measurement of volume data. Siemens' new tool for LV function analysis, Argus 4D VF, enables the user to identify the mitral valve insertion points in end-diastole and end-systole on long-axis planes and automatically adapts the basal border of the LV cavity in every single phase of the cardiac cycle. With Argus 4D VF there is neither missing ventric-

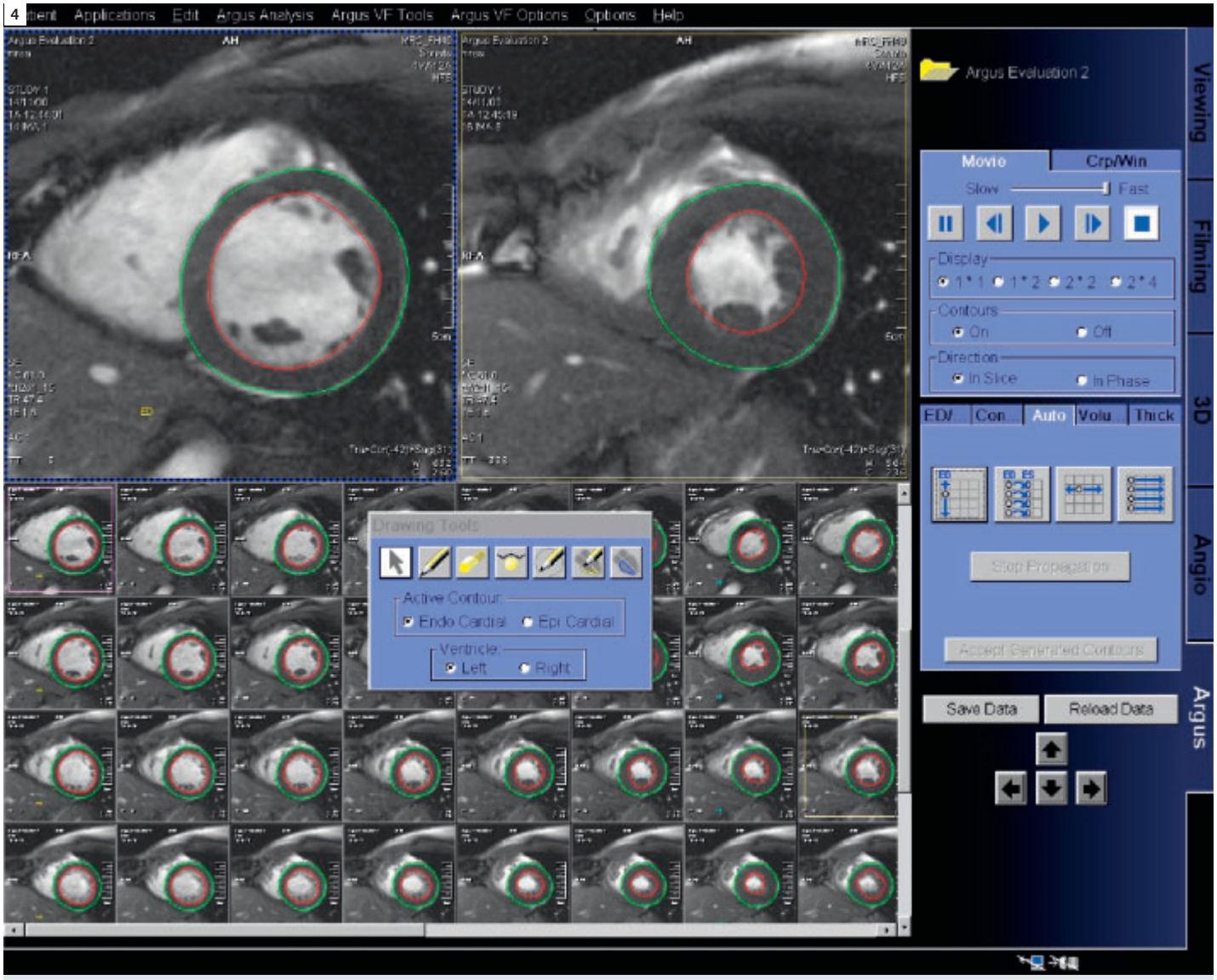

4 User interface of Argus Function®. Contours are drawn initially on one or more slices and then propagated to other slices and phases automatically. Argus Function allows for volume, function and mass analysis for both LV and RV.

ular volume nor additional atrial volume deteriorating the accuracy of the LV volumetric analysis anymore.

Beyond providing higher accuracy, the tool's main advantage is its speed: Using Argus 4D VF, a typical LV function and mass analysis can be done in less than a minute. The reason for this is a new approach: Instead of contour tracing, a heart model-based algorithm enables the user to limit the input to a few mouse clicks with a guided workflow to identify the following anatomical landmarks:

- Center of the LV apex on a apical short-axis cine
- Center of the LV base on a basal short-axis cine
- Mitral valve insertion points on a 2- and/or 4-chamber plane in diastole and systole

The model-based algorithm provides within a few seconds the appropriate endo- and epicardial contours on all slices and phases as well as a summary table including various data for volume, function and mass. A volume-time curve and the key parameters are also integrated into the main window which allows to see parameter changes immediately

5 The user interface of the new Argus 4DVF®. After loading short- and long-axis images, a guided workflow ensures a fast calculation of the contours by use of a heart-model based algorithm and the automatic assessment of LV function **(A)**. Advanced volume rendering options are available for a time-resolved (4D) visualization **(B)**.

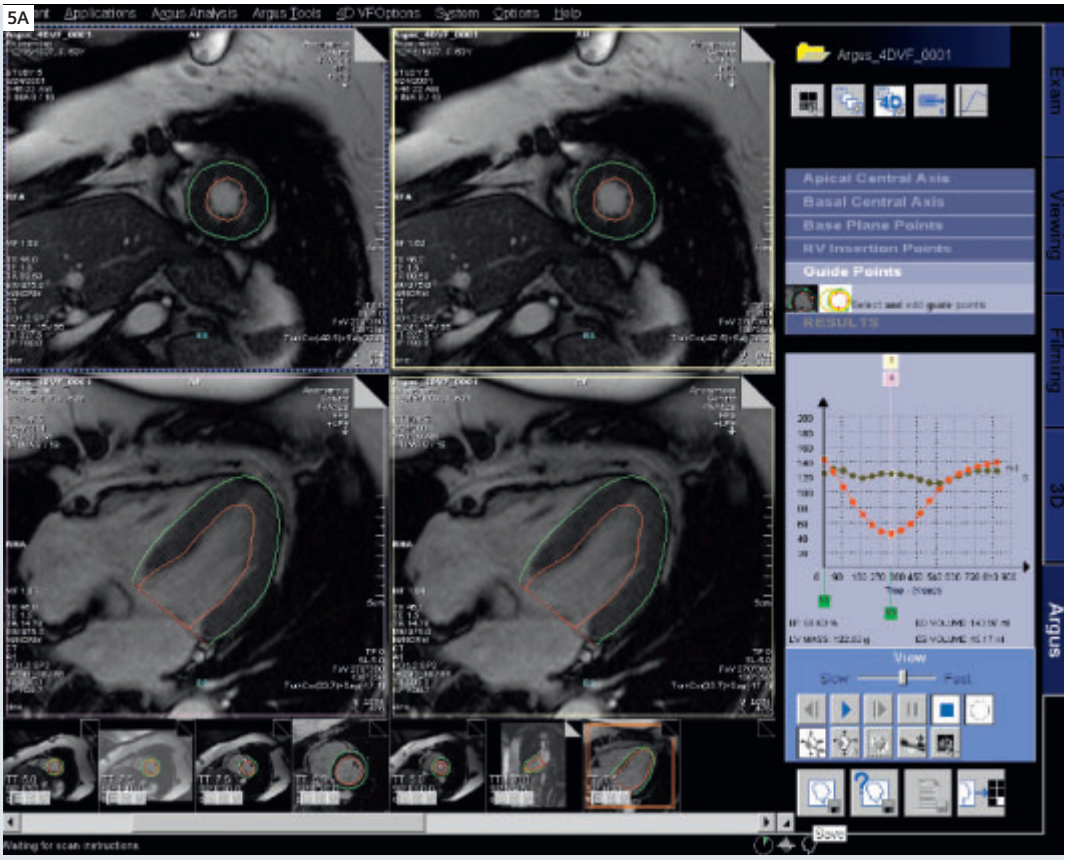

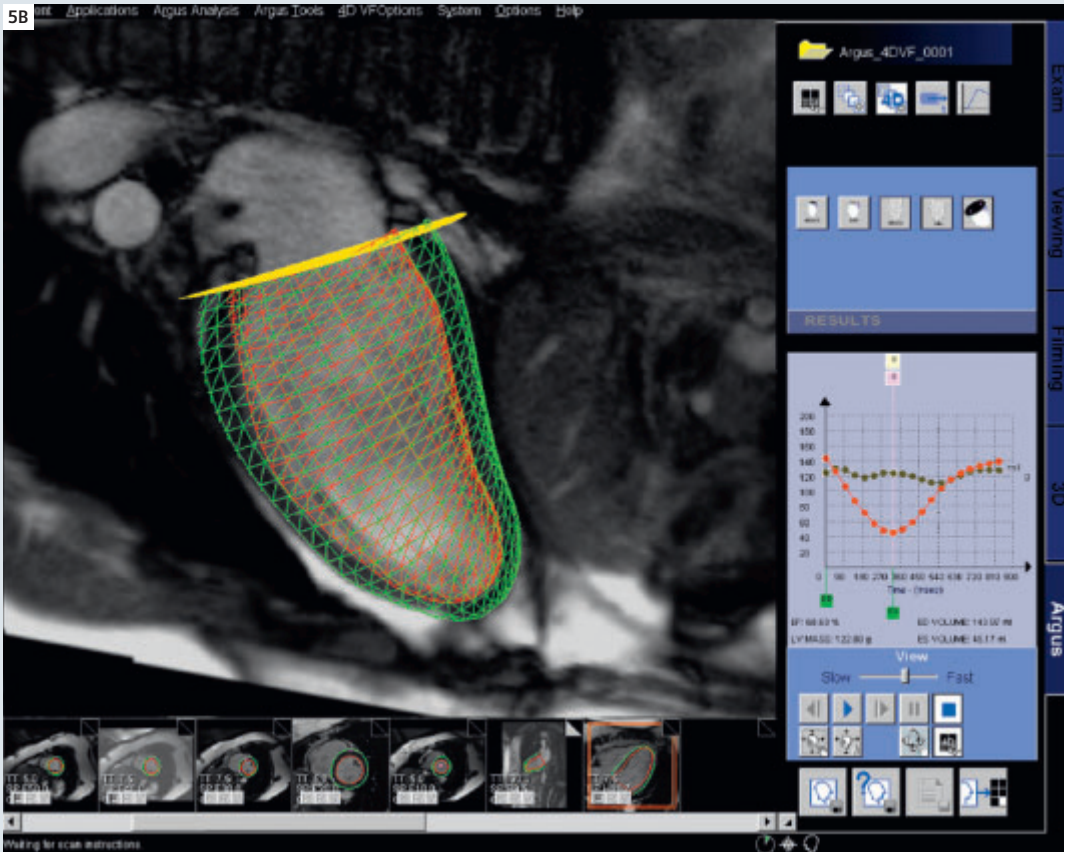

when changes are done on contours (e.g. for papillary muscle inclusion/exclusion, Fig. 5A). A comprehensive visualisation task-card provides various 4D volume visualization options (solid/mesh, endocardium only/epicardium only etc.) with or without spatial integration of the respective 2D cine MR images (Fig. 5B).

Inline VF®

Especially in a high-throughput setting, instead of the necessity of using post-processing tools, one might expect to have the most relevant data available right after a scan – without any user interaction. With another tool, Inline VF, Siemens introduced the first fully automatic LV function assessment tool implemented on the MR acquisition workplace. Inline VF is integrated directly into the acquisition sequence (Fig. 6), enabling the calculation of functional data already during image acquisition. The heart is localized on the short-axis CMR images automatically with the support of a motion compensation algorithm; endo- and epicardial contours are detected and shown on the inline display with no user interaction (Fig. 7A, B). Subsequently the parameters of LV function are generated and shown on the display without additional mouse clicks (Fig. 7C). The images can be loaded and modified in Argus Function, when needed. Inline VF is embedded in *syngo* BEAT, thus can be used with each triggered 2D cine sequence (GRE or TrueFISP contrast, segmented or real-time acquisition, cartesian or radial sampling scheme).

CMR is the gold standard for functional cardiac diagnostics; the new tools further lead to an efficient workflow and will help to increase the utilization of CMR in clinical routine.

Contact
Okan Ekinci, M.D.
Global Segment Manager
Cardiovascular MRI
Siemens Medical Solutions
Karl-Schall-Str. 6
91052 Erlangen
Germany
Phone: +49 9131/84-4391
okan.ekinci@siemens.com

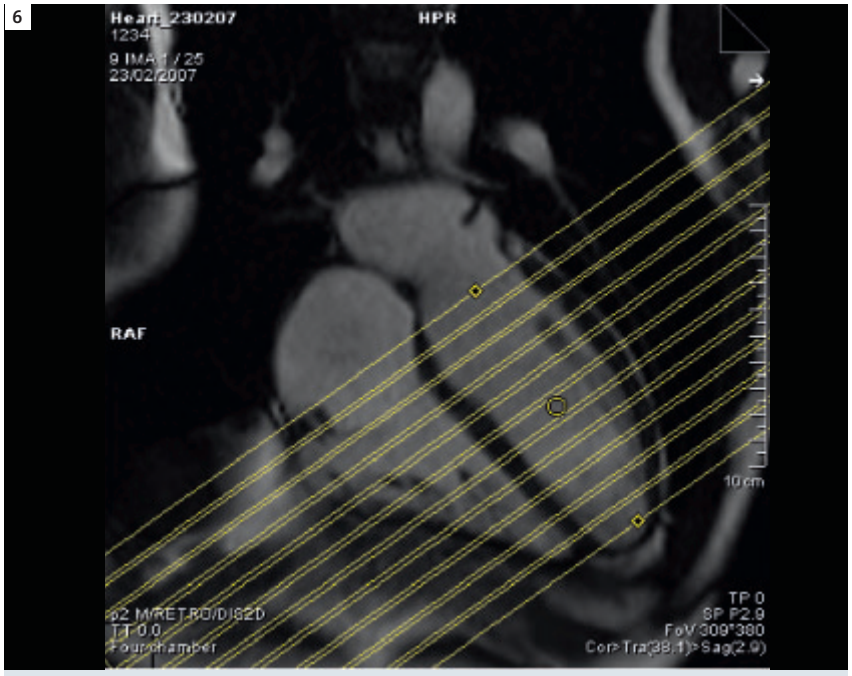

6 Planning of short-axis slices on a 4-chamber view using Inline VF®. The most basal slice is positioned on the mitral valve plane in end-diastole. An automatic algorithm moves the most basal slice for calculation purposes in end-systole to the next slice when necessary, to avoid left atrial volume affecting the volumetric analysis.

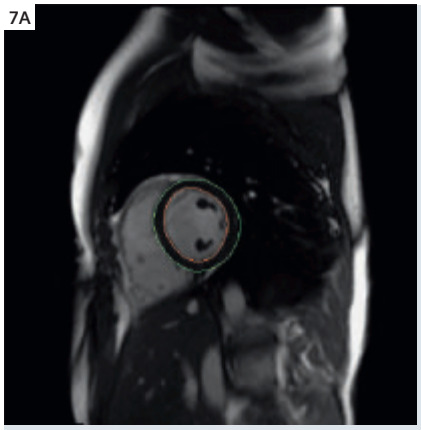

7 Inline VF® automatically locates the heart and detects endo- and epicardial contours in all cardiac slices and phases **(A, B)**. Parameters of left ventricular function (e.g., EDV, ESV, EF, SV etc.) are shown on the inline display right after scan **(C)**.

CMR Delayed Enhancement Imaging in Coronary Artery Disease

Igor Klem, M.D.

Duke Cardiovascular Magnetic Resonance Center, Duke University Medical Center, Durham, USA

Delayed Enhancement MRI – from bench to bedside

Imaging myocardial injury using T1-weighted pulse sequences after the administration of intravenous gadolinium contrast media has been performed since the mid 1980's. A major advance of this technique was achieved with the development of a pulse sequence (segmented inversion-recovery turbo-FLASH) which allowed an increase in signal difference between "normal" and "hyperenhanced" tissue 10-fold compared to older pulse sequences. This technique, named **delayed contrast-enhanced MRI** (DE-MRI) was introduced in the late 1990's and may be considered already the gold-standard for the detection of irreversibly damaged myocardium. This development of DE-MRI and its subsequently emerging clinical applications parallels the steadily increasing importance of cardiovascular magnetic resonance in routine clinical patient care.

Infarcted myocardium accumulates gadolinium and can be visualized as hyperenhanced or "bright" regions on T1-weighted images.

What is hyperenhanced or "bright" myocardium?

The underlying concept is that infarcted tissue accumulates gadolinium and can be visualized as hyperenhanced or "bright" regions on T1-weighted images acquired at least 10 minutes after gadolinium injection. How can we understand that a "non-specific" contrast agent can distinguish between viable and nonviable myocardium, especially across the wide range of tissue environments that occur during infarct healing? One should conceptually not think of DE-MRI as a tissue- or necrosis-specific staining technique or a ligand binding to specific receptors. Gadolinium is an inert extracellular contrast agent and the amount of contrast agent in a given tissue distribution volume determines the image signal intensity – the more contrast per distribution volume the higher the signal. An important physiological fact to remember is that the tissue volume in normal myocardium is predominately intracellular (~ 75% of the water space). Because extracellular contrast media is excluded from this space by the intact sarcolemmal membrane, the volume of distribution of a contrast medium in normal myocardium is quite small (~ 25% of water space), and one can consider viable myocytes as actively excluding contrast media. The unifying mechanism for the hyperenhancement effect of nonviable myocardium may then be the absence of viable myocytes rather than any inherent properties that are specific for acutely

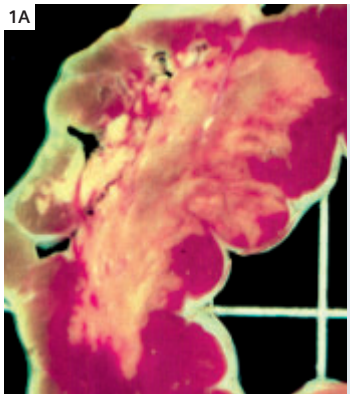

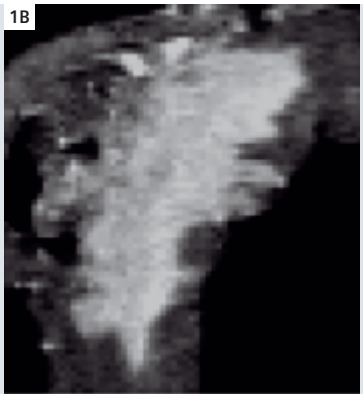

1 Comparison of high-resolution ex-vivo DE-MRI images (right) with acute myocyte necrosis defined by histopathology (left). Note that the size and shape of the infarcted region (yellowish-white region) defined histologically by staining is nearly exactly matched by the size and shape of the hyper-enhanced (bright) region on DE-MRI.
(Adapted from Kim RJ, Fieno DS, Parrish TB, et al. Relationship of MRI delayed contrast enhancement to irreversible injury, infarct age, and contractile function. Circulation 1999; 100: 1996; with permission).

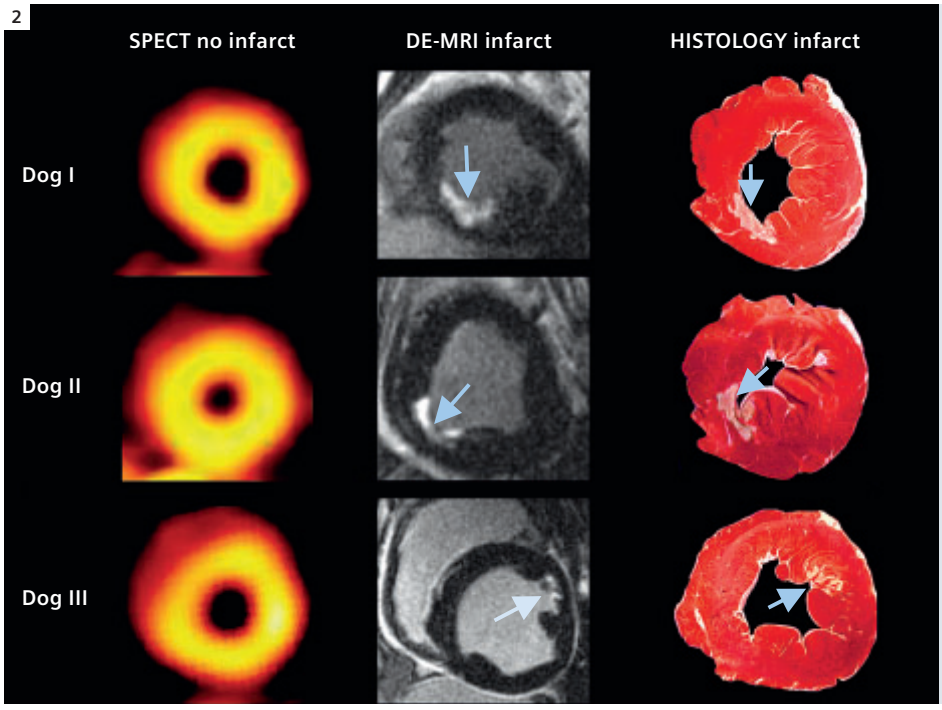

2 Short axis views from three animals with subendocardial infarcts. DE-MRI detected even small infarcts (arrowheads) which were missed by SPECT.
(Adapted from Wagner A, Mahrholdt H, Holly TA, et al. Contrast-enhanced MRI and routine single photon emission computed tomography (SPECT) perfusion imaging for detection of sub-endocardial myocardial infarcts: an imaging study. Lancet 2003; 361: 376; with permission.)

necrotic tissue, collagenous scar, or other forms of nonviable tissue.
In animal models of ischemic injury directly comparing DE-MRI to histopathology a nearly exact agreement between the size and shape of infarcted myocardium by DE-MRI to that by histopathology was demonstrated (Figure 1). It has been shown that DE-MRI can delineate between reversible and irreversible myocardial injury independent of wall motion, infarct age, or reperfusion status. Human studies demonstrate that DE-MRI is effective in identifying the presence, location, and extent of MI in both the acute and chronic settings. Additionally, DE-MRI provides scar size measurements that are closely correlated with positron emission tomography (PET) in patients with ischemic cardiomyopathy, and provides results superior to single-photon emission computed tomography (SPECT) in patients with subendocardial infarctions.

Advantages of DE-MRI over other viability techniques

A DE-MRI scan for assessment of viability is quite simple (see section on protocol), can be performed in a single exam of less than 30 minutes duration and does not require pharmacological or physical stress. Additionally, DE-MRI is rarely performed in isolation, rather it is one component in a more comprehensive study that is tailored to the specific patient. It may be combined with a stress component for ischemia assessment, cine images for functional assessment, flow velocity mapping for evaluation of valvular disease, or a vascular study to assess aortic pathology to mention just a few of the possible combinations.
A major advantage of DE-MRI is the high spatial resolution. With a standard implementation, a group of 10 hyperenhanced pixels (voxel, 1.9 x 1.4 x 6 mm) in a typical image would represent an infarction of 0.16 grams, or a region one thousandth of the LV myocardial mass. This level of resolution, more than 40-fold greater than SPECT, allows visualization of even microinfarcts that cannot be detected by other imaging techniques (Figure 2).
Further, DE-MRI is different from radionuclide imaging in that it provides direct visualization of both non-viable and viable myocardium. For instance, rather than simply identifying a region of acute infarction as non-viable due to reduced tracer activity, DE-MRI can distinguish between acute infarcts with necrotic myocytes and acute infarcts with necrotic myocytes and damaged microvasculature. The latter, termed the "no-reflow phenomenon", indicates compromised tissue perfusion despite restoration of epicardial artery patency. DE-MRI performed 5–10 minutes after contrast provides high image quality and delineates regions with more

DE-MRI can delineate between reversible and irreversible myocardial injury independent of wall motion, infarct age, or reperfusion status.

The voxel resolution of CMR is 40-fold greater than SPECT, allowing visualization of microinfarcts that cannot be detected by other imaging techniques.

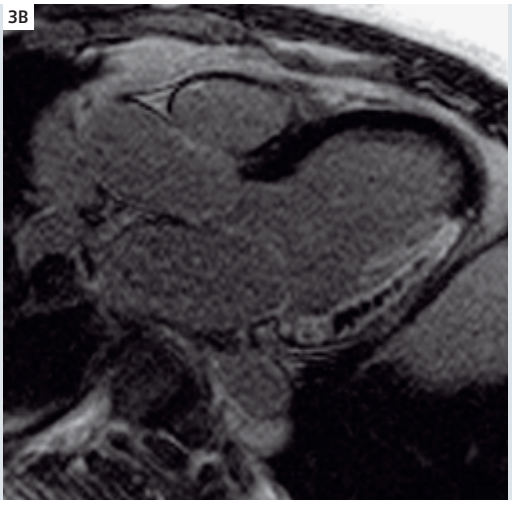

3 Short axis and long axis images from a patient with acute myocardial infarction. Note that the transmural infarct is composed of a bright area with a central black core corresponding to an area of no-reflow.

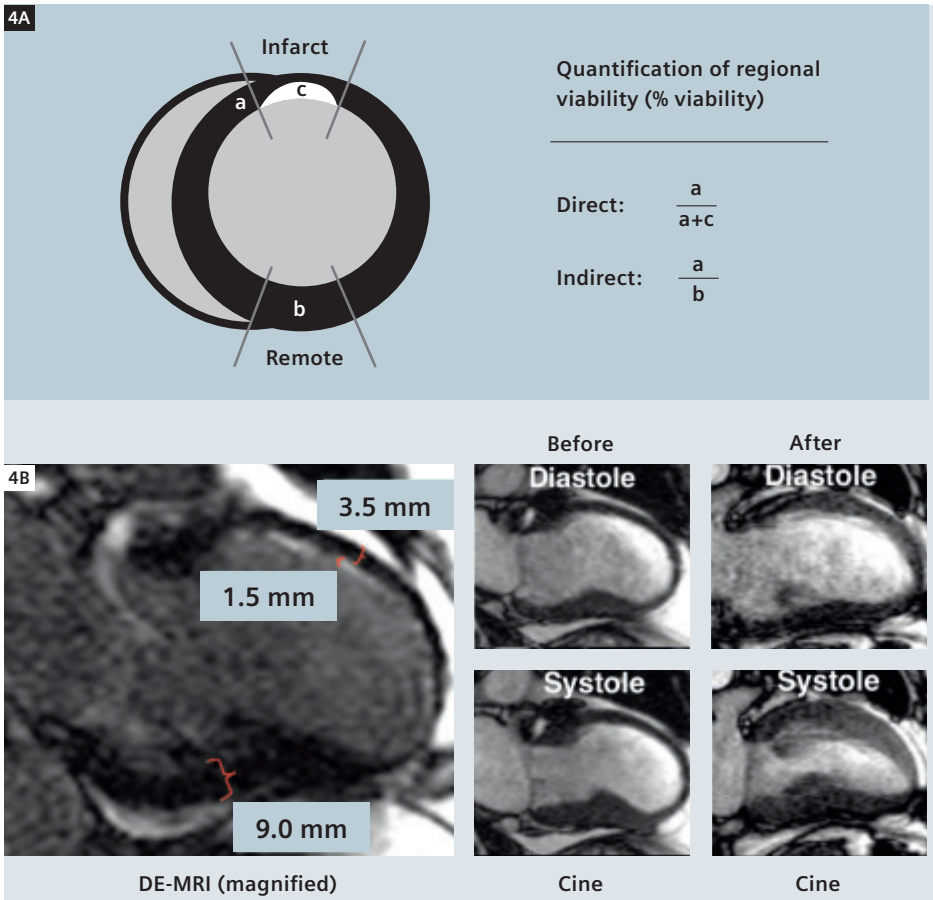

4 **(4A)** Illustration of the differences between a direct and indirect method of quantifying regional viability. Viable myocardium is displayed in black and infarcted myocardium displayed in white.
(4B) Long axis MR images of a patient before and two months after revascularization. Although the akinetic anterior wall is "thinned" (diastolic wall thickness = 5 mm; remote zone = 9 mm), DE-MRI demonstrates that there is only a subendocardial infarction (1.5 mm thick). A direct assessment of viability would show that the anterior wall is predominantly viable (3.5 mm / 5 mm = 70% viable), whereas the indirect method would show that the anterior wall is predominantly nonviable 3.5 mm / 9 mm = 39% viable).
Cine MR images obtained following coronary revascularization demonstrate full recovery of wall motion and diastolic wall thickness. Full motion movies can be viewed at http://dcmrc.duhs.duke.edu/NF10.
(Modified from Heart 2004; 90: 137–140 with permission.)

profound microvascular damage (Figure 3).
The ability to simultaneously visualize non-viable and viable myocardium provides additional advantages. For example, DE-MRI can accurately assess ventricular remodeling following acute MI at an early time point before measurements of ventricular volumes, internal dimensions, and ventricular mass have changed. This is possible since DE-MRI can assess serially, concurrent directionally opposite changes such as resorption of infarcted tissue and hypertrophy of viable myocardium.
When only viable myocardium can be visualized, the "percentage of viability" in a given segment is assessed indirectly and generally refers to the

amount of viability in the segment normalized to the segment with the maximum amount of viability. Conversely, when both viable and infarcted myocardium can be visualized, the "percentage of viability" can be assessed directly and expressed as the amount of viability in the segment normalized to the amount of viability plus infarction in the same segment (Figure 4A). These differences in the way in which viability is measured can alter clinical interpretation. Figure 4B demonstrates MR images in a patient with chronic coronary disease and an akinetic anterior wall. Although the anterior wall is thinned, only a small subendocardial portion of the anterior wall is infarcted. In this case, the indirect method would show that the anterior wall is only 39% viable (compared to the remote region), whereas the direct method would show that the anterior wall is 70% viable. The indirect method would predict no recovery of wall motion after revascularization whereas the direct method would predict recovery. The post-revascularization images (bottom-right panel) demonstrate in this patient the direct method was correct.

Clinical applications of DE-MRI

Prediction of functional recovery in ischemic disease

As the patient example in Figure 4 shows, one clinical application of DE-MRI is to identify patients with potentially reversible ventricular dysfunction from those with irreversible dysfunction. With the ability of DE-MRI to directly visualize the transmural extent of infarction (and viability) functional improvement after revascularization can be predicted in both acute and ischemic disease.
In the context of acute myocardial infarction, prompt revascularization therapy has been shown to result in salvage of ischemic but viable myocardium, improvement in ejection fraction (EF), and long-term improvement in survival. In the immediate post-infarction setting, even after successful reperfusion, myocardial dysfunction may persist, and it is difficult to distinguish whether it is due to myocardial necrosis or to myocardial stunning. Differentiation between these two conditions is important because patients with a large area with dysfunction but only little necrosis (i.e. predominantly stunned) would be expected to have marked functional and clinical improvement. In contrast, patients with a dysfunctional region that is predominantly necrotic would not be expected to have much functional improvement. Studies in patients with acute myocardial infarction and successful revascularization showed that transmural extent of infarction was highly predictive of improvement in wall motion and global function (see recommended reading for details).

DE-MRI allows visualization of the transmural extent of myocardial infarction.

The transmural extent of infarction determined by DE-MRI has also been shown to predict response to myocardial revascularization in patients with chronic ischemic heart disease. Similar to findings in the acute setting, likelihood of functional improvement was inversely related in a progressive stepwise fashion to transmural extent of infarction. Several studies have demonstrated that there is a progressive relationship between the likelihood of contractile response to revascularization and the transmural extent of infarction as evidenced by DE-MRI.

The transmural extent of infarction determined by DE-MRI predicts the response to myocardial revascularization in patients with chronic ischemic heart disease.

DE-MRI for heart-failure assessment

We have discussed thus far the ability of DE-MRI to predict the likelihood and magnitude of functional improvement after revascularization in both acute and chronic ischemic disease. There is however a significant proportion of patients, in whom myocardial dysfunction and heart failure (ischemic cardiomyopathy) persists even after revascularization, or in whom revascularization is not possible due to a variety of reasons (e.g. associated comorbidities, poor distal targets, or diffuse atherosclerotic disease). In addition, a significant proportion of patients have dysfunction in the absence of CAD (nonischemic cardiomyopathy). The utility of DE-MRI for diagnostic assessment of heart failure patients is manyfold. We will discuss here some established and emerging applications:

1. The ability of DE-MRI to provide in-vivo images corresponding to ex-vivo pathological sections allows the determination of underlying pathology of cardiomyopathies. This application is based on the concept that both presence and pattern of scar can be used to discriminate between myopathic processes. The typical pattern of hyperenhancement that occurs in patients with myocardial infarction and thus with ischemic cardiomyopathy can be explained by the pathophysiology of myocardial ischemia. Following approximately fifteen minutes of coronary occlusion, a wavefront of myocardial necrosis begins in the subendocardium and progresses transmurally with increasing duration of occlusion. Therefore, hyperenhancement can

The distribution pattern of DE allows the determination of underlying pathology of cardiomyopathies.

2D/3D & PSIR TurboFLASH/ TrueFISP IR sequences are provided for delayed enhancement imaging in the Advanced Cardiac Package.

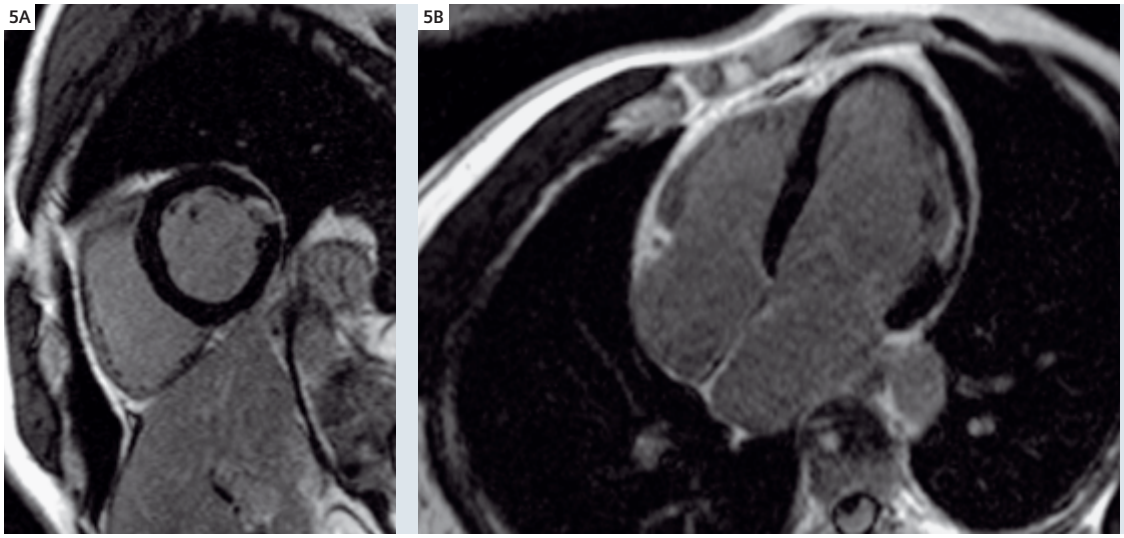

5 Typical DE-MRI images (5A: short-axis and 5B: 4-chamber view) of a patient with coronary artery disease and previous myocardial infarct in the lateral wall. The hyperenhancement of CAD pattern typically involves the subendocardium extending towards the subepicardium. The transmural extent of infarction is well visualized.

Different delayed enhancement patterns can be seen in non-ischemic cardiomyopathies such as HCM, cardiac amyloidosis, cardiac sarcoid or myocarditis.

be classified as "ischemic" type or "non-ischemic" type, the former involving the subendocardium (i.e. subendocardial or transmural) and be located in a region that is consistent with the perfusion territory of an epicardial coronary artery (Figure 5). Hyperenhancement pattern has been shown to provide diagnostic utility for distinguishing between ischemic and non-ischemic cardiomyopathies. While classification of cardiomyopathies as ischemic or non-ischemic is an important means of dichotomizing patients with systolic dysfunction, prior studies have found that disease-specific differences in etiology of myocardial dysfunction alter prognosis and therapy. Among patients with non-ischemic cardiomyopathies, therapeutic options include corticosteroids for treatment of cardiac sarcoid or myocarditis, alkyloids in the setting of cardiac amyloid, α-galactosidase enzyme replacement therapy in the setting of Anderson-Fabry's disease, and septal ablation or myomectomy in the setting of hypertrophic cardiomyopathy. DE-MRI evidenced hyperenhancement can occur in all of these conditions, having been reported in inflammatory conditions such as myocarditis, infiltrative cardiomyopathies such as sarcoid, systemic processes such as amyloid or Chagas disease, and genetic abnormalities such as hypertrophic cardiomyopathy or Anderson-Fabry's disease. Each of these conditions results in myocardial dysfunction as a result of diverse pathological processes and is associated with differences in hyperenhancement patterns (Figure 6).

For CMR stress studies, cine and perfusion studies at rest and stress are combined with DE to identify scar tissue.

2. In patients with congestive heart failure, several studies have shown that medical therapy using beta-blockers can result in improvement in LV function, heart failure symptoms, and long-term survival. A significant heterogeneity exists, however, in the response to beta-blockers among individual patients. It has been shown that patients with the most advanced disease have less capacity to respond to beta-blockers, because less viable myocardium exists. Similar to the situation in patients undergoing coronary revascularization, an inverse relationship was found between the transmural extent of infarction and the likelihood of improvement in regional contractility and LVEF after beta-blocker therapy. Furthermore, this parameter from DE-MRI was directly related to the magnitude of reverse remodeling (i.e. a decrease in LV enddiastolic volume index and LV end-systolic volume index).

DE-MRI as part of a multi-component stress test

MRI stress testing is being increasingly performed in clinical practice for evaluation of patients with ischemic heart disease. There are two techniques available, dobutamine cine CMR, analogous to dobutamine stress echocardiography, and vasodilator (adenosine) stress perfusion. The latter appears to be more practical and faster in the clinical scenario. In addition to providing information on stress perfusion, which could be obtained in approx. 5 minutes scan time, CMR can provide a very comprehensive evaluation if stress perfusion is combined with other CMR components. In our experience, the optimum combination is stress/rest perfusion CMR with delayed enhancement CMR (Figure 7). While the former detects perfusion

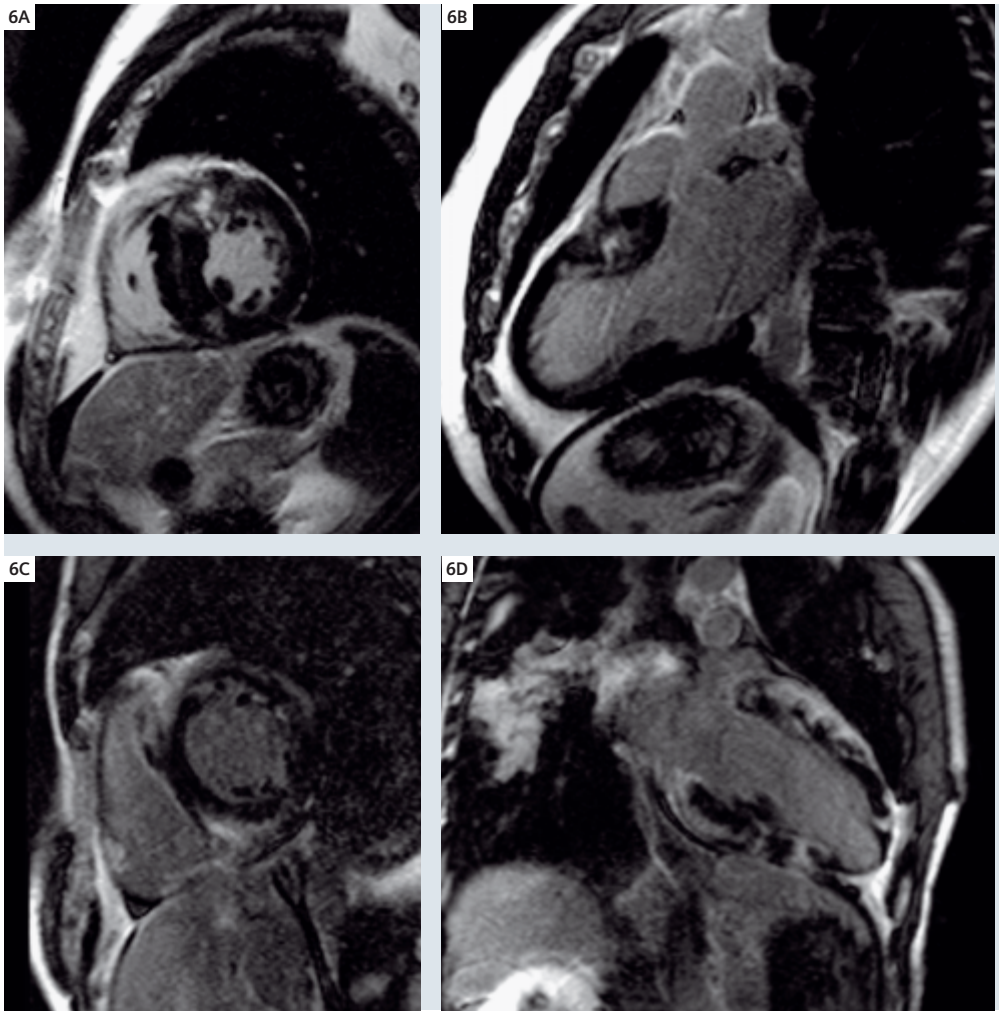

6 Examples of patient images with non-CAD type of hyperenhancement. Patient 1 is a 32-year-old male with hypertrophic cardiomyopathy. DE-MRI revealed extensive scarring at the right ventricular insertion sites into the septum **(A, B)**.
Patient 2 is a 28-year-old male with pulmonary sarcoidosis, an MRI scan performed for further evaluation of ventricular tachycardia revealed extensive cardiac involvement **(C, D)**.

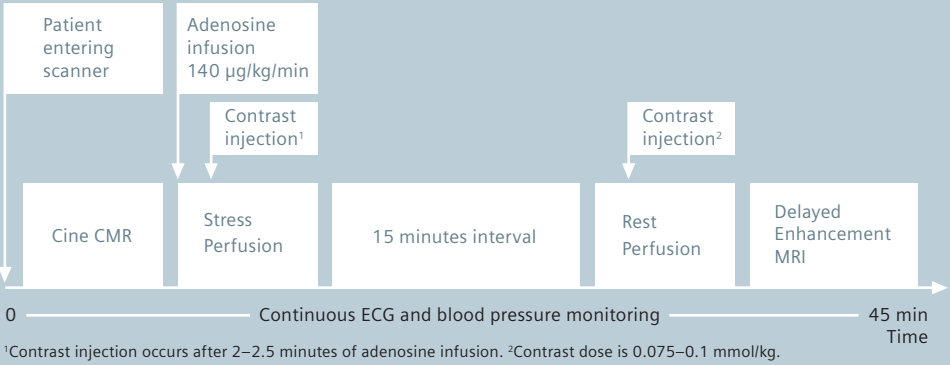

[1]Contrast injection occurs after 2–2.5 minutes of adenosine infusion. [2]Contrast dose is 0.075–0.1 mmol/kg.

7 Flow-diagram of a multi-component CMR stress perfusion study. Note that DE-MRI is performed after two injections of gadolinium contrast (2 x 0.07–0.1 mmol/kg) for stress and rest perfusion, which provides sufficient contrast for delayed enhancement imaging without additional contrast injections.

defects, DE-CMR provides further information regarding the cause of those defects. For example, perfusion defects that are matching in spatial extent to bright areas (scar) on DE-CMR are caused by infarcted myocardium (Figure 8). In contrast, a perfusion defect detected in dark (viable) myocardium by DE-CMR is consistent with inducible ischemia. Occasionally, artifactual defects are observed on perfusion CMR which may impose difficulties in image interpretation. We found DE-CMR to be also useful to differentiate artifactual perfusion defects from true perfusion defects due to coronary artery disease. Artifactual defects occur in identical location, intensity and extent on serial

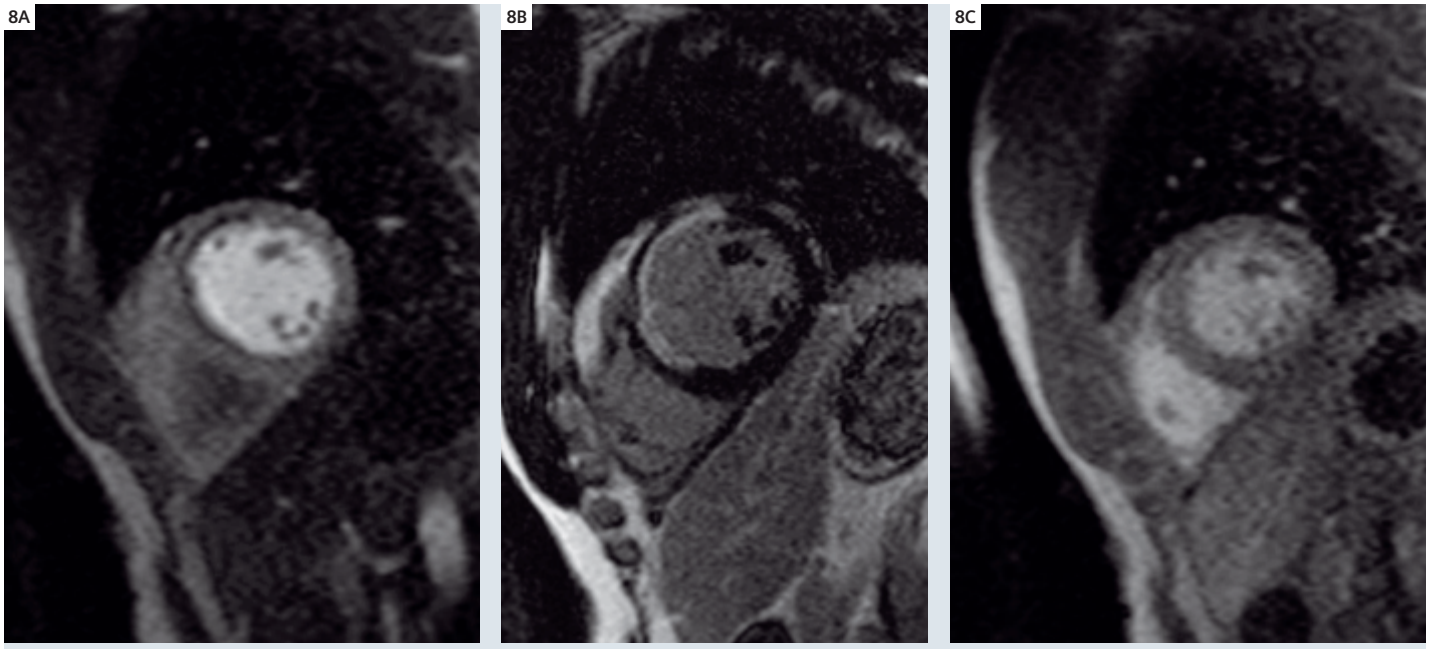

8 Patient example of a stress CMR study demonstrating complementary information of stress/rest perfusion and DE-MRI. Note that the subendocardial perfusion defect seen during stress **(A)** matches in spatial extent the scarred area on DE-MRI **(B)** indicating that there is infarct but no ischemic viable myocardium. Rest perfusion images **(C)** can be useful for differentiation of true perfusion defects from artifacts.

DE-MRI provides an important non-invasive tool for studying associations between scar characteristics and arrhythmic risk.

image acquisitions if imaging parameters are kept unchanged. Therefore we acquire for every patient both stress and rest perfusion images and compare these to DE-CMR findings. The only physiological scenarios where myocardial perfusion is thus severely reduced to cause rest defects are a) resting ischemia and b) infarcts. In the former scenario, the patient would likely be symptomatic at rest, thus not a good candidate for stress testing. In the latter scenario, which is more common in clinical practice, we have an independent technique for infarct detection to confirm our perfusion findings: DE-CMR. Consequently, if matched defects are not confirmed to be infarcts on DE-CMR they can be identified as artifactual. We found that considering these physiologic principles when interpreting the multi-component CMR stress test can increase the accuracy significantly (see recommended reading for details).

DE-MRI can be performed as a stand-alone procedure and takes less than 30 minutes.

DE-CMR for assessment of patients with arrhythmias

Myocardial scar forms a substrate for ventricular tachyarrhythmias, with a relationship between scar morphology and arrhythmic risk demonstrated in both experimental and epidemiologic studies. Data from animal studies indicates that both scar size and scar morphology influence arrhythmic risk. DE-MRI evidenced hyperenhancement provides highly accurate assessment of both scar size and morphology, with improved scar detection in comparison to other modalities such as myocardial scintigraphy (SPECT). Thus, DE-MRI provides an important non-invasive tool for studying associations between scar characteristics and arrhythmic risk. Interesting insights into the relationship between hyperenhancement and arrhythmogenic potential has been provided in several investigations and has started to transition into clinical trials to investigate the potential of this technique for prediction of clinical SCD risk.

DE-MRI imaging protocol – as simple as it is

A DE-MRI scan can be performed in a single brief examination which requires only a peripheral intravenous catheter which is placed before the patient enters the MRI scanner, and does not require pharmacologic or physiologic stress. After obtaining scout images to delineate the short and long axis views of the heart, cine images are acquired to provide a matched assessment of left ventricular (LV) morphology and contractile function with the viability characterization from DE-MRI. Short-axis views (e.g. 6 mm slice thickness with 4 mm gap to

match contrast-enhancement images) are taken every 10 mm from mitral valve insertion to LV apex along with two to three long-axis views in order to encompass the entire LV. The patient is then given a bolus of 0.10–0.20 mmol/kg intravenous gadolinium by hand or power injection. After a 10–15 minute delay to allow the contrast media to distribute, high spatial resolution delayed enhancement images of the heart are obtained at the same slice locations as the cine images, using a 2D segmented inversion recovery fast gradient-echo (seg IR-GRE, e.g. 2D IR TurboFLASH) pulse sequence. For patients who are acutely ill and unable to perform breath-holds an alternative is offered by using a subsecond "snapshot" imaging technique. This single-shot, inversion-recovery, steady state free-precession sequence can be used in analogy to the segmented gradient echo sequence. Parallel Acquisition Techniques (iPAT) are used to speed up imaging. This technique has been shown to be highly accurate with only mildly reduced sensitivity and possible underestimation of the transmural extent of infarction. Another option is a 3D sequence during free breathing using the navigator technique to account for breathing motion.

The pulse sequence parameters are set up similar to any other cardiac MRI sequence, the only specific parameter to DE-MRI is the inversion time (TI). This is the time required from the inversion prepulse (which provides T1-weighting) to the center of the read-out portion of the sequence and should be set to "null" signal from normal myocardium. What that means is that the signal from myocardium is minimized i.e. black, thereby the infarct which has different T1-characteristics than normal myocardium has the largest difference in signal and appears bright on the image. The correct TI has to be determined for each scan and depends on factors such as the contrast dose and timing of imaging after administration of contrast. Obtaining the correct TI can be accomplished with little training. For those starting with DE-MRI the cardiac pulse-sequence package includes tools to allow the beginner to identify the right TI time: the TI-Scout displays the identical scan location with an array of different TI-times, which allows the scanner operator to determine the correct TI (where myocardium appears black) for subsequent acquisitions using the IR-GRE sequence. Alternatively a phase-sensitive IR-GRE (e.g. PSIR) sequence can be used which can be used over a broad range of TI-time, thus making it unnecessary to optimize the TI. In general, most delayed enhancement images are acquired during an 8–10 s breath-hold, single shot phase-sensitive IR-GRE (PSIR) images in even less than 4 seconds. The imaging time for the entire examination is under 30 minutes. Figures 3, 5 and 6 demonstrate DE-MRI images from typical patient scans.

Summary

Delayed enhancement MRI provides clinically important information in a wide range of cardiac pathologies, in those frequently encountered in cardiology practice such as coronary artery disease and heart failure as well as less common problems such as in patients with cardiomyopathies or ventricular arrhythmias. It provides in-vivo information to the clinician that used to be only available to the pathologist on macroscopic exploration. In our institution DE-MRI is part of every cardiac exam. DE-MRI is a very robust technique and can be performed easily on a standard MRI scanner equipped with a cardiac package.

Single-shot PSIR sequences can be used for accurate DE-MRI especially in patients with breath-holding difficulties or arrhythmia.

Contact
Igor Klem, M.D.
Duke Cardiovascular Magnetic Resonance Center
Duke University Medical Center 3934
Durham, NC 27710
USA
igorklem@duke.edu

DE-MRI provides in-vivo information to the clinician that used to be only available to the pathologist on macroscopic exploration.

Recommended Reading

1 Kim RJ, Shah DJ, Judd RM. How we perform delayed enhancment imaging. JCMR 2003;5:505–514.
2 Kim RJ, Fieno DS, Parrish TB, et al. Relationship of MRI delayed contrast enhancement to irreversible injury, infarct age, and contractile function. Circulation 1999;100:1992–2002.
3 Kim RJ, Wu E, Rafael A, et al. The use of contrast-enhanced magnetic resonance imaging to identify reversible myocardial dysfunction. N Engl J Med 2000;343:1445–53.
4 Wagner A, Mahrholdt H, Holly TA, et al. Contrast-enhanced MRI and routine single photon emission computed tomography (SPECT) perfusion imaging for detection of subendocardial myocardial infarcts: an imaging study. Lancet 2003;361: 374–79.
5 Choi KM, Kim RJ, Gubernikoff G, et al. Transmural extent of acute myocardial infarction predicts long-term improvement in contractile function. Circulation 2001;104:1101–7.
6 Klem I. Heitner JF, Shah DJ, et al. Improved detection of coronary artery disease by stress perfusion cardiovascular magnetic resonance with the use of delayed enhancement infarction imaging. J Am Coll Cardiol 2006;47:1630–8.

Differentiation of Cardiomyopathies by use of CMR

Rory O'Hanlon, M.D.; Dudley J. Pennell, M.D., FCRP, FESC
CMR Unit, Royal Brompton Hospital, London, UK

Jeanette Schulz-Menger, M.D., FESC; Ralf Waßmuth, M.D.
Charité Campus Buch, Franz-Volhard-Klinik, Berlin, Germany

Introduction

CMR can yield information on cardiac anatomy, function, tissue characterization, perfusion, and valvular flow in one single study.

Primary cardiomyopathies (CMP) are diagnosed by exclusion of other cardiac diseases. Secondary or specific cardiomyopathies are defined as distinct myocardial diseases with specific origin as ischemic, hypertensive, inflammatory. The identification of the etiology for a non-ischemic cardiomyopathy is often difficult and suboptimal with conventional imaging and invasive testing. A "standard" investigative route is focused around a detailed history, ECG, transthoracic echocardiography, holter monitoring, exercise treadmill testing, and invasive angiography. These tests often produce a clear diagnosis, such as coronary artery disease, valvular heart disease, dilated cardiomyopathy, or hypertrophic cardiomyopathy. Nevertheless, establishing a diagnosis of cardiomyopathy can still be difficult and may be not possible to do with certainty. In recent years, advances in cardiovascular magnetic resonance (CMR) have brought this technology into routine clinical use. In a single 45–60 minute study, CMR can yield information on cardiac anatomy, function, tissue characterization, perfusion, and valvular flow. This technology not only helps to determine the etiology and presence for a cardiomyopathic process, but also provides a robust imaging tool to follow patients over time and provide prognostic information.

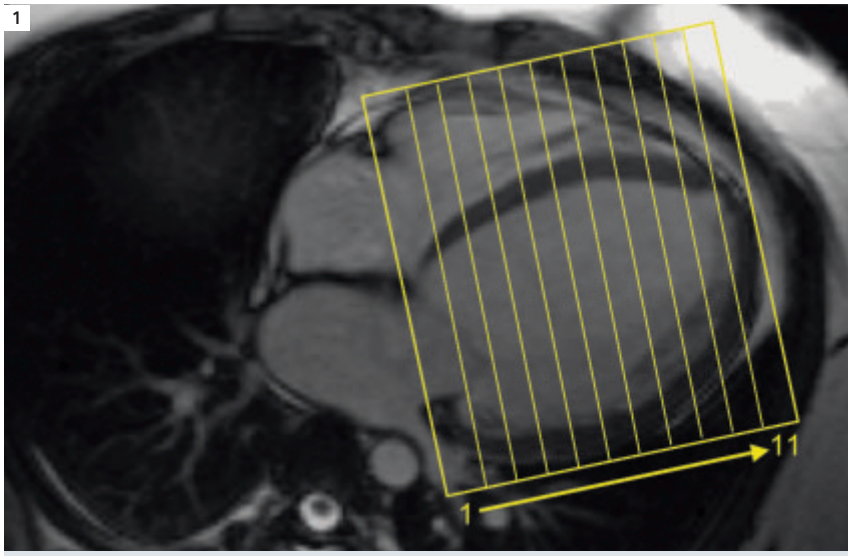

1 Method of acquisition of short axis stack of cine-images from base to apex. The first slice (1) is typically taken parallel to the annulus of the mitral and tricuspid valve. Serial slices 10 mm apart are acquired from base to apex (slice 11) usually with a slice thickness of 7 mm and 3 mm gaps, at our institution. Breath-hold is typically no longer than 8–10 seconds.

A number of CMR techniques are useful in the assessment of cardiomyopathy. Initially a detailed assessment of cardiac anatomy is performed using at least transaxial (and also usually coronal and sagittal) HASTE (Half-Fourier Acquisition Single-Shot Turbo Spin-Echo) imaging, which can be completed in approximately 3 minutes. This serves to identify at an early stage important shunts, anomalous pulmonary venous drainage, or congenital anomalies which may explain increased chamber dimensions suggestive of a cardiomyopathy. Alternatively, a multislice single-shot True-FISP morphology sequence can be performed. TrueFISP cine imaging of long and short axis function is performed to assess overall myocardial function, followed by a stack of 8–12 short axis TrueFISP cines of the LV and RV from base to apex, which is regarded as the "gold standard" test for quantitative assessment of biventricular volumes and function (Fig. 1). Assessment of volumes and mass can be performed by manual planimetry of the epi- and endocardial border in diastole and the endocardial border in systole (Fig. 2). Alternatively, the analysis can be performed using semi-

automated software (Fig. 3). A completely automatic VF analysis tool has recently been introduced by Siemens Medical Solutions (Inline VF). For patients with subtle reductions in function by echocardiography, CMR can establish ventricular dysfunction with greater confidence because of the availability of normal values which are corrected for age, sex and body surface area. CMR also provides a more suitable method for follow up of serial measurements given the superior interstudy reproducibility over other imaging modalities which are more routinely used, especially 2D echocardiography.

A number of other more specialized imaging sequences are also performed in a patient with suspected cardiomyopathy. T1 and T2-weighted turbo-spin echo (TSE) sequences are useful to assess the pericardium where the clinical question resolves around constrictive vs. restrictive cardiomyopathy. Short TI Inversion Recovery (STIR) imaging with a triple inversion protocol, nulls signal from fat, is T2-weighted and is used to identify areas of increased myocardial water content, indicative of myocardial oedema and inflammation which are seen in conditions such as acute myocarditis and acute myocardial infarction. Myocardial T2*-weighted imaging is used to quantify myocardial iron. Imaging performed immediately (1–3 minutes) following intravenous gadolinium is a sensitive tool to detect intracardiac thrombi by providing the best delineation between the enhanced blood-pool and myocardium on one side and the dark thrombus on the other side. Further, late gadolinium enhancement (LGE) imaging using sequences such as inversion recovery TurboFLASH (IR GRE) or phase-sensitive inversion recovery (PSIR) sequences is then performed approximately 5–20 minutes after gadolinium administration (the delay between contrast administration and image acquisition depends on the concentration of gadolinium given, typically 0.1–0.2 mmol/kg body weight). The presence of LGE is indicative of abnormal myocardial interstitium such as myocardial fibrosis and infarction. In non-ischemic cardiomyopathy, there are several typical patterns of LGE which are very helpful in determining etiology and providing prognostic information. Please refer to the article of I. Klem (pg. 14) for details about typical LGE pattern caused by ischemic heart disease.

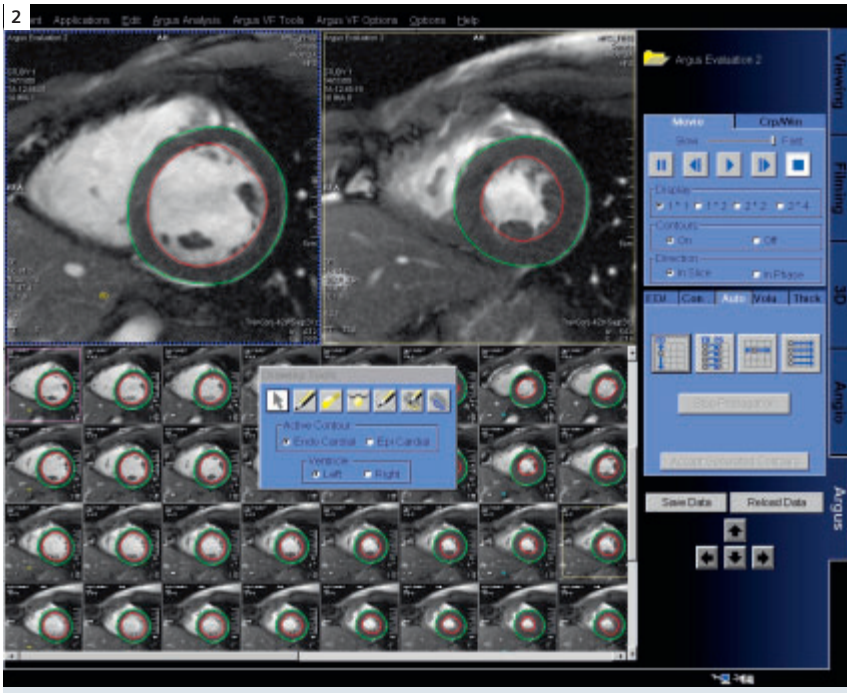

2 Contouring of epicardial and endocardial borders in diastole and systole to measure LV mass, volumes, and function. The volumes are calculated by summing the volume of the blood in each slice. The mass is determined from the volumes of myocardium in diastole multiplied by the myocardial density (1.05 g/cm^2).

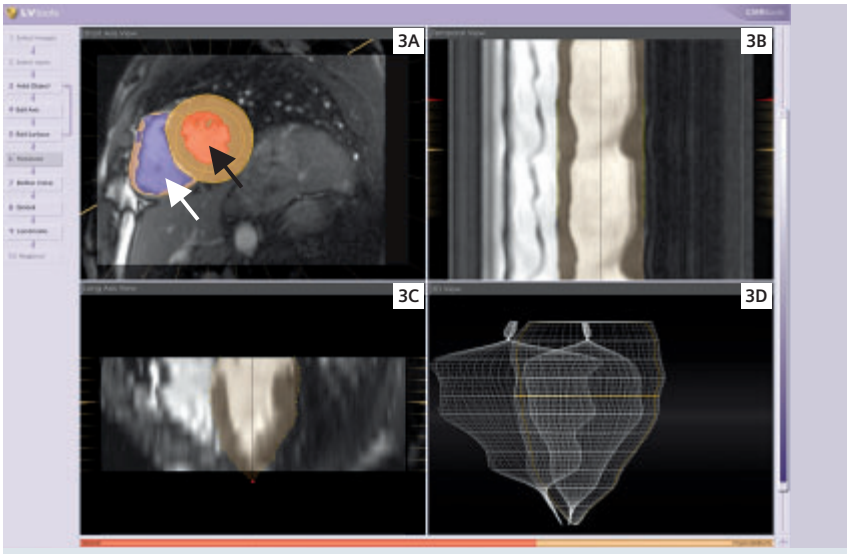

3 Semiautomated analysis of left and right ventricular mass, volume, and function. There are several software packages that can perform this assisted analysis and the one shown here is CMRtools® (Cardiovascular Imaging Solutions, London, UK; www.cmrtools.com). A 3-dimensional model of the epicardial and endocardial contours is generated, incorporating user-defined guide-points and shown in panel D. This model calculates the contours for all slices and is fully adjustable. The model is checked against a composite long axis image (panel C) and the time activity image (panel B) to ensure it is consistent through planes and time. Finally, thresholding of blood to account for papillary muscles is performed with an intensity based tool (LV blood orange with black arrow; RV blood blue with white arrow). The atrial contribution to volumes is excluded in diastole and systole by defining the mitral and tricuspid valve annuli from the long-axis cines.

Dilated Cardiomyopathy

CMR is superior to nuclear scintigraphic techniques to distinguish non-ischemic from ischemic etiologies of cardiomyopathy.

We use the term dilated cardiomyopathy to refer to patients with systolic dysfunction, a dilated heart and a cause from muscle dysfunction which has not resulted from the various manifestations of coronary artery disease. For many patients who present with systolic dysfunction and dilated heart, the ruling out of coronary artery disease as the etiology is of importance since this has a major impact on prognosis and treatment strategies [1-3]. There are studies using LGE as a novel non-invasive test to determine if LV dysfunction has an ischaemic etiology. In the absence of LGE in those with a dilated heart, an ischaemic etiology is extremely unlikely (97% negative predictive value), and in the presence of an ischaemic etiology, the amount of LGE correlates with the degree of severity of underlying CAD [4-7]. By contrast, patients with normal coronaries by angiography and LV dysfunction may still have an ischemic etiology for LV dysfunction (thrombosis on a non-stenotic plaque, or embolism in up to 13% of individuals), and may have been inappropriately diagnosed as having a dilated cardiomyopathy [5]. The results of the LGE technique as a non-invasive method of differentiating ischaemic and dilated cardiomyopathy are superior to other techniques because the myocardial substrate can be interrogated with such high resolution. Additionally, CMR is superior to nuclear scintigraphic techniques to distinguish non-ischemic from ischemic etiologies. CMR is not limited by attenuation artefacts, which lead to false positive results for presence of myocardial infarction. Comparative studies between SPECT and CMR perfusion imaging have also demonstrated that CMR can better identify small myocardial infarctions than nuclear techniques [9]. Perfusion can also be assessed by both techniques to identify ischaemia, but CMR has superior spatial resolution and provides sensitivity and specificity values ranging between 83% and 95% and 53% and 95% respectively [10]. While the absence of LGE does not completely rule out an ischemic etiology in the rare setting of global myocardial hibernation in the absence of infarction, first-pass myocardial perfu-

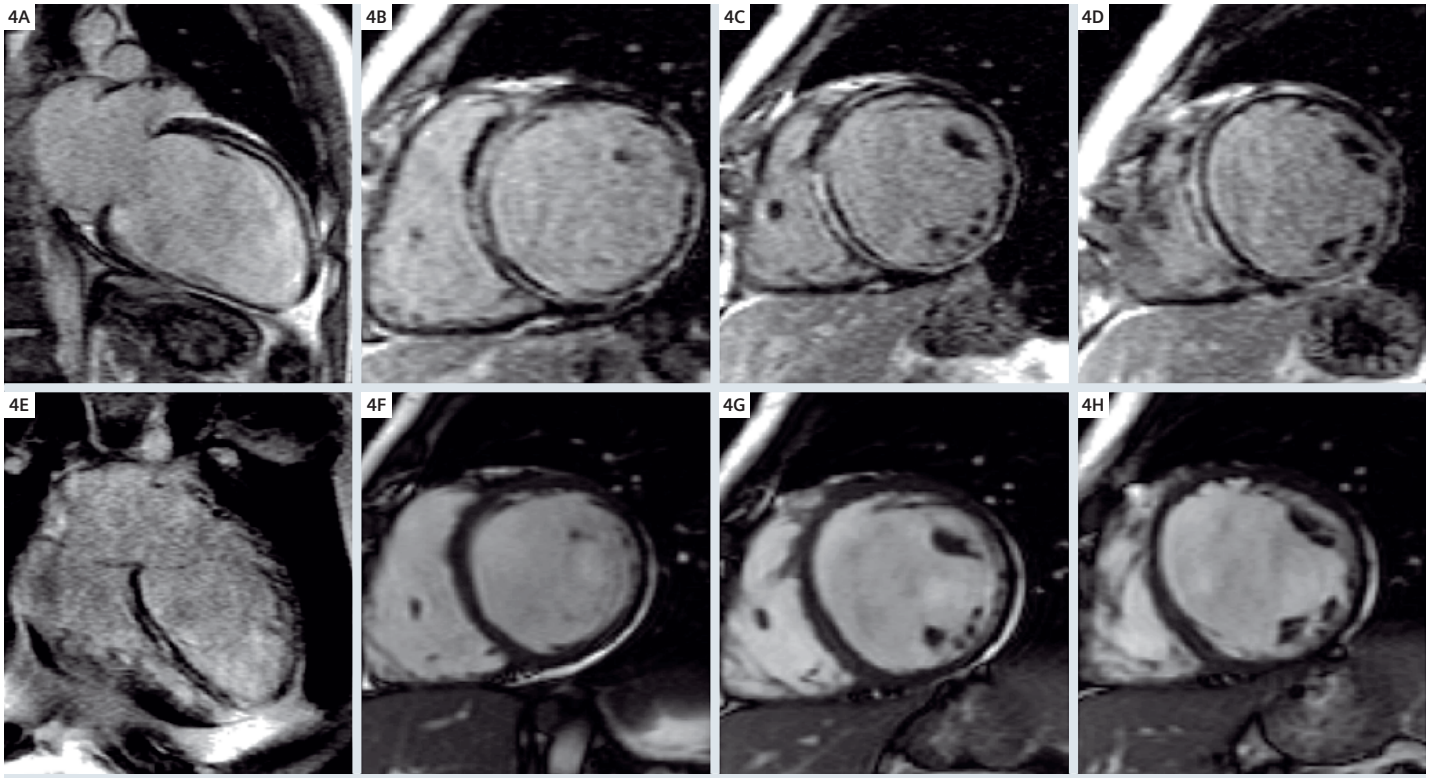

4 Late gadolinium enhancement in dilated cardiomyopathy. There is mid-wall enhancement which is most marked in the septum. Vertical (A) and horizontal (E) long axis and three short axis (B, C, D) planes. Corresponding frames from the SSFP short axis cines are shown (F, G, H).

sion imaging or proximal coronary artery MR angiography can be performed.
Myocardial fibrosis, in a non-infarct pattern, is seen in up to 30% of patients with DCM, typically in a mid-wall septal distribution ("mid-wall striae", Fig. 4). The presence of fibrosis has important prognostic implications, with the presence of mid-wall fibrosis in DCM being associated with an increased risk of sudden cardiac death and ventricular tachycardia (VT), independent of other more traditional markers of increased risk [11]. These findings might also suggest the use of CMR for better identification of patients with need for an ICD implantation.
As highlighted above, CMR is the reference standard method of assessment of myocardial volumes and function. The interstudy and interindividual variability is less than 5%, thus making this technique accurate for picking up subtle reductions in ventricular function. This low variability also allows for accurate serial measurements over time to monitor for changes in function and monitor response to medical therapies. Furthermore, given the excellent interstudy reproducibility, smaller sample sizes are needed to detect true clinical differences between patient populations in research studies [12]. One example of this would be in a drug trial designed to detect a 10 g difference in LV mass with anti-hypertensive treatment, a sample size of 505 would be needed with 2D echo versus only 14 with CMR, for a power of 80% and P-value of 0.05 [13].

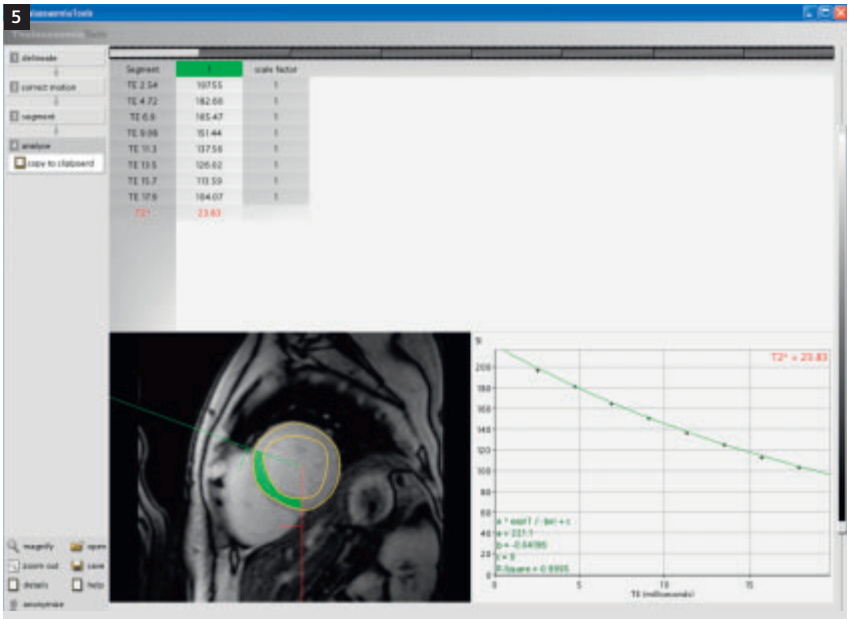

5 Myocardial T2* analysis using Thalassemia-Tools® (plug-in of CMRtools®). The gradient echo images are loaded and the interventricular septum is defined. This area is least affected by variable susceptibility artefact commonly seen adjacent to the anterior and inferior walls (cardiac veins with deoxygenated blood) and the lateral wall (lungs). The software generates the signal against echo-time points and best fits the decay curve to estimate the T2* (in this case normal at 23.8 ms). When the myocardial T2* is very short (<10 ms), the latter points are comprised of noise rather than signal and the software can be instructed to discount such points to ensure the curve fits the "signal rich" initial decay points. This method is known as truncation. Other mathematical solutions for the data fitting exist including modeling of a constant for the baseline offset, and bi-exponential decay modeling. The truncation technique has been used for the major randomized controlled trials and its performance is well understood. The other techniques yield slightly different T2* values and therefore consistent analysis technique is important.

Thalassemia

Heart failure due to iron overload is the principle cause of death in patients with thalassemia, accounting for up to 71% of all deaths, with 50% of these patients dying before the age of 35, despite iron-chelating therapy [14-16]. This form of cardiomyopathy is reversible but intensive iron chelation is necessary to remove myocardial iron [17]. Unfortunately once heart failure symptoms occur in iron overload cardiomyopathy, the prognosis is poor. In the past, total body iron stores and approximation of myocardial iron loading were assessed by serum ferritin levels and liver biopsy, and indeed these parameters were also used to monitor success or failure of chelation therapy. It is now recognized that there can be marked discordance between liver and heart iron loading making early detection of myocardial iron challenging using conventional techniques [18]. Since 2000 a new CMR technique has been able to address this problem. T2* is a relaxation parameter assessed by CMR arising principally from local magnetic field inhomogeneities that are increased with particulate storage iron deposition. This parameter is reproducible and correlates with liver and myocardial iron stores. It can be easily imaged and quantified in the heart using gradient echo techniques (Fig. 5). There is no better method of quantification of myocardial iron content than with this new CMR technique.
Using T2* it has been shown that there is no clinically useful correlation between myocardial iron and liver iron or ferritin levels confirming that reliance on these conventional parameters as a marker of cardiac iron loading is unreliable [18, 19]. The

CMR Thalassemia protocols are available with the Cardiac Suite (standard package) on all 1.5T MAGNETOM Tim systems.

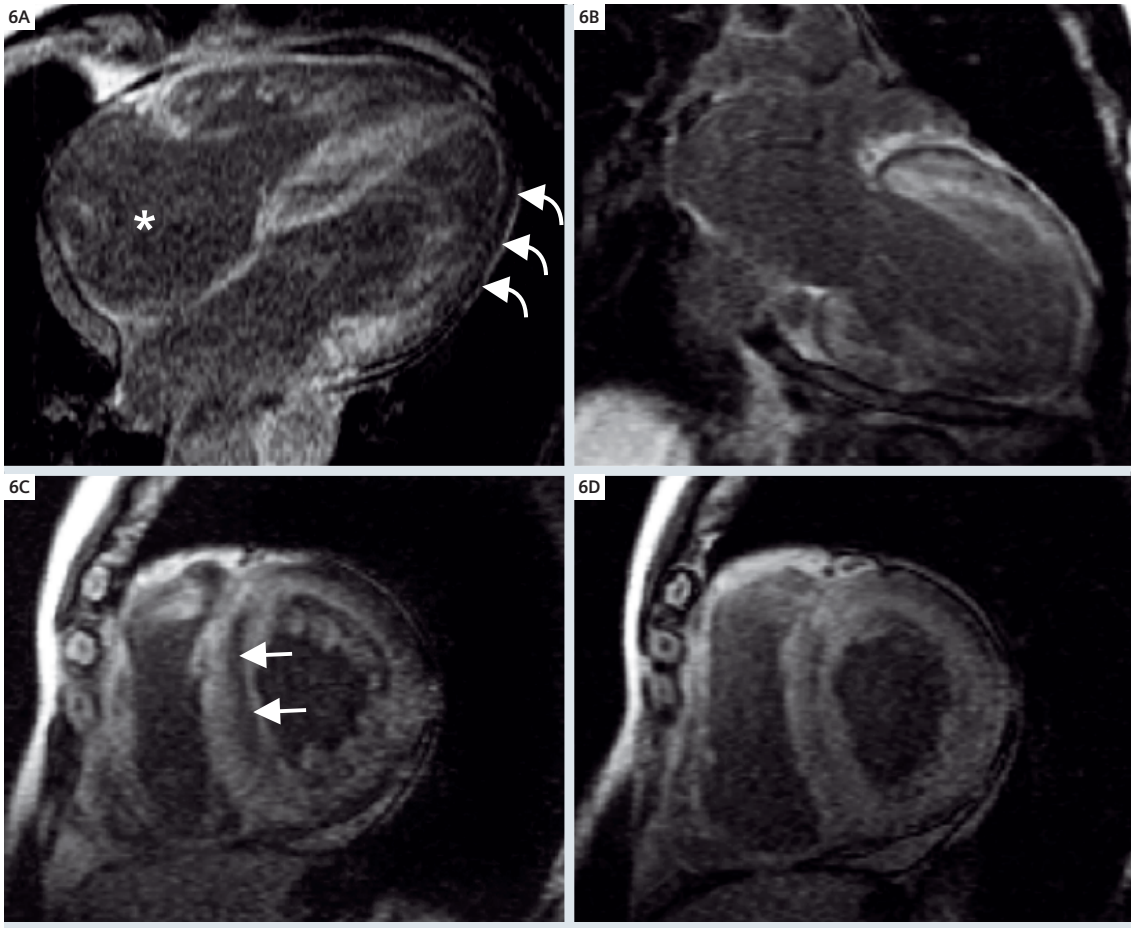

6 Late gadolinium enhancement in cardiac amyloidosis. Horizontal **(A)** and vertical **(B)** long axis and two short axis **(C, D)** planes. Typical findings are shown including low intensity blood pool marked by * (LGE usually has high signal in the blood pool), and general enhancement favoring the subendocardium – the short curly white arrows show epicardial sparing. Mid-wall "sparing" is seen in the septum (zebra pattern – short white arrows).

The incidence of development of heart failure in those with a T2* < 6 ms is very high, whereas it is uncommon in patients with a T2* > 10 ms.

degree of myocardial iron is directly correlated with the severity of LV dysfunction. In a cross-sectional study, 89% of thalassemia patients with new onset cardiac failure had a T2* less than 10 ms. Therefore the threshold of <10 ms for myocardial T2* is now taken as indicating severe iron loading. Mild to moderate iron loading is indicated by a myocardial T2* of 10–20 ms, and >20 ms is normal (the median for the normal population is approximately 40 ms). In a prospective follow-up study, the incidence of development of heart failure in those with a T2* <6 ms is very high, whereas it is uncommon in patients with a T2* >10 ms. Arrhythmias however occur with a wider distribution of myocardial T2*. T2* has been also used to monitor success of chelation therapy. Improvement in both cardiac function and myocardial T2* over a one-year period was found using 24-hour continuous intravenous deferoxamine for 12 months in heart failure [20]. A cross-sectional study showed that the oral chelator deferiprone was associated with superior ejection fraction and myocardial T2* than the standard treatment of injected subcutaneous deferoxamine [21]. Recently 2 prospective randomized controlled trials have confirmed that deferiprone has superior efficacy in removing cardiac iron. The first study indicated superiority of deferiprone as monotherapy over deferoxamine in reducing cardiac iron overload and improving ejection fraction [22]. In a second trial, the authors found that combination chelation therapy (deferiprone plus deferoxamine) improved both myocardial T2* and ejection fraction in comparison with deferoxamine monotherapy [23].

Since the introduction of the T2* technique to the management of thalassemia patients, with particular emphasis on intensification or alteration of chelation therapies, UK mortality rates in this condition have reduced by 80% [24]. This pattern has also been documented in Italy [15], and Cyprus [25]. This is a substantial health improvement for beta-thalassemia patients which has world-wide importance.

Myocardial inflammation: Viral Myocarditis, Sarcoidosis, SLE

Viral myocarditis is a common cause of dilated cardiomyopathy. In Europe, Parvovirus, Herpes virus and Coxsackie virus are most often found to be the culprit. Myocardial inflammation on the basis of systemic disease often determines the overall prognosis of the patient. However, based on autopsy studies, myocardial involvement is often clinically underdiagnosed, e.g. in sarcoidosis about 50% of cases are positive at autopsy [28]. Moreover, myocarditis can be of different origin including bacterial, viral, toxic or involvement in systemic diseases [29]. Focal and diffuse tissue changes on a histological level vary depending on the agents and the time course of the disease. Cellular infiltration with and without myocyte necrosis has been described [30, 31]. The broad clinical spectrum from subclinical disease to severe heart failure and a course of the disease from complete convalescence to dilated cardiomyopathy depends on the extent of the myocardial damage and its immediate detection. Therefore an early non-invasive differentiation is warranted.

Contrast-enhanced CMR (ceCMR) has been used to detect myocardial inflammation for several years [32]. A good correlation between ceCMR and endomyocardial biopsy including a relation to severity of disease was published recently [33,34]. Nevertheless, in our experience, some patients with inflammatory myocardial reaction may be overlooked by only applying LGE imaging. Exploiting the unique tissue characterization capabilities of CMR, a multi-sequential approach was introduced, which was shown to increase the diagnostic accuracy of magnetic resonance imaging to detect myocarditis [35]. This includes

- T2-weighted fast spin echo for oedema detection,
- T1-weighted spin echo imaging before and early after contrast to delineate increased interstitial space and
- LGE imaging to visualize necrotic areas.

The combined approach differentiates between reversible and irreversible damage and allows to a certain extent to assess the acuity of inflammation.

Applying a similar approach, we were able to detect myocardial involvement in sarcoidosis even when left-ventricular function was still preserved [36]. Different CMR techniques have proven useful during follow-up including steroid therapy in sarcoidosis [37, 38]. The extent of LGE may indicate the risk of the patients, but larger prospective trials are needed to address this issue. Interestingly, there is also first evidence that in systemic lupus erythematosus quantification of T2 is helpful in characterizing myocardial involvement [39].

Currently we recommend the combination of T1 and T2-weighted sequences. The proposed approach is published and is meanwhile optimized for different types of scanners. Nevertheless, we expect further technical improvement including more robust techniques.

Since the introduction of the CMR T2* technique, mortality rates in thalassemia patients could be reduced by 80% in the UK.

There is a good correlation between ceCMR and endomyocardial biopsy including a relation to severity of myocardial inflammation.

T2-weighted imaging

For T2 we use a short TI fast spin-echo sequence with triple inversion (STIR). More recent approaches (works in progress) include T2-weighted gradient echo attempting to overcome some of the drawbacks of the spin-echo approach: Insufficient blood suppression in areas of slow flow and posterolateral signal loss due to mistriggering, but they have not been proven in that setting yet.

Used parameters are as follows: TR = 2RR, TE 65 ms, TI 140 ms, slice thickness 15 mm, gap 5 mm, FoV 340–380 mm, matrix 256 x 256. Global instead of regional myocardial signal is measured. Skeletal muscle is used as a reference structure to minimize heart rate effects.

TSE T1 & T2, 2D IR/PSIR sequences are provided in the Cardiac Suite (standard) on all MAGNETOM Tim systems.

Contrast-enhanced T1-weighted imaging

For contrast enhanced T1-weighted imaging we recommend differentiating an early from a late phase. The early phase encloses the first 4 minutes after contrast administration, encompasses the steady-state during the whole period (non-breath-hold sequence). Hyperemia, increased distribution volume in the intercellular space and capillary leakage result in increased contrast enhancement in this phase. Here, we recommend a continuous non-breathhold interleaved multislice T1-weighted fast spin-echo sequence.

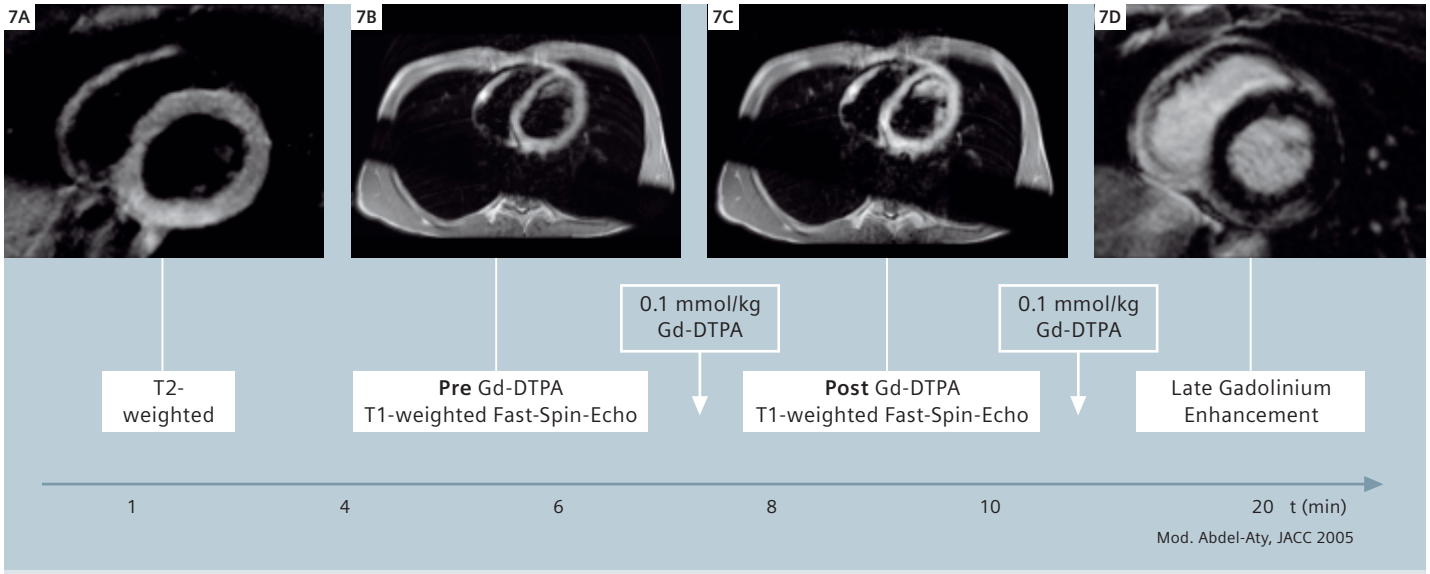

7 Myocarditis CMR Protocol. Multi-sequential approach for assessment of myocardial inflammation. After assessment of left-ventricular function, T2- and T1-weighted sequences are acquired. See text for more details.

Quantitative analysis of the T1-weighted sequences for the assessment of the „relative enhancement" takes ~5-10 minutes.

It is prone to flow artifacts, so saturation bands across the atria and the aorta might be helpful. Typical parameters:
TR 475–480 ms, TE 30 ms, matrix 256 x 256; slice thickness 6 mm, number of acquisitions 4–6.
We compare signal intensity before and after contrast and calculate a ratio of myocardial over skeletal muscle enhancement (a number we have called "relative enhancement") to control for heart rate effects. In addition to optimization for different scanners, normal values for the quantification of signal enhancement were established. The complete quantitative analysis of all sequences takes ~5–10 minutes.

LGE imaging

ACC & SCMR classified the use of CMR in inflammatory CMP as a „Class A Indication".

The third part of the protocol includes the assessment of late Gd enhancement images. The interpretation for clinical use is usually done qualitatively. In contrary to the "ischemic pattern", LGE in patients with myocarditis is usually not located at myocardial segments consistent with coronary territories and can be located subepicardially or intramyocardially. According to recent studies there is even suspicion of a predominant localization of certain viruses in particular myocardial segments. LGE may appear grayish (instead of white) in myocarditis and have a patchy or solid appearance. LGE may reduce in size over the course of myocarditis – however, it is still unknown, whether shrinkage of disseminated fibrotic areas, reduction of interstitial space (e.g. after oedema), or both cause this phenomenon (Figs. 7-9). CMR has been accepted, meanwhile, as clinically helpful in the diagnosis of myocarditis even if certain technical questions remain under discussion. Accordingly the recent conjoint report of the American College of Cardiology and the SCMR has classified its use as "appropriate" or "Class A Indication" in inflammatory cardiomyopathy [31].

Hypertrophic Cardiomyopathy (HCM)

As a screening tool, echocardiography is used but it was recently shown that localized apical and anterolateral hypertrophies are under-diagnosed when applying echo [40]. This is of potential impact for risk stratification and screening of relatives. In CMR, the detection and quantification of hypertrophy can be easily done by application of cine-images (state of the art: steady-state free precession sequences, e.g. TrueFISP). The combination with parallel imaging (iPAT) allows a fast and robust coverage of the heart. The routinely used protocol includes standard long-axis and full coverage short-axis slices (Fig. 10). The localization of obstruction can be visualized by a signal loss due to the turbulent flow, the dimension of the left ventricular outflow tract can be measured applying cine-images of the LVOT [41]. This approach is not only helpful for the differentiation

8A

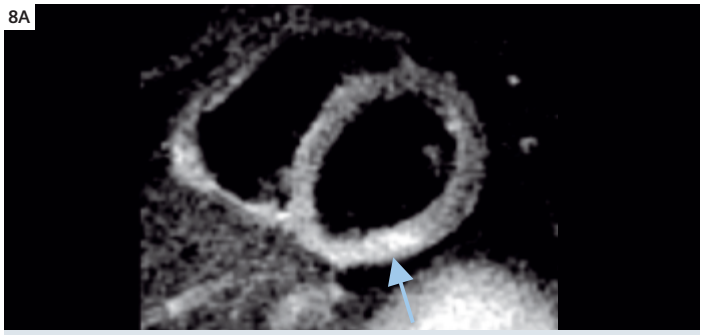

8 Myocarditis. 24-year-old male patient, admitted to our emergency unit with severe chest pain, history of respiratory infection, no known risk factors for coronary artery disease. ECG: left bundle branch block. Laboratory: Increased cardiac markers.
A) Oedema imaging: T2-weighted (T2w) images, increased global signal (ratio = 2.5), inferiorly a focal oedema can be visualized (arrow). Recovery during follow-up.

8B

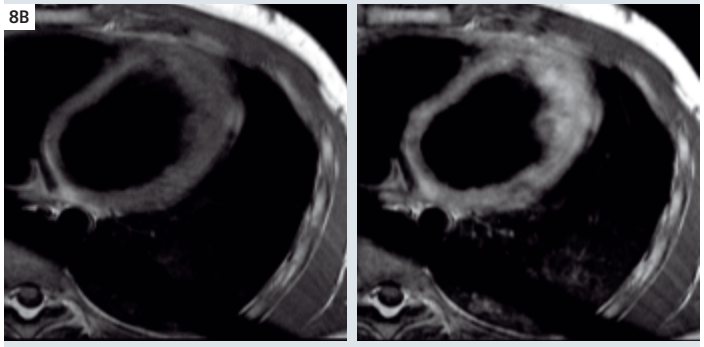

B) Early enhancement: T1w FSE before and after contrast application. Quantification of signal increase showed an increased value (ratio = 4.9) Normalization could be verified during follow-up.

8C

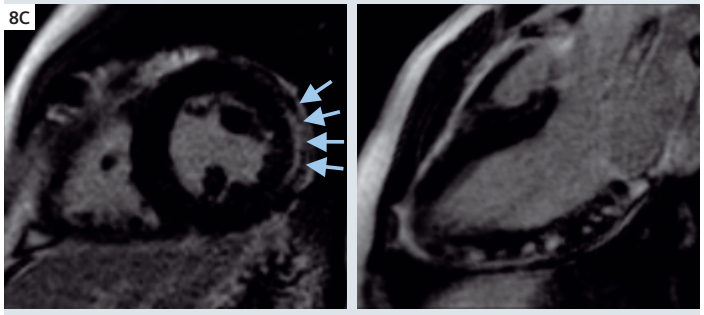

C) Late gadolinium enhancement (LGE): Typical subepicardial enhancement in the lateral wall as seen in the mid-cavity short axis orientation (left, arrows) and patchy enhancement in the inferolateral wall from base to apex as seen in the LVOT orientation (bright spots, right), indicative of fibrotic areas – persistent during follow-up. Note the saturation bands on both images, placed to prevent artefacts due to flow in atria or aorta. Diagnosis: active myocarditis.

9A

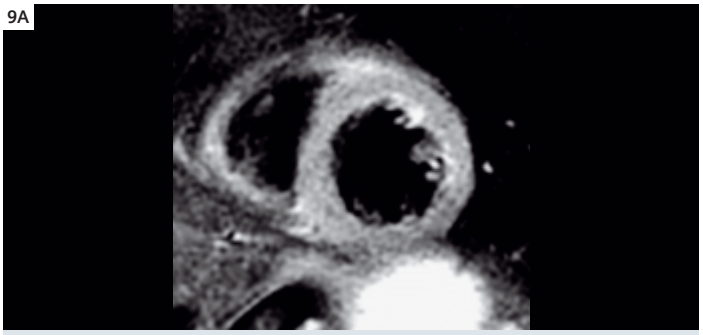

9 Myocarditis. 64-year-old female patient, admitted to the emergency room with severe chest pain, history of diarrhea. ECG: ST-Elevation in leads I, II, aVL, V5-6; T-wave inversion in lead II. Laboratory findings: CK two-fold elevated, Troponin highly elevated, leucocytes 16 Gpt/l, CRP 28 mg/dl (normal <5 mg/dl). Transthoracic echo: wall motion abnormalities in anteroseptal and anterolateral segments, LV ejection fraction 28%. Coronary angiography: exclusion of significant coronary artery disease (CAD). CMR-findings:
A) Oedema imaging: T2-weighted images, increased global signal (ratio = 2.3) – normalization during follow up.

9B

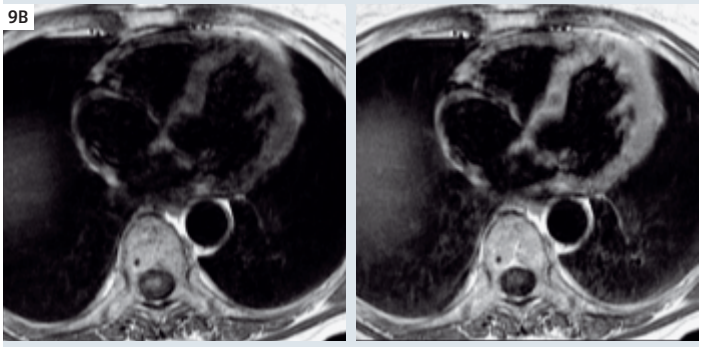

B) Early enhancement: Showing T1w FSE before and after contrast application. Quantification of signal-increase showed a significant increase (ratio = 5.6) – normalization during follow up.

9C

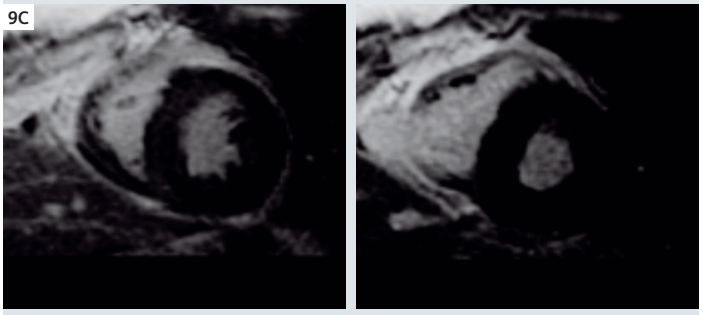

C) Late gadolinium enhancement (LGE): no evidence for LGE
Diagnosis: active myocarditis.

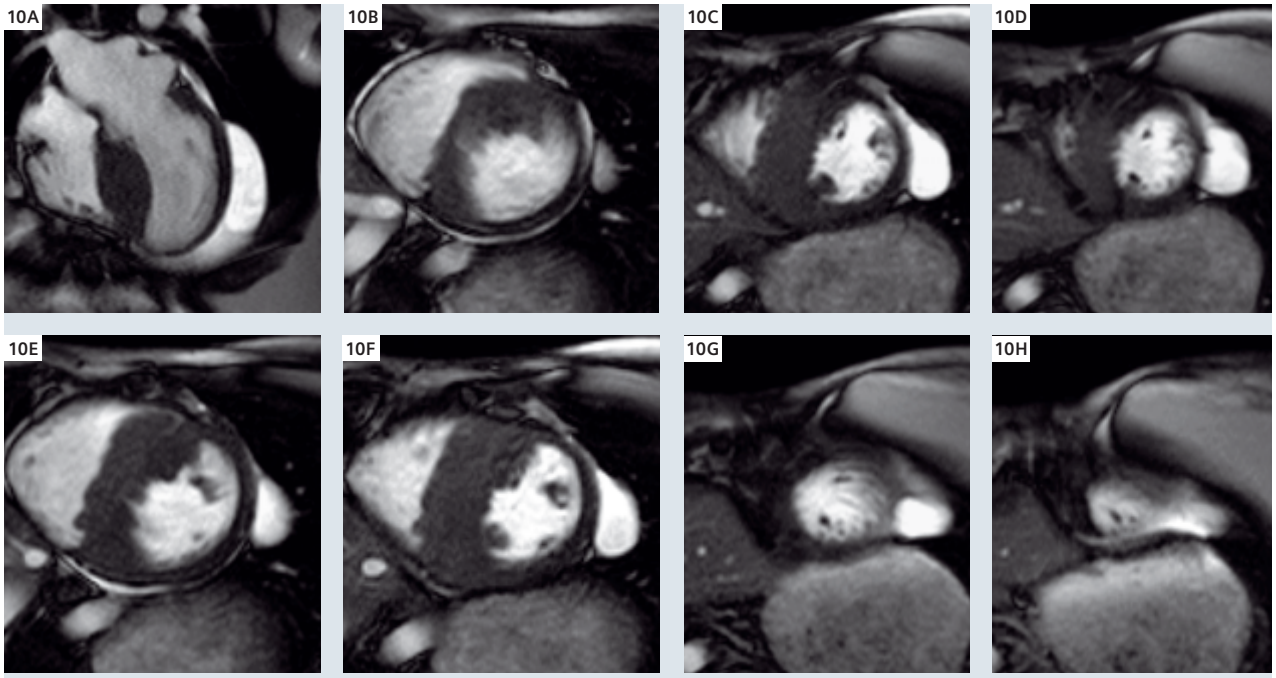

10 Hypertrophic Obstructive Cardiomyopathy. TrueFISP cine-images. Long-axis (4-chamber view) showing septal hypertrophy (A). Complete coverage of the left ventricle in short-axis orientation (B–H).

between obstructive and non-obstructive forms, but also allows us to understand the relationship between the evolution of obstruction and post-interventional tissue changes, e.g. following septal embolisation [42] (Fig. 11). The verification of new therapeutic approaches like septal ablation can be improved using ce CMR which is also useful during follow-up [43, 44].

There is initial evidence for a correlation of LGE to higher risk regarding development of heart failure and sudden cardiac death in HOCM.

We believe that the application of LGE is promising for further risk stratification in HOCM. There is initial evidence for a correlation to higher risk regarding development of heart failure and sudden cardiac death [45] (Fig. 12). LGE in HOCM usually appears as intramyocardial spots in the ventricular septum at the junction of RV and LV, and may extend as patchy areas throughout the hypertrophic myocardium. CMR is unique in simultaneously correlating the morphological abnormalities in HCM to their underlying tissue injury, thus providing a comprehensive characterization of the disease phenotype and elucidating the cause of LVH. Those data are not available by use of other non-invasive modalities free of ionizing radiation.

CMR is a reliable method for diagnosing cardiac amyloid by the presence of a typical LGE pattern, which is not seen in other LVH pathologies.

Amyloidosis

Cardiac involvement is frequent in AL amyloidosis, and is a key determinant of treatment options and prognosis. Unfortunately, cardiac involvement remains the principle cause of death in approximately half of patients with AL amyloidosis. In general, the diagnosis of cardiac amyloidosis is made by echocardiography, demonstrating left ventricular hypertrophy and variable degrees of diastolic dysfunction in the setting of a histological diagnosis of amyloidosis (usually from outside the heart). In the presence of concurrent risk factors for LVH, however, the diagnosis can be difficult to make. By contrast, CMR is a reliable method for diagnosing cardiac amyloid by the presence of a typical LGE pattern, which is not seen in other LVH pathologies, with widespread enhancement preferentially affecting the subendocardium (Fig. 6). The wash-in and wash-out kinetics of gadolinium are markedly abnormal. LGE imaging therefore typically shows a dark blood pool. Since the mid-wall is relatively spared in the ventricular septum, there may be a characteristic zebra pattern with subendocardial enhancement of the LV and RV endocardium (for optimal LGE imaging in patients with suspicion of cardiac amyloidosis, see article of Voros et al., p. 86). Other features which are characteristic of cardiac amyloidosis include a thickened inter-atrial septum and RA free wall hypertrophy. Significant-

ly, the LGE in amyloidosis is not representative of fibrosis but instead of interstitial expansion by amyloid fibrils (protein). Most recently the gadolinium kinetics has been shown to predict prognosis. This CMR technique allows for more robust diagnosis of cardiac amyloid without the need for cardiac biopsy, and may also prove useful for monitoring serial changes over time with new treatments.

Arrhythmogenic Right Ventricular Dysplasia/Cardiomyopathy

ARVD/ARVC is a genetically determined disease with the risk of malignant arrhythmias and sudden cardiac death (SCD) even in young patients. Current guidelines require a composite of clinical, functional and morphologic criteria to diagnose ARVC.

For years, CMR has been presented in the textbooks as particularly suitable for diagnosing ARVC especially through detection of right ventricular (RV) fatty infiltration. In daily practise, however, it is a lot more cumbersome.

It is indeed easier to visualize and quantify the right ventricle by applying CMR than by use of echocardiography. We prefer the axial and sagittal orientation to a classical short axis approach for better delineation of the tricuspid valve plane and the outflow tract area. Due to the thinner RV walls, reproducibility of volume and functional measurements is still lower than for the left ventricle. Slice thickness should be reduced to 5 or 6 mm as a maximum; contiguous slice acquisition is warranted [46].

The literature has suggested the use of fast spin-echo T1-weighted images with and without fat saturation technique to detect fatty infiltration in the RV wall. In the "real world", sensitivity, specificity and reproducibility of this approach have been disappointing [47]. Indeed, pathologists have described fibro-fatty infiltration instead of pure fatty infiltration. This matches the first reports describing delayed enhancement in the RV wall [48] which nevertheless await verification from other groups. Newer sequence developments allow fat suppression in LGE images which offers the opportunity to investigate the fibro-fatty infiltration and may bring us closer to the proposed criteria of ARVC.

In agreement with other groups we found the detection of global and regional wall motion abnormalities the most helpful criterion in daily practise. Micro-aneurysms and bulging are highly suggestive of ARVC. However, one has to be familiar with the typical regional RV contraction patterns (e.g. around the moderator band or RVOT) to avoid false positive reports (Fig. 13).

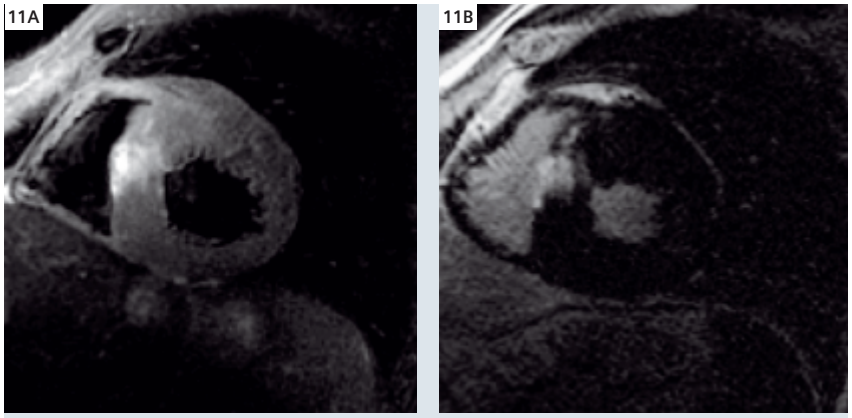

11 Hypertrophic Obstructive Cardiomyopathy. 57-year-old patient, scan was done seven days after interventional septal ablation. **Left:** Bright signal in the septal wall showing the oedema (STIR sequence). The oedema was resolved after 6 weeks. **Right:** After contrast application bright signal in the septal wall showing scar tissue (late gadolinium enhancement imaging). Lesion persists.

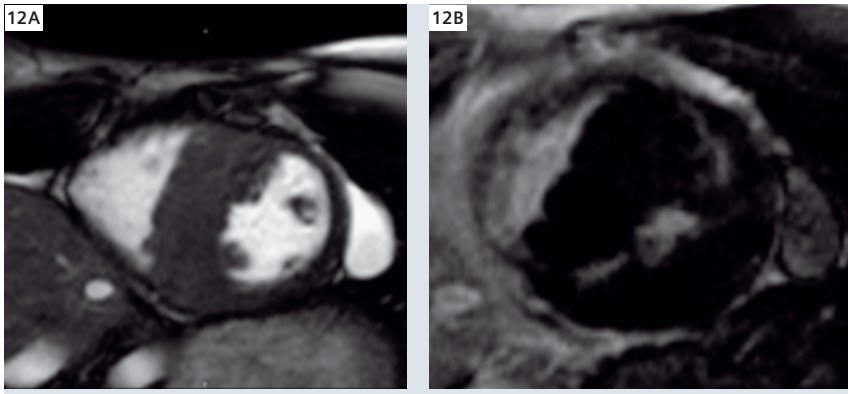

12 Fibrosis in hypertrophic cardiomyopathy. **Left:** Short-axis image showing septal hypertrophy. Right: Same short-axis view with LGE imaging: Bright signal shows fibrosis. The primary location of the enhancement at the insertion points of RV is a typical finding in HCM.

T1-weighted TSE and delayed enhancement sequences can be used to detect fibro-fatty infiltrations in ARVD.

Conclusion

CMR allows not only to differentiate ischemic from non-ischemic cardiomyopathic origins but also allows to establish the etiology within the non-ischemic category such as myocarditis, amyloidosis, thalassaemia or ARVD. CMR enables this by providing multiple different sequences that allow for visualization (and sometimes also quantification)

There is an incremental value of CMR in the risk assessment of certain cardiomyopathies (e.g. HOCM, DCM).

of tissue alterations such as iron deposition, oedema, fibrosis etc. with high diagnostic accuracy. Since recent studies showed an incremental value of CMR in the risk assessment of certain cardiomyopathies (e.g. for sudden cardiac death and VT in HOCM and DCM), CMR has been increasingly used to ensure the best treatment for the right patient at the right time.

Acknowledgement

All 2D sequences needed for cardiomyopathy evaluation are provided in the Cardiac Suite as standard on all MAGNETOM Tim systems.

The whole Cardiac MR working group of the Franz Volhard-Klinik, Charité Campus Buch is engaged in all topics discussed in the Berlin sub-chapters of this manuscript. I want to acknowledge especially the work of Anja Zagrosek and André Rudolph who provided the case examples, and also to thank Hassan Abdel-Aty for his excellent and critical review.

Contacts
Prof. Dudley Pennell, M.D.
CMR Unit
Royal Brompton Hospital
Sydney Street
London SW3 6NP, UK
d.pennell@ic.ac.uk
+44 20 7351 8802
+44 207 351 8816

Assoc. Prof. Jeanette Schulz-Menger, M.D.
Franz-Volhard-Klinik
Charité Universitätsmedizin Berlin
Helios-Klinikum Berlin
Schwanebecker Chaussee 50
13125 Berlin, Germany
jeanette.schulz-menger@charite.de
+49 30 940152903
http://www.charite-buch.de/fvkweb/CMR

References

1 Likoff MJ, Chandler SL, Kay HR. Clinical determinants of mortality in chronic congestive heart failure secondary to idiopathic dilated or to ischemic cardiomyopathy. Am J Cardiol 1987;59:634–8.
2 Bart BA, Shaw LK, McCants Jr CB, et al. Clinical determinants of mortality in patients with angiographically diagnosed ischemic or nonischemic cardiomyopathy. J Am Coll Cardiol 1997;30: 1002–8.
3 Allman KC, Shaw LJ, Hachamovitch R, et al. Myocardial viability testing and impact of revascularization on prognosis in patients with coronary artery disease and left ventricular dysfunction: a meta-analysis. J Am Coll Cardiol 2002;39:1151–8.
4 Casolo G, Minneci S, Manta R, et al. Identification of the ischaemic etiology of heart failure by cardiovascular magnetic resonance imaging: diagnostic accuracy of late gadolinium enhancement. Am Heart J 2006;151:101–108.
5 McCrohon JA, Moon JC, Prasad SK, et al. Differentiation of heart failure related to dilated cardiomyopathy and coronary artery disease using gadolinium-enhanced cardiovascular magnetic resonance. Circulation 2003;108:54–9.
6 Bello D, Shah DJ, Farah GM, et al. Gadolinium cardiovascular magnetic resonance predicts reversible myocardial dysfunction and remodeling in patients with heart failure undergoing beta-blocker therapy. Circulation 2003;108:1945–53.
7 Soriano CJ, Ridocci F, Estornell J, et al. Late gadolinium-enhanced cardiovascular magnetic resonance identifies patients with standardized definition of ischemic cardiomyopathy: a single centre experience. Int J Cardiol 2007;116:167–173.
8 Bulkley BH, Hutchins GM, Baileyy I, et al. Thallium 201 imaging and gated cardiac blood pool scans in patients with ischemic and idiopathic congestive cardiomyopathy: a clinical and pathological study. Circulation 1977;55:753–760.
9 Wagner A, Mahrholdt H, Holly TA, Elliott M.D., Regenfus M, Parker M, Klocke FJ, Bonow RO, Kim RJ, Judd RM. Contrast-enhanced MRI and routine single photon emission computed tomography (SPECT) perfusion imaging for detection of subendocardial myocardial infarcts: an imaging study. Lancet 2003; 361: 374–9.
10 Barkhausen J, Hunold P, Jochims M, et al. Imaging of myocardial perfusion with magnetic resonance. J Magn Reson Imaging 2004;19:750–7.
11 Assomull RG, Prasad SK, Lyne J, et al. Cardiovascular magnetic resonance, fibrosis, and prognosis in dilated cardiomyopathy. J Am Coll Cardiol 2006;48:1977–1985.
12 Keenan NG, Pennell DJ. CMR of ventricular function. Echocardiography 2007;24:185–193.
13 Bottini PB, Carr AA, Prisant M, et al: Magnetic resonance imaging compared to echocardiography to assess left ventricular mass in the hypertensive patient. Am J Hypertens 1995;8:221–228.
14 Olivieri NF, Nathan DG, MacMillan JH, Wayne AS, Liu PP, McGee A, Martin M, Koren G, Cohen AR. Survival in medically treated patients with homozygous beta-thalassemia. N Engl J Med. 1994;331: 574 –578.
15 Borgna-Pignatti C, Rugolotto S, De Stefano P, Zhao H, Cappellini M.D., Del Vecchio GC, Romeo MA, Forni GL, Gamberini MR, Ghilardi R, Piga A, Cnaan A. Survival and complications in
patients with thalassemia major treated with transfusion and deferoxamine. Haematologica. 2004;89:1187–1193.
16 Modell B, Khan M, Darlison M. Survival in beta thalassaemia major in the UK: data from the UK Thalassaemia Register.

Lancet. 2000; 355:2051–2052.
17 Wacker Ph.D., Balmer-Ruedin D, Oberhansli I, Wyss M. Regression of cardiac insufficiency after ambulatory intravenous deferoxamine in thalassaemia major. Chest 1993; 103: 1276–8.
18 Anderson LJ, Holden S, Davis B, et al. Cardiovascular T2-star (*) magnetic resonance for the early diagnosis of myocardial iron overload. Eur Heart J 2001;21:2171–2179.
19 Tanner MA, Galanello R, Dessi C, et al. Myocardial iron loading in patients with thalassemia major on deferoxamine chelation. J Cardiovasc Magn Reson 2006;8:543–547.
20 Anderson LJ, Westwood MA, Holden S, et al. Myocardial iron clearance during reversal of siderotic cardiomyopathy with intravenous desferrioxamine: a prospective study using T2* cardiovascular magnetic resonance. Br J Haematol 2004;127:348–355.
21 Anderson LJ, Wonke B, Prescott E, et al. Comparison of effects of oral deferiprone and subcutaneous desferrioxamine on myocardial iron concentrations and ventricular function in beta-thalassemia. Lancet 2002;360:516–520.
22 Pennell DJ, Berdoukas V, Karagiorga M, et al. Randomised controlled trial of deferiprone or deferoxamine in beta-thalassemia major in patients with asymptomatic myocardial siderosis. Blood 2006;107:3738–3744.
23 Tanner MA, Galanello R, Dessi C, et al. A randomized, placebo-controlled , double-blind trial of the effect of combined therapy with deferoxamine and deferiprone on myocardial iron in thalassemia major using cardiovascular magnetic resonance. Circulation 2007;115:1876–1884.
24 Modell B, Khan M, Darlison M, Westwood MA, Pennell DJ, David Ingram D. Falling mortality and changing causes of death in thalassaemia major: data from the UK thalassaemia register and possible contribution from T2* cardiovascular magnetic resonance. J Cardiovasc Magn Reson In review.
25 Telfer P, Coen PG, Christou S, Hadjigavriel M, Kolnakou A, Pangalou E, Pavlides N, Psiloines M, Simamonian K, Skordos G, Sitarou M, Angastiniotis M. Survival of medically treated thalassemia patients in Cyprus. Trends and risk factors over the period 1980–2004. Haematologica 2006; 91: 1187–92.
26 Falk RH, Skinner M. The systemic amyloidoses: an overview. Adv Intern Med. 2000;45:107–137.
27 Maceira AM, Joshi J, Prasad SK, et al. Cardiovascular magnetic resonance in cardiac amyloidosis. Circulation 2005;111: 186–193.
28 Iwai K, Tachibana T, Takemura T, et al. Pathological studies on sarcoidosis autopsy. I. Epidemiological features of 320 cases in Japan. Acta Pathol Jpn. Jul–Aug 1993;43(7–8):372–376.
29 Feldman AM, McNamara D. Myocarditis. N Engl J Med. Nov 9 2000;343(19):1388–1398.
30 Kawai C. From myocarditis to cardiomyopathy: mechanisms of inflammation and cell death: learning from the past for the future. Circulation. Mar 2 1999;99(8):1091–1100.
31 Magnani JW, Dec GW. Myocarditis: current trends in diagnosis and treatment. Circulation. Feb 14 2006;113(6):876–890.
32 Friedrich MG, Strohm O, Schulz-Menger J, et al. Contrast media-enhanced magnetic resonance imaging visualizes myocardial changes in the course of viral myocarditis. Circulation. May 12 1998;97(18):1802–1809.
33 Mahrholdt H, Goedecke C, Wagner A, et al. Cardiovascular magnetic resonance assessment of human myocarditis: a comparison to histology and molecular pathology. Circulation. Mar 16 2004;109(10):1250–1258.
34 Mahrholdt H, Wagner A, Deluigi CC, et al. Presentation, patterns of myocardial damage, and clinical course of viral myocarditis. Circulation. Oct 10 2006;114(15):1581–1590.
35 Abdel-Aty H, Boye P, Zagrosek A, et al. Diagnostic performance of cardiovascular magnetic resonance in patients with suspected acute myocarditis: comparison of different approaches. J Am Coll Cardiol. Jun 7 2005;45(11): 1815–1822.
36 Schulz-Menger J, Wassmuth R, Abdel-Aty H, et al. Patterns of myocardial inflammation and scarring in sarcoidosis as assessed by cardiovascular magnetic resonance. Heart. Mar 2006;92(3):399–400.
37 Smedema JP, Snoep G, van Kroonenburgh MP, et al. Cardiac involvement in patients with pulmonary sarcoidosis assessed at two university medical centers in the Netherlands. Chest. Jul 2005;128(1):30–35.
38 Vignaux O, Dhote R, Duboc D, et al. Detection of myocardial involvement in patients with sarcoidosis applying T2-weighted, contrast-enhanced, and cine magnetic resonance imaging: initial results of a prospective study. J Comput Assist Tomogr. Sep-Oct 2002;26(5):762–767.
39 Singh JA, Woodard PK, Davila-Roman VG, et al. Cardiac magnetic resonance imaging abnormalities in systemic lupus erythematosus: a preliminary report. Lupus. 2005;14(2):137–144.
40 Rickers C, Wilke NM, Jerosch-Herold M, et al. Utility of cardiac magnetic resonance imaging in the diagnosis of hypertrophic cardiomyopathy. Circulation. Aug 9 2005;112(6):855–861.
41 Schulz-Menger J, Abdel-Aty H, Busjahn A, et al. Left ventricular outflow tract planimetry by cardiovascular magnetic resonance differentiates obstructive from non-obstructive hypertrophic cardiomyopathy. J Cardiovasc Magn Reson. 2006;8(5):741–746.
42 Schulz-Menger J, Gross M, Messroghli D, et al. Cardiovascular magnetic resonance of acute myocardial infarction at a very early stage. J Am Coll Cardiol. Aug 6 2003;42(3):513–518.
43 van Dockum WG, ten Cate FJ, ten Berg JM, et al. Myocardial infarction after percutaneous transluminal septal myocardial ablation in hypertrophic obstructive cardiomyopathy: evaluation by contrast-enhanced magnetic resonance imaging. J Am Coll Cardiol. Jan 7 2004;43(1):27–34.
44 van Dockum WG, Beek AM, ten Cate FJ, et al. Early onset and progression of left ventricular remodeling after alcohol septal ablation in hypertrophic obstructive cardiomyopathy. Circulation. May 17 2005;111(19):2503–2508.
45 Moon JC, McKenna WJ, McCrohon JA, et al. Toward clinical risk assessment in hypertrophic cardiomyopathy with gadolinium cardiovascular magnetic resonance. J Am Coll Cardiol. May 7 2003;41(9):1561–1567.
46 Tandri H, Friedrich MG, Calkins H, et al. MRI of arrhythmogenic right ventricular cardiomyopathy/dysplasia. J Cardiovasc Magn Reson. 2004;6(2):557–563.
47 Bluemke DA, Krupinski EA, Ovitt T, et al. MR Imaging of arrhythmogenic right ventricular cardiomyopathy: morphologic findings and interobserver reliability. Cardiology. 2003;99(3):153–162.
48 Tandri H, Saranathan M, Rodriguez ER, et al. Noninvasive detection of myocardial fibrosis in arrhythmogenic right ventricular cardiomyopathy using delayed-enhancement magnetic resonance imaging. J Am Coll Cardiol. Jan 4 2005;45(1):98–103.

Myocardial Stress Perfusion Imaging using CMR

Andrew E. Arai, M.D.

National Heart, Lung and Blood Institute, National Institutes of Health, Bethesda, M.D., USA

Clinical role

Stress testing is one of the most powerful diagnostic approaches to detecting coronary artery disease.

Adult cardiology and medicine focuses tremendous emphasis on the evaluation of patients with known or suspected coronary artery disease since this is one of the leading causes of death in industrialized nations. There are three major clinical presentations of coronary artery disease: chest pain syndromes, acute coronary syndromes (including acute myocardial infarction) and sudden death. Since relatively few patients suffering from coronary artery disease can be resuscitated from sudden death, most efforts are aimed at detecting coronary artery disease at earlier stages of the disease and at preventing permanent myocardial damage. Stress testing is one of the most powerful diagnostic approaches to detecting coronary artery disease. In general terms, it is necessary to understand why it is necessary to perform stress testing to detect physiologically significant coronary artery disease when using technologies that do not directly image the coronary arteries.

Coronary interventions should primarily be performed when there is clinical evidence of myocardial ischemia associated with the coronary stenosis.

Coronary artery disease causes symptoms of chest discomfort in two major presentations: acute coronary syndromes or in chronic stable angina. In acute coronary syndromes, a thrombus developed on an unstable coronary plaque resulting in intermittent or complete obstruction of a coronary artery. In the most extreme cases this will cause an ST elevation myocardial infarction. In patients with unstable angina, no permanent myocardial damage may have occurred and further testing with either coronary angiography or stress testing may be needed to determine whether coronary disease could explain the symptoms or needs intervention.

Outside of the setting of acute myocardial infarction or the most severe rest perfusion defects associated with hibernating myocardium, perfusion of the heart is generally normal at rest. Even in the presence of a severe coronary stenosis, autoregulation of the heart's blood vessels maintains normal perfusion to the heart muscle. Thus, at rest, a patient can feel normal and have no chest pain. Likewise, images of rest perfusion can look quite normal and uniform in the heart. A stress test uncovers the coronary stenosis by challenging the adequacy of the heart's ability to regulate blood flow. As the patient exercises or vasodilator medicines are administered, blood flow increases in the heart muscle served by a normal coronary artery. However, blood flow cannot increase as much downstream from a significantly stenosed coronary artery. Thus, high levels of exercise may induce chest pain and ST segment abnormalities. During a stress perfusion study, a relative defect in blood flow to some regions of the heart may be imaged by nuclear methods (SPECT) or by CMR. Alternatively, imaging can be performed during stress to detect a new or worsening wall motion abnormality. Such testing can performed by echocardiography (during exercise or dobutamine) or by CMR (during dobutamine).

Stress imaging tests are generally indicated when a patient has an equivocal stress ECG or uninterpretable ECG due, for example, to baseline ST segment abnormalities. Pharmacological stress testing is generally required in patients that cannot adequately exercise. For an exercise stress test to be diagnostic, peak heart rate must be at least 85% maximal predicted for age. Such high heart rates can be difficult to attain if a patient has problems such as arthritis.

Directly imaging the coronary arteries is an alternative approach to detecting coronary artery disease. However, the consensus of medical experts indicates that coronary interventions should primarily be performed in clinical situations where

Table 1: Non-CMR stress tests used for the detection of coronary artery disease

	# of patients	Sensitivity	Specificity
Exercise ECG	2456	52	71
Exercise SPECT	4480	87	73
Stress Echocardiography	2637	85	77

Adapted from Fleischmann et al. and Klocke et al. [1, 2]

Among stress tests, exercise ECG has the lowest sensitivity and specificity for detecting coronary artery disease.

Table 2: Sensitivity and specificity of stress perfusion CMR for detecting coronary artery disease

Reference	N	Stress	Sensitivity (%)	Specificity (%)
Klem *et al. [3]*	92	adenosine	89	87
Ingkanisorn *et al. [4]*	135	adenosine	100	93
Okuda *et al. [5]*	33	dipyridamole	84	87
Sakuma *et al. [6]*	40	dipyridamole	81	68
Plein *et al. [7]*	92	adenosine	88	82
Takase *et al. [8]*	102	dipyridamole	93	85
Paetsch *et al. [9]*	49	adenosine	79	75
Paetsch *et al. [10]*	79	adenosine	91	62
Wolff *et al. [11]*	99	adenosine	93	75
Thiele *et al. [12]*	32	adenosine	75 80	97 91
Plein *et al. [13]*	72	adenosine	88	83
Bunce *et al. [14]*	35	adenosine	74	71
Nagel *et al. [15]*	84	adenosine	88	90
Ishida *et al. [16]*	104	dipyridamole	84	82
Doyle *et al. [17]*	184	dipyridamole	57 52	78 82
Kinoshita *et al. [18]*	27	dipyridamole	55 77	77 81
Ibrahim *et al. [19]*	25	adenosine	69	89
Schwitter *et al. [20]*	48	dipyridamole	87 91	85 94
Panting *et al. [21]*	26	adenosine	79, 72, 60 77	83, 83, 43 83
Al-Saadi *et al. [22]*	34	dipyridamole	90	83
Totals	**1392**		**~83%**	**~80%**

Taking all studies into account, the sensitivity and specificity of stress perfusion CMR is around 83% and 80% respectively.

there is clinical evidence of myocardial ischemia associated with the coronary stenosis. Thus, even in patients with known intermediate stenosis of a coronary artery, there is frequently a need for stress testing to define whether the stenosis is physiologically significant in that individual. Now that non-invasive coronary CT angiography has progressed to a point where it can detect high-

Table 3: Image acquisition parameters for different perfusion pulse sequences

Method	SR-SSFP	SR-FLASH	SR-GRE-EPI (research WIP)
TE (ms)	1.1	1.3	1.1 (TE1)
TR (ms)	2.3	2.2	6.1
BW (Hz/pixel)	1400	780	1630
Echotrain length	1	1	4
Readout Flip Angle	50	12	25
Matrix	128 × 80	128 × 80	128 × 80
Parallel Imaging Factor	R = 2	R = 2	R = 2
TD (ms) (to 1st line)	39	41	54
TI (ms) (to center)	85	85	85
Tslice (ms) (total)	132	130	117
Slices per RR @ 60/90/120 bpm	7/5/3	7/5/3	8/5/4

grade coronary artery stenosis in asymptomatic patients, there will be increasing need to define the physiological significance of these abnormalities. There is also a need to define the physiological significance of possible stenosis associated with highly calcified coronary arteries or in smaller coronary stents that cannot be adequately resolved with current generation CT scanners.

Cardiac risk factors are widely used clinically to help guide preventive treatments and to delay the onset of clinically overt coronary artery disease. The common risk factors for coronary disease include age, male gender, family history of premature coronary disease, diabetes, hypertension, hyperlipidemia, smoking, obesity, and physical inactivity. In addition, coronary calcium as detected and quantified by a CT scan has independent and additive risk as well as prognostic significance. Of the coronary risk factors identified, diabetes, hypertension, hyperlipidemia, smoking, obesity, and activity can all be modified through medical or individual intervention.

The diagnostic accuracy of stress perfusion CMR is comparable to the other stress imaging modalities.

However, risk factors have a relatively weak short-term predictive value for coronary artery disease. For example, the Framingham risk score is commonly used to assess the likelihood that a patient has coronary artery disease but reports risk in probability of disease occurring over a 10-year period. For example, a non-smoking 55-year-old male patient with a cholesterol of 240 mg/dL, an HDL of 40 mg/dL, hypertension with a systolic blood pressure of 130 mmHg has a 10% risk of developing coronary artery disease over the next 10 years. That level of risk warrants intervention if the LDL cholesterol is high enough (130 mg/dL) per the ATP III guidelines [National Cholesterol Education Program, National Heart, Lung, and Blood Institute, National Institutes of Health, NIH Publication No. 01-3670, May 2001] but remains a low enough risk for direct detection of asymptomatic disease to be controversial.

In summary, stress testing and risk factor analysis or preventive cardiology perform complementary approaches to detecting and managing patients with coronary artery disease. At the current time, the primary role of stress testing is in detection of coronary disease or physiological assessment of coronary disease. Risk factor analysis focuses on optimizing management of medically modifiable risk factors either in the prevention of disease or in more aggressive management of patients with known disease.

Diagnostic accuracy

There are many forms of stress tests and significant differences in the sensitivity, specificity, and accuracy of these tests. Table 1 summarizes the sensitivity and specificity of non-CMR stress tests used for the detection of coronary artery disease. Table 2 presents similar statistics for stress perfusion CMR. The diagnostic accuracy of stress perfusion CMR is clearly comparable to the other stress imaging modalities and all stress imaging modalities have clinically significant increased sensitivity relative to stress ECG.

Sequences and protocols

To perform first pass perfusion imaging, a series of T1 weighted images must be obtained every heartbeat or every other heart beat while a bolus of contrast passes through the heart and myocardium. As with many aspects of diagnostic testing, choices need to be made with regard to balance between anatomic coverage, spatial resolution within each imaging plane, temporal resolution, and image quality. We generally image 3 slices of the heart in a short axis orientation to assess at least 16 segments of the heart. In general, this allows acquiring all three slices every cardiac cycle. However, this choice was made since our group has focused much effort on developing fully quantitative analysis methods. It would be equally reasonable to image a total of 6 slices every other heartbeat to improve the anatomic coverage of the heart. Three main sequences have been used to acquire stress perfusion images: TurboFLASH (GRE), TrueFISP (SSFP), and hybrid echoplanar methods (GRE-EPI or hybrid EPI). Of these, TurboFLASH and TrueFISP are available as product level software and the hybrid echoplanar method is under evaluation as a research "work-in-progress." The main advantages of TurboFLASH are its simplicity and the minimal image artifacts. The main consideration for using the TrueFISP sequence is the higher signal-to-noise ratio and improved contrast-to-noise ratio. Either sequence produces high quality perfusion images. Examples of stress perfusion defects obtained with TurboFLASH, TrueFISP, and the hybrid echoplanar methods are shown in figures 1–4.

SR TrueFISP (SSFP) and SR TurboFLASH (GRE) sequences are available for CMR myocardial perfusion imaging.

Table 3 summarizes recommended starting parameters for first pass perfusion studies. These are parameter sets that we have studied at the National Institutes of Health. Many groups push for higher spatial resolution but one must recognize that the time used to acquire more lines of k-space will lengthen the duration of the readout during the cardiac cycle opening the possibility of artifacts due to motion and will reduce the number of images per heartbeat (slices per RR). We have tried to aim for short imaging time during the cardiac cycle to minimize dark rim artifacts at the endocardial-blood interface. Parallel imaging factors (iPAT factors) are quite effective at im-

Up to 8 slices can be acquired in one or more orientations during the CMR first-pass perfusion imaging.

1 Inferior perfusion defect during stress using the SR TurboFLASH perfusion sequence.

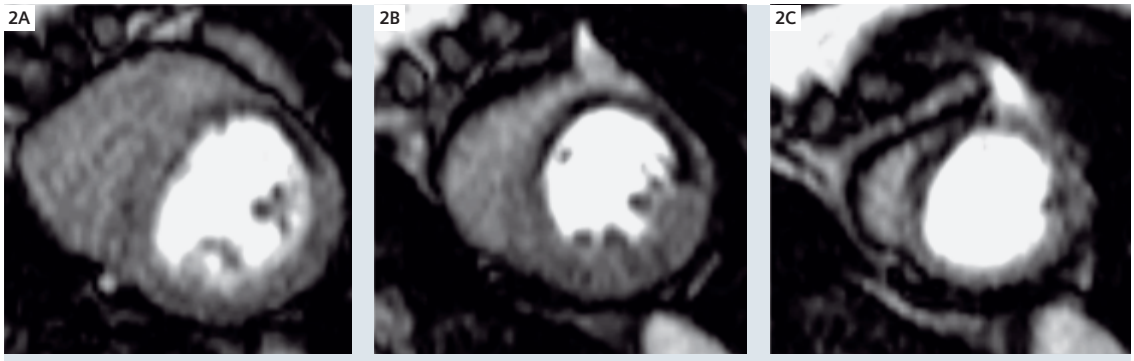

2 Example of stress perfusion defect using SR TrueFISP.

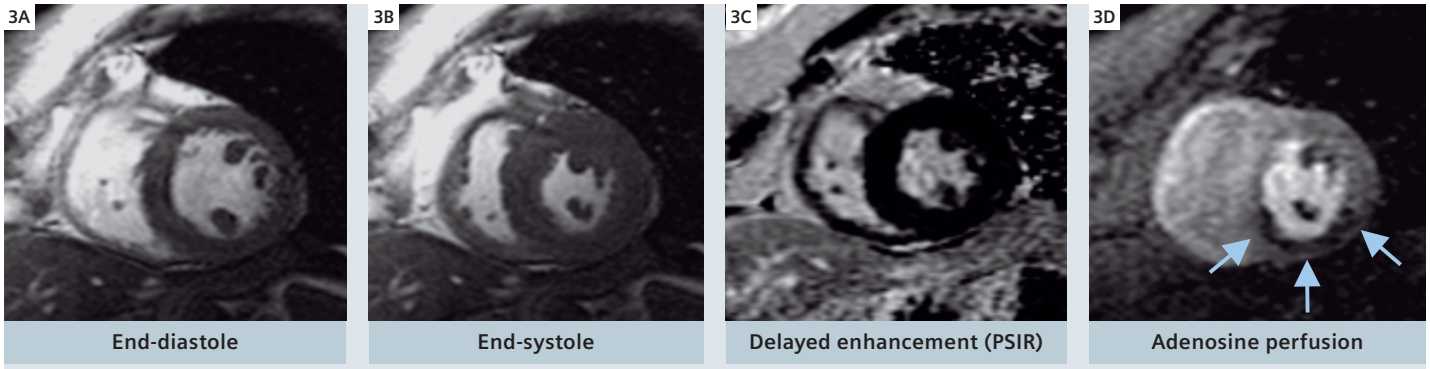

3 Patient with stress induced perfusion defects but no myocardial scar.

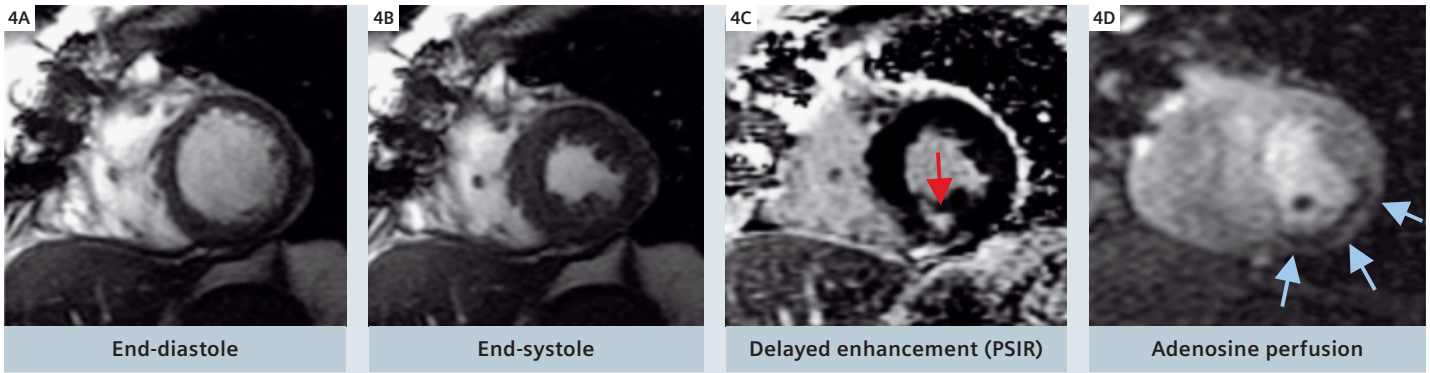

4 Patient with prior bypass surgery, small inferior myocardial infarction, larger wall motion abnormality and perfusion defect. Findings consistent with stunned myocardium and inducible ischemia. PSIR is used as a fast technique for Delayed Enhancement MRI.

proving temporal resolution and well worth the tradeoff in signal-to-noise ratio. In our general experience, artifacts are a much larger issue than signal-to-noise ratio for perfusion images.

Typical protocol for CMR stress perfusion imaging

Figure 5 shows the typical timing of a stress perfusion protocol. After localizer images, the vasodilator stress agent is started. In the case of adenosine, we recommend mixing enough adenosine to provide a 6 minute infusion at 140 micrograms/kg/min. By 3 minutes into the infusion, adequate vasodilation should be achieved to allow performing the stress perfusion imaging. Once the stress perfusion images are acquired, the adenosine infusion can be stopped. When using dipyridamole, we recommend a net dose of 0.56 mg/kg infused over 4 minutes. Peak vasodilation with dipyridamole may not be achieved until several minutes after completing the infusion. We usually do the stress perfusion imaging 4 minutes after finishing the dipyridamole unless severe symptoms require us to image earlier. Aminophylline 100 mg IV is sometimes needed to reverse the effects of dipyridamole symptoms due to the significantly longer half-time. When carrying out a rest perfusion study after the stress perfusion, it is generally a good idea to reverse the dipyridamole since it may have lingering effects that alter the rest perfusion.

Due to the very short half-life time (< 30 s), adenosine is mostly used as a vasodilator for stress tests.

After stabilizing the patient following the stress test, cine CMR can be performed to assess anatomy, ejection fraction, and regional wall motion. Some centers acquire rest cine images prior to the injection of adenosine and additionally during adenosine stress. A rest perfusion study is then performed using identical parameters to the stress test to facilitate comparisons. Finally, delayed enhancement imaging of myocardial infarction can be performed. If additional imaging is required one could do velocity encoded phase contrast before or after the rest perfusion study. Turbo spin echo (black blood imaging) should be completed prior to the stress perfusion imaging to avoid poor blood suppression related to having contrast in the circulation. A contrast-enhanced MRA could

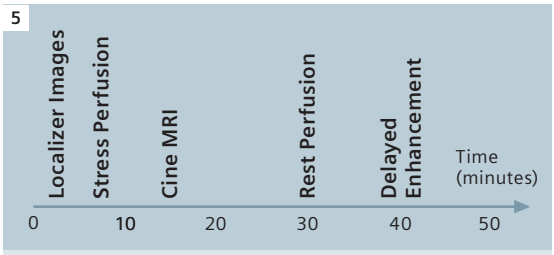

5 Timing of a stress perfusion CMR exam

be performed in place of the rest perfusion study if desired. Coronary MRA can generally be performed at any point along the time line since most of the sequences are not too severely affected by the presence of contrast. As regards the dosage of contrast, several factors have to be considered in the main decision. In general, for a given set of parameters, the signal. -noise ratio will be better for higher doses of contrast but the linearity between gadolinium concentration and signal intensity may become an issue. The dual bolus and dual sequence methods were introduced by researchers attempting to benefit from higher doses of contrast for the myocardium but to preserve the linearity in the blood pool necessary to quantify perfusion [23, 24]. If one is not performing quantitative analysis, it is reasonable to use a dose of gadolinium contrast of 0.5 mmol/kg.

Pitfalls with CMR first-pass perfusion imaging

The pitfall in CMR first pass perfusion imaging is making a reasonable balance between sensitivity and specificity when interpreting images. There is no substitute for experience that includes correlation with invasive coronary angiography. Even as a center with experience in over 1000 stress perfusion cases, we found it extremely helpful to go back to correlation with cardiac catheterization when we switched imaging methods to the True-FISP perfusion sequence. You learn the most from cases with an unequivocal normal angiogram and also from true defects in patients with a significant stenosis in the absence of a myocardial infarction. When we project a perfusion study to a group of physicians, it is inevitable that one or more physicians will have a question about a gray rim near the endocardial border on one or more slices of a perfusion scan. There are many tricks that can be used to help determine the likelihood that these defects may or may not be real perfusion defects:

- Perfusion defects tend to follow the typical perfusion territories of the coronary artery.
- Perfusion defects tend to affect distal segments first depending on how distal or proximal the location of the stenosis is.
  - Exception: Patients with coronary artery bypass surgery.
  - Exception: Branch vessel disease such as diagonal or septal perforators.
- True perfusion defects tend to last several heartbeats beyond the initial rapid upslope of myocardial enhancement. Susceptibility artifacts tend to be worst during peak concentration of gadolinium during the intracavity RV and LV phases of enhancement and tend to disappear rapidly.
  - Corollary: If a dark rim disappears by the time most segments have reached about 90% maximal enhancement, then the rim is probably an artifact.
- Perfusion defects tend to be subendocardial except in the most severe cases. This allows using differences between endocardial and epicardial enhancement as another way to control for issues like surface-coil intensity drop off. It also makes it possible to detect balanced ischemia associated with multi-vessel disease.
- True perfusion defects usually have significantly lower enhancement than normal segments. If in doubt, place a small region of interest on the questionable dark rim artifact and a region of normal heart (close proximity to avoid surface coil intensity issues). Many of the things people list as possible defects are within 3–4% of the signal intensity of neighboring myocardium. A 15 or 20% difference in signal intensity is more likely to be a real defect.
- Use all information available to you when interpreting images. The delayed enhancement is a very specific tool for diagnosing coronary artery disease (see figure 6). The group at Duke University tested a simple interpretation algorithm that they find helps improve the specificity of reading perfusion scans [3]. Essentially, if the patient has a myocardial infarction on delayed enhancement imaging, it is very likely he has significant coronary disease. If an apparent perfusion defect is seen at rest and at stress in the absence of an MI on delayed enhancement imaging, it must be an artifact (only in the absence of wall motion abnormalities!). A defect

A typical stress MRI exam consists of function, perfusion and delayed enhancement imaging.

Low doses of Gadolinium are used for quantitative perfusion analysis, in order to preserve linearity between gadolinium concentration and signal intensity.

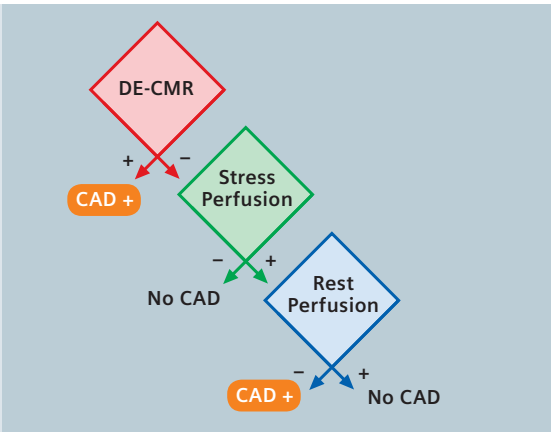

6 Duke method for using delayed enhancement and rest perfusion to improve the accuracy of interpreting stress perfusion images (Adapted from Klem et al.).

seen at stress but not at rest is most likely to represent a true defect.

- An unequivocal regional wall motion abnormality on cine CMR can also be very informative. However, do not put too much weight on marginal variations in wall motion.
- Also look for artifacts associated with sternal wires, vascular clips, and coronary stents. These findings increase the pretest likelihood of disease considerably.
- Time-intensity curves can also help distinguish true defects from false positive defects. It is not uncommon that one or more segments of the heart appears delayed by 1–2 heartbeats relative to the other segments. This can create a region of the heart being 25% or more darker than all other segments and appear like a severe perfusion defect. Time-intensity curves show such a region enhances at a similar rate to the other segments but is simply delayed in time relative to the other segments.

CMR and echo stress tests have comparable exam times, however, CMR comes with significantly more diagnostic information about ischemia and viability.

Advantages and benefits of CMR stress perfusion imaging

The main advantages of CMR stress perfusion imaging relate to the completeness and quality of the information obtained during this single examination. Figure 4 shows the utility of a CMR stress perfusion exam in a patient with known coronary artery disease. Thus, the clinical question is not a simple binary presence or absence of coronary disease. This patient had prior bypass surgery and a prior myocardial infarction. She presented with chest pain that occurred at rest but remained troponin negative throughout her hospitalization. The clinically relevant question is whether there is myocardial ischemia beyond the infarct. Following the principles listed in the section on "pitfalls," there are many pieces of useful information. Starting with the delayed enhancement image, there is a small inferior myocardial infarction (red arrow). Interestingly, the wall motion abnormality is more extensive than the small infarct and includes the inferolateral segment. The cine CMR also shows the sternal wire artifacts in the chest wall. Finally, the stress perfusion defect is also more extensive than the infarct. This study thus shows a patient with known coronary disease with evidence of stunned myocardium (viable myocardium with a wall motion abnormality in the setting of recent clinical suspicion of ischemia) and a stress induced perfusion defect consistent with inducible ischemia.

Compared to SPECT, CMR offers an at least 10 times higher volumetric image resolution.

There are also advantages of stress CMR in terms of diagnostic workflow. A high-quality exam can be accomplished within 45–60 minutes covering cine CMR, stress perfusion, rest perfusion, and delayed enhancement images. This exam allows assessment of ejection fraction, regional wall motion, the valves, evidence of inducible perfusion defects, and the extent of myocardial infarction. The fact that these imaging methods can be displayed side-by-side in the same imaging planes facilitates interpretation, particularly for subtle abnormalities. Thus, stress CMR studies can be performed with an efficiency that is significantly higher than most nuclear methods. The time of exams is comparable to echocardiographic stress tests but with significantly more diagnostic information about ischemia and viability. Thus, as a complete package, the rest-stress CMR study provides more information than either echocardiography or SPECT.

The image resolution of CMR perfusion studies is also unique and a distinct advantage. Compared with SPECT, the image resolution is at least 10 times higher on a volumetric basis. Considering the normal left ventricular wall is only about 10 mm thick, SPECT operates at an acquisition resolution incapable of resolving epicardial from endocardial perfusion. Typical resolution CMR perfusion scans operate at an acquisition resolution smaller than ~3 mm and thus routinely resolve endocardial from epicardial perfusion abnormalities. The greatest advantage of this comes in detecting multivessel disease, left main disease, or microvascular disease [16, 25]. Recent papers have documented that stress perfusion imaging has prog-

nostic value. In a series of patients studied after presenting to the emergency department, adenosine stress CMR had excellent sensitivity and specificity for diagnosing coronary artery disease [4]. A negative adenosine stress CMR study had excellent prognosis. In another study, the prognosis of positive or negative stress tests was nearly identical if the stress agent was adenosine or dobutamine [26]. Last but not least, when compared to SPECT imaging, instead of 4-20 mSv, no ionizing radiation is needed to perform a CMR stress exam.

Conclusions

In a center with the equipment and expertise to perform stress CMR, vasodilator stress tests are a very powerful tool for diagnosing and managing ischemic heart disease. The stress perfusion information is an important step beyond viability imaging since the presence or absence of inducible perfusion defects can alter the management of a patient. The combined evaluation of function, perfusion, and viability provides the information needed for managing complicated patients with coronary artery disease.

References

1 Fleischmann, K.E., et al., Exercise echocardiography or exercise SPECT imaging? A meta-analysis of diagnostic test performance. J Nucl Cardiol, 2002. 9(1): p. 133–4.
2 Klocke, F.J., et al., ACC/AHA/ASNC guidelines for the clinical use of cardiac radionuclide imaging-executive summary: a report of the American College of Cardiology/American Heart Association Task Force on Practice Guidelines (ACC/AHA/ASNC Committee to Revise the 1995 Guidelines for the Clinical Use of Cardiac Radionuclide Imaging). Circulation, 2003. 108(11): p. 1404–18.
3 Klem, I., et al., Improved detection of coronary artery disease by stress perfusion cardiovascular magnetic resonance with the use of delayed enhancement infarction imaging. J Am Coll Cardiol, 2006. 47(8): p. 1630–8.
4 Ingkanisorn, W.P., et al., Prognosis of negative adenosine stress magnetic resonance in patients presenting to an emergency department with chest pain. J Am Coll Cardiol, 2006. 47(7): p. 1427–32.
5 Okuda, S., et al., Evaluation of ischemic heart disease on a 1.5 Tesla scanner: combined first-pass perfusion and viability study. Radiat Med, 2005. 23(4): p. 230–5.
6 Sakuma, H., et al., Diagnostic accuracy of stress first-pass contrast-enhanced myocardial perfusion MRI compared with stress myocardial perfusion scintigraphy. AJR Am J Roentgenol, 2005. 185(1): p. 95–102.
7 Plein, S., et al., Coronary artery disease: myocardial perfusion MR imaging with sensitivity encoding versus conventional angiography. Radiology, 2005. 235(2): p. 423–30.
8 Takase, B., et al., Whole-heart dipyridamole stress first-pass myocardial perfusion MRI for the detection of coronary artery disease. Jpn Heart J, 2004. 45(3): p. 475–86.
9 Paetsch, I., et al., Myocardial perfusion imaging using OMNISCAN: a dose finding study for visual assessment of stress-induced regional perfusion abnormalities. J Cardiovasc Magn Reson, 2004. 6(4): p. 803–9.
10 Paetsch, I., et al., Comparison of dobutamine stress magnetic resonance, adenosine stress magnetic resonance, and adenosine stress magnetic resonance perfusion. Circulation, 2004. 110(7): p. 835–42.
11 Wolff, S.D., et al., Myocardial first-pass perfusion magnetic resonance imaging: a multicenter dose-ranging study. Circulation, 2004. 110(6): p. 732–7.
12 Thiele, H., et al., Color-encoded semiautomatic analysis of multi-slice first-pass magnetic resonance perfusion: comparison to tetrofosmin single photon emission computed tomography perfusion and X-ray angiography. Int J Cardiovasc Imaging, 2004. 20(5): p. 371–84; discussion 385–7.
13 Plein, S., et al., Assessment of non-ST-segment elevation acute coronary syndromes with cardiac magnetic resonance imaging. J Am Coll Cardiol, 2004. 44(11): p. 2173–81.
14 Bunce, N.H., et al., Combined coronary and perfusion cardiovascular magnetic resonance for the assessment of coronary artery stenosis. J Cardiovasc Magn Reson, 2004. 6(2): p. 527–39.
15 Nagel, E., et al., Magnetic resonance perfusion measurements for the noninvasive detection of coronary artery disease. Circulation, 2003. 108(4): p. 432–437.
16 Ishida, N., et al., Noninfarcted myocardium: correlation between dynamic first-pass contrast-enhanced myocardial MR imaging and quantitative coronary angiography. Radiology, 2003. 229(1): p. 209–16.
17 Doyle, M., et al., The impact of myocardial flow reserve on the detection of coronary artery disease by perfusion imaging methods: an NHLBI WISE study. J Cardiovasc Magn Reson, 2003. 5(3): p. 475–85.
18 Kinoshita, M., et al., Myocardial perfusion magnetic resonance imaging for diagnosing coronary arterial stenosis. Jpn Heart J, 2003. 44(3): p. 323–34.
19 Ibrahim, T., et al., Assessment of coronary flow reserve: comparison between contrast-enhanced magnetic resonance imaging and positron emission tomography. J Am Coll Cardiol, 2002. 39(5): p. 864–70.
20 Schwitter, J., et al., Assessment of myocardial perfusion in coronary artery disease by magnetic resonance: a comparison with positron emission tomography and coronary angiography. Circulation, 2001. 103(18): p. 2230–2235.
21 Panting, J.R., et al., Echo-planar magnetic resonance myocardial perfusion imaging: parametric map analysis and comparison with thallium SPECT. J Magn Reson Imaging, 2001. 13(2): p. 192–200.
22 Al-Saadi, N., et al., Noninvasive detection of myocardial ischemia from perfusion reserve based on cardiovascular magnetic resonance. Circulation, 2000. 101(12): p. 1379–83.
23 Christian, T.F., et al., Absolute myocardial perfusion in canines measured by using dual-bolus first-pass MR imaging. Radiology, 2004. 232(3): p. 677–84.
24 Gatehouse, P.D., et al., Accurate assessment of the arterial input function during high-dose myocardial perfusion cardiovascular magnetic resonance. J Magn Reson Imaging, 2004. 20(1): p. 39–45.
25 Panting, J.R., et al., Abnormal subendocardial perfusion in cardiac syndrome X detected by cardiovascular magnetic resonance imaging. N Engl J Med, 2002. 346(25): p. 1948–53.
26 Jahnke, C., et al., Prognostic value of cardiac magnetic resonance stress tests: adenosine stress perfusion and dobutamine stress wall motion imaging. Circulation, 2007. 115(13): p. 1769–76.

Contact
Andrew E. Arai, MD
Senior Investigator
National Heart,
Lung and Blood Institute
National Institutes
of Health
Bethesda, MD, 20892
USA

High-Dose Dobutamine Stress Cardiac MR Imaging for Detection of Myocardial Ischemia

Markus Jochims M.D.; Oliver Bruder M.D.; Christoph Jensen M.D.; Georg V. Sabin M.D.
Department of Cardiology and Angiology, Elisabeth Hospital Essen, Germany

Introduction

Stress induced impairment of regional left ventricular function is a reliable indicator of transient myocardial ischemia [1, 13]. Therefore, the analysis of wall motion abnormalities by echocardiography in conjunction with a variety of different stress modalities has grown to a clinically established non-invasive test for the assessment of myocardial ischemia [2]. However, optimal echocardiographic image acquisition depends on the skill of the operator and the presence of an adequate acoustic window. Approximately 15% of patients admitted to stress-echo yield suboptimal or non-diagnostic images [3, 4, 5, 6]. Formerly these patients were referred to myocardial scintigraphy performed in single-photon emission computed tomography (SPECT) technique. High-dose dobutamine stress cardiac magnetic resonance imaging (CMR) emerged as an alternative high-resolution and noninvasive method for the detection of stress induced myocardial ischemia, which does not expose the patient to radiation and provides a diagnostic accuracy for the detection and localization of functional significant coronary artery disease (CAD) comparable to stress echocardiography and SPECT technique [6, 16]. Various studies have shown that CMR permits acquisition of images with high-spatial and improved temporal resolution in any tomographic plane [7] and allows accurate determination of left ventricular function in terms of wall motion and wall thickening at rest and during pharmacological stress [8, 9]. High dose dobutamine stress testing can be safely performed with a standard dobutamine/atropine stress protocol similar to stress echocardiography studies and proved to be a clinically feasible tool for the assessment of hemodynamically significant coronary artery stenoses [6, 10, 11, 12, 14, 22, 23, 26].

The diagnostic accuracy of dobutamine stress MRI is comparable to stress echocardiography and SPECT.

Dobutamine stress cardiac MR imaging

Due to its high spatial resolution and good tissue contrast, CMR has been shown to be the most accurate imaging modality for determination of wall thickening and volume measurements [13, 14, 15]. Recent technical developments, providing stronger gradient systems with new ultrafast sequences and fast data reconstruction procedures providing "near real-time" imaging facilitate clinically feasible cardiac MRI stress testing. Cine CMR with retrospective ECG-gating displays myocardial contractility of the entire cardiac cycle and permits evaluation of global and regional function [17].

MR sequence

The image quality of gradient echo techniques, which offer a shorter acquisition time as spin-echo sequences, depends on flow effects and may decrease depending on impaired regional or global ventricular function. Steady-state free precession sequences (e.g. TrueFISP) provide much higher signal intensity and signal-to-noise ratio (SNR) [18]. They enable rapid data acquisition and a high contrast between blood and myocardium without flow artifacts. Because of the distinguished delineation of anatomic structures steady-state free precession sequences are ideally suited for evalua-

TrueFISP cine sequences provide rapid image acquisition and high contrast between blood pool and myocardium.

tion of wall motion and wall thickening. Parallel imaging techniques reduce imaging time even more, but there is a partial loss of SNR depending on the accelerating factor. Currently, steady state free precession sequences in combination with parallel image acquisition and retrospective gating are state of the art. New real-time imaging sequences with improved spatial and temporal resolution will lead to further improvement in cardiac MR imaging especially during stress testing [17].

Image acquisition

Primary rapid multi-slice localizing images are acquired to define the cardiac axes. By means of single-angulated tomograms intersecting the mitral valve and the cardiac apex on a transverse view double-angulated long-axis tomograms that also intersect the mitral valve plane and the apex are planned. Based upon these images contiguous true short-axis cine scans are acquired to cover the whole left ventricle. In addition, three long-axis tomograms – two chamber view, four chamber view and three chamber view – are acquired according to the equatorial short axis orientation. Scanning by breath-holding in end-expiration reduces breathing artifacts. True short-axis and long-axis cine images are obtained at each stress level.

iPAT (integrated Parallel Acquisition Techniques) allow fast acquisition of cine images in multiple orientations.

Standard high-dose dobutamine protocol

As a primarily beta1-adrenergic catecholamine with positive inotropic and positive chronotropic effect, dobutamine increases the myocardial oxygen consumption. Coronary arteries with severe stenosis do not allow adequate increase of blood flow to compensate elevated myocardial oxygen consumption under stress conditions. Myocardial ischemia leads to impairment of regional myocardial function, depressed systolic contractility and loss of systolic wall thickening. ECG changes and clinical symptoms manifest later and inconsistently in the "cascade of ischemia" [13].

For stress testing dobutamine is infused intravenously during 3-minute stages at doses of 10, 20, 30 and 40 µg per kilogram of body weight per minute under continuously monitoring of heart rhythm, blood pressure and symptoms. If the submaximal stress level described by a target heart rate of ((220-age) × 0.85) is not reached, additional fractionated atropine doses of 0.25 mg every 60 seconds up to a maximal dose of 1.0 mg are administered intravenously. The same true short-axis and long-axis cine images are obtained at each stress level as acquired at rest (Figure 1). Immediately after acquisition images are displayed

Dobutamine stress MRI is performed using the same incremental dobutamine protocol as known from stress echocardiography.

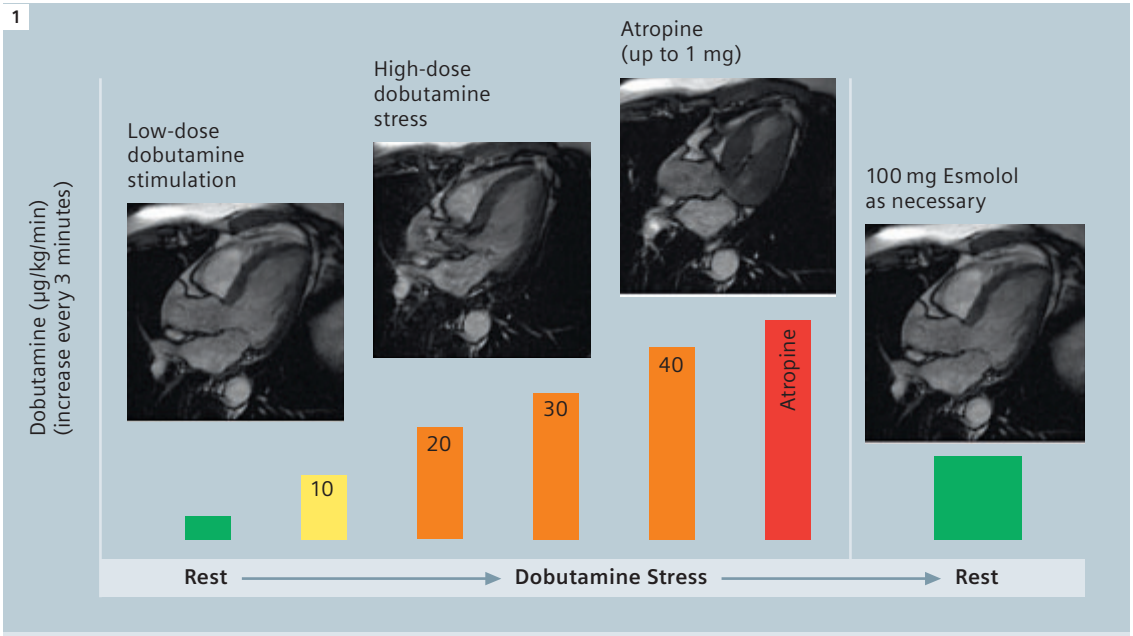

1 Schematic illustration of a dobutamine stress CMR examination consisting of cine imaging at rest, dobutamine stress and rest imaging.

Table 1: Contraindications to dobutamine stress MRI

Unstable angina pectoris
Left main coronary artery disease
Higher-grade aortic stenosis
Hemodynamically relevant obstructive hypertrophic cardiomyopathy
Myocarditis, endocarditis, pericarditis
Aortic dissection / higher-grade aortic aneurysm
Higher-grade complex ventricular arrhythmia
History of sudden death
Mobile left ventricular / left atrial thrombus
Severe systemic hypertension (systolic blood pressure > 240 mmHg and/or diastolic blood pressure > 120 mmHg)
Intractable anxiety / claustrophobia
Contraindications to atropine
Advanced heart block
Glaucoma
Pyloric stenosis
Prostatic hypertrophy

Table 2: Side effects during dobutamine / atropine stress:

Mild complications (10–50%): Anxiety, nausea and vomiting, palpitations, heat sensations, tachypnoea, angina pectoris, hypertension, hypotension, premature ventricular beats, atrial and ventricular arrhythmia, atrial fibrillation, transient atrioventricular blocks
Severe complications (0.1– 0.3%): Sustained ventricular tachycardia, ventricular fibrillation and myocardial infarction

Table 3: Termination criteria for dobutamine stress MRI

Target heart rate reached ((220 – age) × 0.85)
New or worsening wall-motion / thickening abnormalities
Complex cardiac arrhythmias
Systolic blood pressure increase > 240 mmHg and/or diastolic blood pressure > 120 mmHg
Blood pressure decrease > 20 mmHg below baseline systolic blood pressure and/or decrease > 40 mmHg from a previous level
Severe chest pain or other intractable symptoms

for observation of new wall motion abnormalities. If clinically relevant symptoms of arrhythmia or angina occurs or if the age predicted target heart rate or a systolic blood pressure over 240 mmHg or a diastolic blood pressure over 120 mmHg is reached, the dose of dobutamine must not increased further. An advantage of dobutamine is its rapid onset of action and short half-life of about 120 seconds allowing for gradual drug titration. After stress termination, dobutamine side effects can be reversed by administration of a beta-blocker. To increase the sensitivity of the test, it is recommended to stop beta-blocker treatment 24–48 h prior to the examination [20].
Contraindications to dobutamine stress CMR, side effects, and termination criteria are listed in Tables 1, 2 and 3, respectively.
Due to the risk of severe side effects of stress testing, patients have to be closely monitored for their safety. Resuscitation equipment and trained personnel must be available.

Diagnostic criteria and image analysis

For standardized assessment and documentation of CMR the use of the 17-segment model of the American Heart Association is recommended [21]. It is generally accepted and enables comparability to other imaging modalities. The left ventricle will be divided into a

- basal,
- mid-cavity and
- apical short axis section.

With regard to the circumferential location, the basal and mid-cavity slices are further subdivided into six segments of 60° each, named

- anterior,
- anteroseptal,
- inferoseptal,
- inferior,
- inferolateral,
- anterolateral

and numbered anticlockwise from 1 (basal anterior) to 6 (basal anterolateral) respectively from 7 (mid anterior) to 12 (mid anterolateral). The apical slice is subdivided into four segments, named

- anterior,
- septal,
- inferior and
- lateral

and numbered anticlockwise from 13 (apical ante-

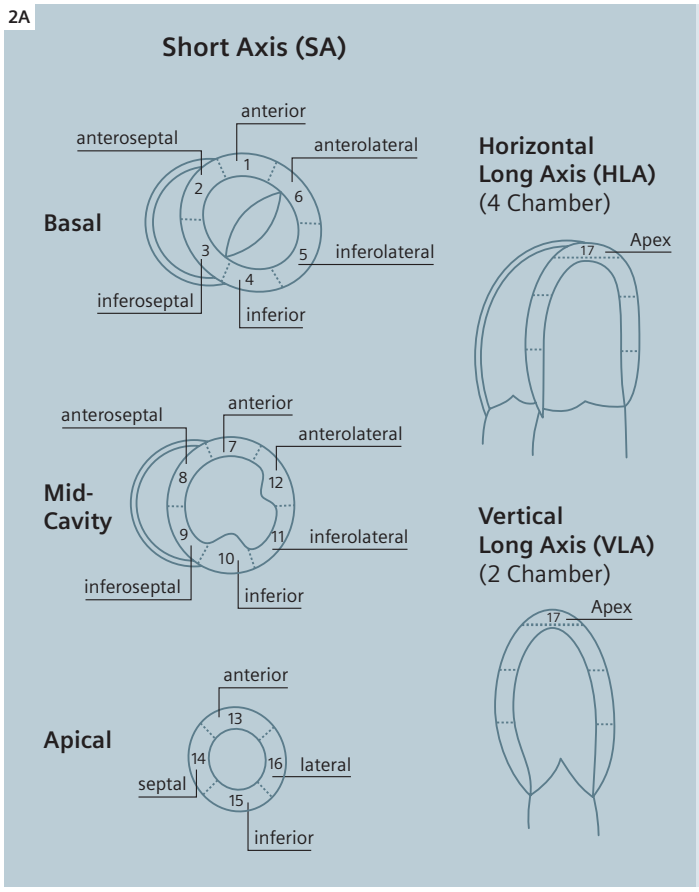

2 Recommendation of the American Heart Association for standardized myocardial segmentation and nomenclature in cardiac imaging. (Adapted from Cerqueira et al. [21])

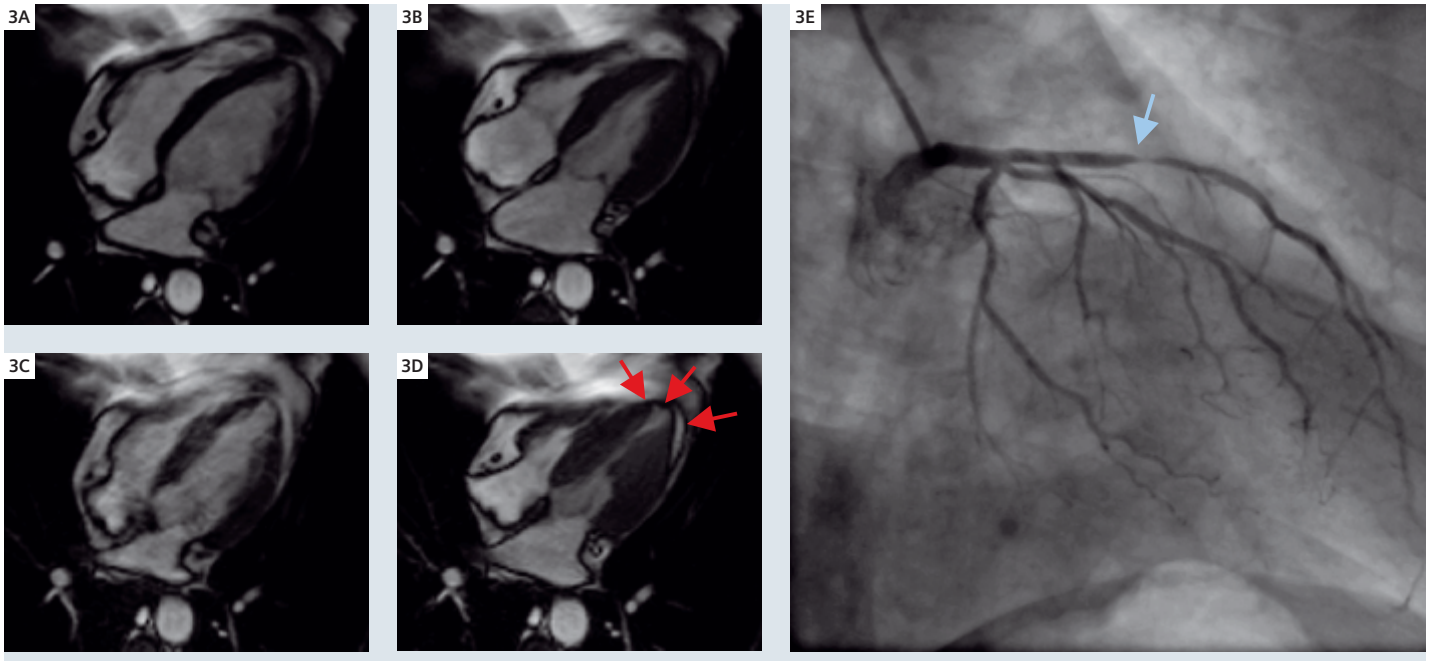

3 **(A–D):** CMR images at rest (top) and at peak dobutamine stress (bottom) showing LV end-diastolic (l.), and end-systolic (r.) frames from a four-chamber view in a patient with normal contraction at rest and with inducible ischemia clearly visible as hypokinesia apical (red arrows). **(E):** Corresponding angiogram of the left coronary artery showing a high-grade LAD stenosis (blue arrow) in the same patient.

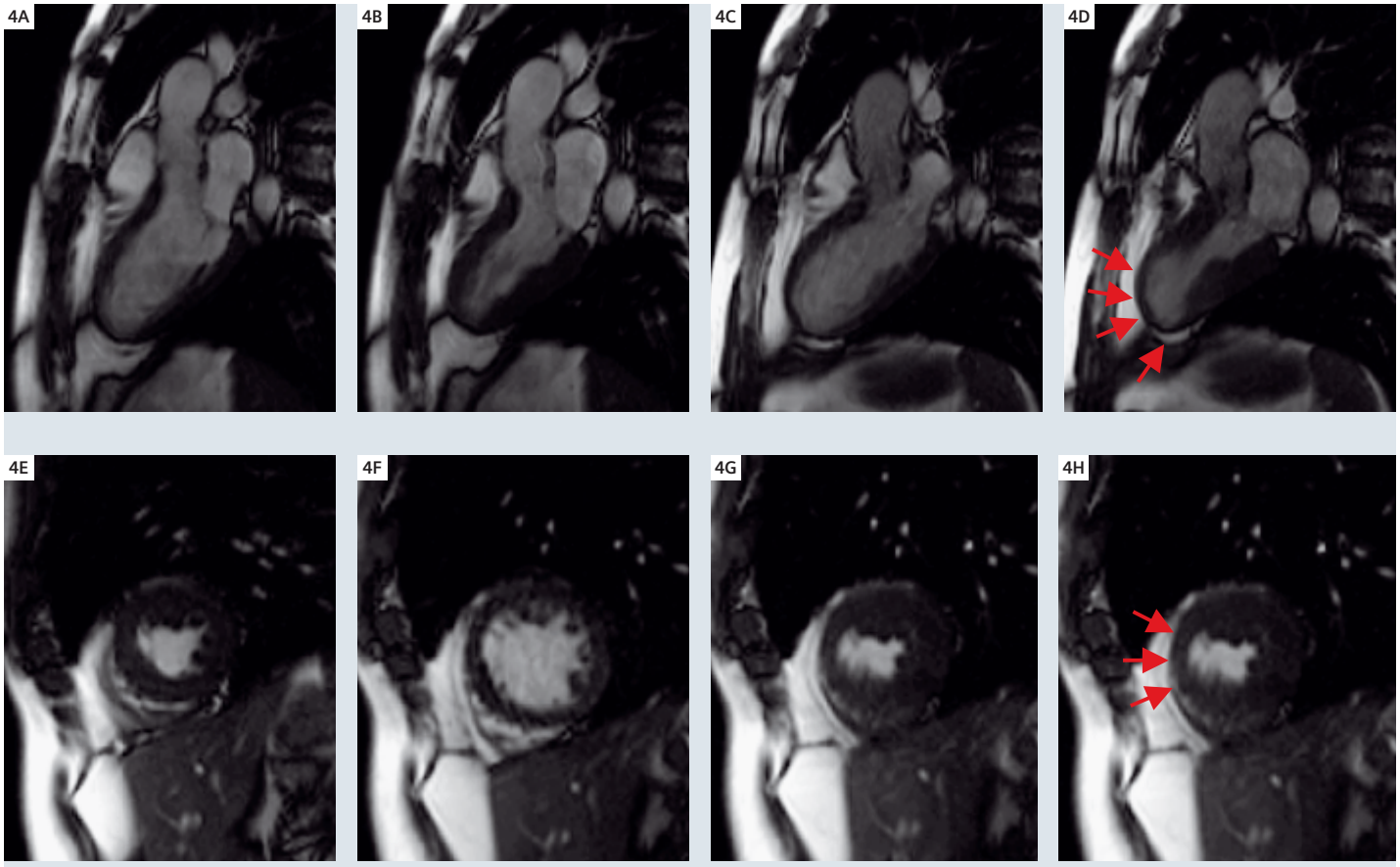

4 (A–D): End-diastolic and end-systolic frames from an apical long-axis view of the left ventricle (three chamber view) and **(E–H)**: midventricular shortaxis view at rest (left) and at peak dobutamine stress (right) in a patient with inducible ischemia. Red arrows mark the region from anteroseptal midventricular to the apex that shows an impaired contractile response with pronounced wall motion abnormality and reduced thickening.

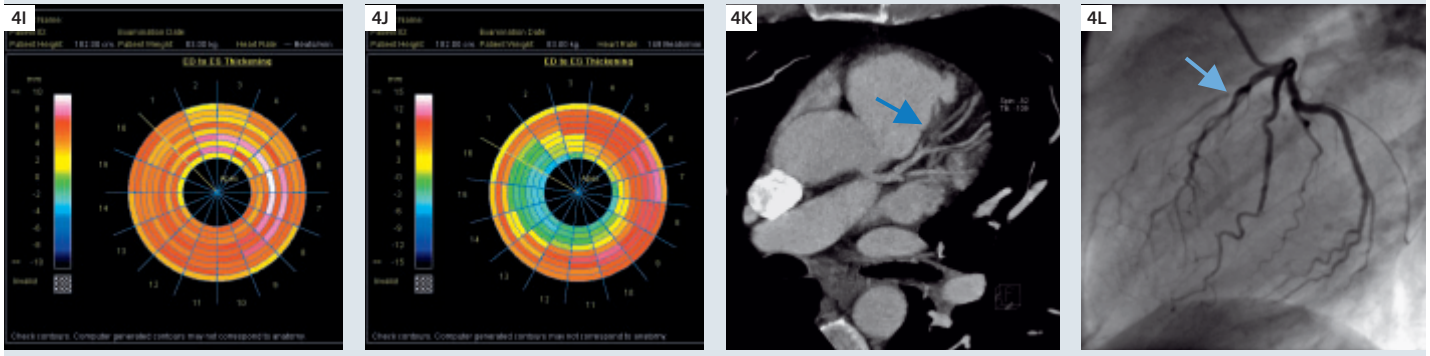

4 (I–J): Bulls eye plots of enddiastolic to endsystolic thickening at rest (left) and at peak dobutamine stress (right) in the same patient.

4 (K–L): Dual source computed tomography (DSCT) coronary angiography (left) and conventionally coronary angiography (right) reveal a subtotal stenosis of the LAD (blue arrows).

rior) to 16 (apical lateral). The apical cap represents the muscle at the tip of the ventricle and is defined as segment 17, called the apex (Figure 2). During high-dose dobutamine stress CMR all 17 left ventricular segments should be analyzed. Therefore, the acquisition of not less than three short-axis slices (basal, mid-cavity, apical) and at least one additional long-axis plane (two- , four- or three-chamber view) is recommended for evaluation of the apical region. At all stress levels an assessment of regional myocardial contractility is performed, including rest and post-stress phase. A **normal** wall motion response at dobutamine stress CMR is defined as development of hyperkinetic wall motion or preservation of the resting contraction pattern during dobutamine infusion. A pathologic response is characterized by transient wall motion abnormalities in at least one segment that was graded normal at rest (Figure 3). Segmental wall motion is graded **hypokinetic**, if endocardial inward movement and systolic wall thickening appeared decreased but not absent. A segment is graded **akinetic** if it shows lack of inward endocardial motion and absence of systolic wall thickening. A segment is graded **dyskinetic** if it demonstrated paradoxical systolic outward movement of the endocardial border or systolic wall thinning [2].

The location of segments with normal and pathologic wall motion are compared to the perfusion territory of the main epicardial coronary arteries which are defined by the AHA recommendations [21]. Wall motion abnormalities in anterior, anteroseptal, and septal segments are usually attributed to the left anterior descending artery (LAD), those in inferior and inferoseptal segments to the right coronary artery (RCA), and those in lateral segments to the circumflex artery (RCX). A coronary artery is considered as significantly stenosed if at least one of the segments located in its territory was abnormal at dobutamine stress CMR (Figure 4). If no segment was abnormal, the corresponding coronary artery is graded to have no relevant stenosis.

A coronary artery is considered as significantly stenosed if at least one of the segments located in its territory was abnormal at dobutamine stress CMR.

Discussion

High-dose dobutamine stress CMR is currently an established method for the assessment of stress inducible regional left ventricular wall motion abnormalities due to its high diagnostic accuracy, feasibility and versatility (Table 4).

Table 4: Dobutamine stress MRI for detection of significant CAD compared with conventional coronary angiography.

Author	Year	Sensitivity	Specificity	Number of patients
Pennell et al.	1992	91%	–	25
van Rugge et al.	1993	81%	100%	45
Baer et al.	1994	84%	–	35
van Rugge et al.	1994	91%	80%	39
Nagel et al.	1999	86%	86%	172
Hundley et al.	1999	83%	83%	41
Kuijpers et al.	2003	96%	95%	68
Paetsch et al.	2004	89%	80%	79
Wahl et al.	2004	89%	84%	160
Syed et al.	2005	89%	100%	19

Dobutamine stress MRI is a reliable, clinically safe and robust method to evaluate the functional significance of coronary lesions with high diagnostic accuracy.

Previous studies have demonstrated the clinical feasibility of CMR in conjunction with pharmacological stress testing for the detecting of relevant CAD [6, 10, 12, 14]. Pennell et al. [10] reported the first use of dobutamine stress in conjunction with CMR in 25 patients with chest pain by using an intermediate dose of dobutamine (up to 20 µg/kg/min). He found a 91% incidence of dobutamine–induced reversible wall motion abnormalities in patients with CAD.

Baer et al. [11] and van Rugge et al. [12] have shown that dobutamine MRI detects overall CAD with a sensitivity of 85% and 91%, respectively by using moderate doses of dobutamine up to 20 µg/kg/min.

Nagel et al. provided the first report on the efficacy and safety of high-dose dobutamine (up to 40 µg/kg/min and additional use of atropine as needed) combined with CMR for the detection of CAD in a larger patient population. In this study dobutamine stress CMR proved to be superior to dobutamine stress echocardiography in terms of sensitivity (86% vs. 74%) and specificity (86% vs. 70%) in 172 patients. The superior results of CMR were attributed to its better overall image quality, which was graded good or very good in 82%, but only in 51% of echocardiography studies [6].

Hundley et al. performed high-dose dobutamine CMR for the detection of ischemia in 41 patients who were not well suited for second harmonic stress echocardiography because of poor acoustic windows and reported a sensitivity and specificity of 83% for the detection of a coronary stenosis > 50% luminal diameter [22].

Wahl et al. performed high-dose dobutamine-atropine stress CMR after coronary revascularization in 160 consecutive patients with pre-existing wall motion abnormalities at rest. CMR displayed good results, with sensitivity of 89% and specificity of 84% for detection of significant CAD [23].

Using TrueFISP or SSFP cine sequences Paetsch et al. found high-dose dobutamine stress CMR to be superior to adenosine stress perfusion MR for detection of significant CAD, with sensitivities and specificities of 89% and 80% and 91% and 62%, respectively in 79 patients without history of prior infarction [26].

Syed et al. had shown a high interstudy reproducibility ($p = 0.91$) and a low interobserver variability (kappa = 0.81) of dobutamine stress MRI in 19 patients with severe coronary disease [27].

The overall sensitivity and specificity for the assessment of ischemia induced wall motion abnormalities for detecting CAD achieved with dobutamine stress CMR is in good agreement with stress echocardiography studies yielding sensitivities of 78% to 96% and specificities of 66% to 85% [28–32].

Conclusion

Dobutamine stress CMR using a state of the art fast imaging sequence is a reliable and clinically safe and robust method to evaluate the functional significance of coronary lesions by detecting ischemic induced wall motion abnormalities.

Contact
Markus Jochims, M.D.
Department of Cardiology and Angiology
Elisabeth Hospital
Klara-Kopp-Weg 1
45138 Essen
Germany
m.jochims@elisabeth-essen.de

References and recommended reading

1 Sugishita J, et al. Dissociation between regional myocardial dysfunction and ECG changes during myocardial ischemia induced by exercise in patients with angina pectoris. Am Heart J 1883;106:1–8.
2 Geleijnse ML ,et al. Methodology, feasibility, safety and diagnostic accuracy of dobutamine stress echocardiography. J Am Coll Cardiol 1997;30(3):595–606.
3 La Canna G, et al. Echocardiography during infusion of dobutamine for identification of reversibly dysfunction in patients with chronic coronary artery disease. J Am Coll Cardiol 1994;23:617–26.
4 Hoffmann R, et al. Analysis of interinstitutional observer agreement in interpretation of dobutamine stress echocardiograms. J Am Coll Cardiol 1996;27:330–6.
5 Zoghbi AW, Barasch E. Dobutamine MRI: A serious contender in pharmacological stress imaging? Circulation 1999;99:730–2.
6 Nagel E, et al. Noninvasive diagnosis of ischemia-induced wall motion abnormalities with the use of high-dose Dobutamine Stress MRI: Comparison with dobutamine stress echocardiography. Circulation 1999;99:763–70.
7 Sechtem U, et al. Cine MR imaging: potential for the evaluation of cardiovascular function. AJR 1987;148:239–46.
8 Pflugfelder PW, et al. Quantification of regional myocardial function by rapid cine MR imaging. AJR 1988;150:523–9.
9 Reichek N. Magnetic resonance imaging for assessment of myocardial function. Magn Reson 1991;Q 7:255–74.
10 Penell DJ, et al. Magnetic resonance imaging during dobutamine stress in coronary artery disease. Am J Cardiol 1992;70:34–40.
11 Baer FM, et al. Coronary artery disease: Findings with GRE MR Imaging and Tc-99m-Methoxyisobutyl-Isonitrile SPECT during simultaneous dobutamine stress. Radiology 1994;193:203–9.
12 Van Rugge FP, et al. Magnetic resonance imaging during dobutamine stress for detection and localization of coronary artery disease: quantitative wall motion analysis using a modification of centerline method. Circulation 1994;90: 127–38.
13 Pennell DJ, et al. Dipyridamole magnetic resonance imaging: a comparison with thallium-201 emission tomography. Br Heart J 1990;64(6):362–9.
14 Pennell DJ, et al. Magnetic resonance imaging during dobutamine stress in coronary artery disease. Am J Cardiol 1992;70(1):34–40.
15 Baer FM, et al. Feasibility of high-dose dipyridamole-magnetic resonance imaging for detection of coronary artery disease and comparison with coronary angiography. Am J Cardiol 1992;69(1):51–6.
16 Jochims, et al.Dobutamine stress magnetic resonance imaging: a reliable alternative to stress echocardiography in patients with insufficient image quality? Eur Heart J 1999;20:678 (abstract).
17 Finn, et al. Cardiac MR Imaging: State of the Technology. Radiology 2006;241(2):338–54.
18 Barkhausen J, et al. MR evaluation of ventricular function: true fast imaging with steady-state precession versus fast low-angle shot cine MR imaging—feasibility study. Radiology 2001;219:264–9.
19 Nesto RW, et al. The ischemic cascade: temporal sequence of hemodynamic, electrocardiographicand symptomatic expressions of ischemia. Am J Cardiol 1987;59(7):23C–30C.
20 Nagel E, et al. Stress cardiovascular magnetic resonance: consensus panel report. J Cardiovasc Magn Reson 2001;3(3):267–81.
21 Cerqueira, et al. Standardized myocardial segmentation and nomenclature for tomographic imaging of the heart. A statement for healthcare professionals from the Cardiac Imaging Committee of the Council on Clinical Cardiology of the American Heart Association. Int J Cardiovasc Imaging 2002;18(1):539–42.
22 Hundley WG, et al. Utility of fast cine magnetic resonance imaging and display for the detection of myocardial ischemia in patients not well suited forsecond harmonic stress echocardiography. Circulation 1999;100(16):1697–702.
23 Wahl A, et al.High-dose dobutamine-atropine stress cardiovascular MR imaging after coronary revascularization in patients with wall motion abnormalities at rest. Radiology 2004;233 (1):210–6.
24 Secknus MA, et al. Evolution of dobutamine echocardiography protocols and indications: safety and side effects in 3,011 studies over 5 years. J Am Coll Cardiol 1997;29(6):1234–40.
25 Wahl A, et al. Safety and feasibility of high-dose dobutamineatropine stress cardiovascular magnetic resonance for diagnosis of myocardial ischaemia: experience in 1000 consecutive cases. Eur Heart J 2004;25(14):1230–6.
26 Paetsch I, et al. Comparison of dobutamine stress magnetic resonance, adenosine stress magnetic resonance, and adenosine stress magnetic resonance perfusion. Circulation 2004;110 (7):835–42.
27 Syed MA, et al.Reproducibility and inter-observer variability of dobutamine stress CMR in patients with severe coronary disease: implications for clinical research. J Cardiovasc Magn Reson 2005;7(5):763–8.
28 Marcowitz PA, Armstrong WF. Accuracy of dobutamine stress echocardiography in detecting coronary artery disease. Am J Cardiol 1992;69:1269–73.
29 Mazeika PK, et al. Dobutamine stress echocardiography for detection and assessment of coronary artery disease. J Am Coll Cardiol 1990;19:1203–11.
30 Sawada SG, et al. Echocardiographic detection of coronary artery disease during dobutamine infusion. Circulation 1991;83:1605–14.
31 Segar DS, et al. Dobutamine stress echocardiography: Correlation with coronary lesion severity as determined by quantitative angiography. J Am Coll Cardiol 1992;19:1197–202.
32 Takeuchi M, et al. Comparison of dobutamine stress echocardiography and stress thallium-201 single-photon emission computed tomography for detecting coronary artery disease. J Am Soc Echocardiogr 1993;6:539–602.
33 Kuijpers D, et al. Dobutamine cardiovascular magnetic resonance for the detection of myocardial ischemia with the use of myocardial tagging. Circulation 2003;107(12):1592–7.
34 Strach K, et al. Cardiac stress MR imaging with dobutamine. Eur Radiol 2006;16: 2728–38.
35 Mandapaka S, et al. Dobutamine Cardiovascular Magnetic Resonance: A Review. J. Magn. Reson. Imaging 2006;24:499–

CMR for Assessment of Valvular Disease

Brett Cowan[1], Alistair Young[1], Chris Occleshaw[2], Andrew Kerr[3]

[1]Centre for Advanced MRI, University of Auckland, Auckland, New Zealand
[2]Department of Cardiology, Auckland City Hospital, Auckland, New Zealand
[3]Department of Cardiology, Middlemore Hospital, Auckland, New Zealand

Introduction

CMR is able to provide accurate quantitative and qualitative data to support the decision-making process of therapy in valvular disease.

Surgical treatment of valvular heart disease (VHD) has the potential to revolutionize the lives of affected patients. Unfortunately, surgery carries the peri-operative risks of stroke, myocardial infarction and occasionally death. Longer term risks include anticoagulation for mechanical valves and the need for re-operation particularly in patients receiving bio-prosthetic valves. In patients presenting or being followed with VHD, decisions need to be made regarding appropriate medical therapy and when this should give way to surgical management. In addition to clinical factors, these decisions are dependent on the type and severity of the lesion, the presence of cardiac decompensation, and also in part on the type of operation required. Cardiac magnetic resonance (CMR) is able to provide accurate quantitative and qualitative data to inform this decision-making process. We review typical applications of CMR in the assessment of VHD, focusing on common indications, case reviews and current limitations, and concluding with exciting new applications in the area of valve mapping.

Background

CMR allows a comprehensive evaluation of valvular disease by imaging morphology, hemodynamics and ventricular volumes.

The majority of stenotic and regurgitant VHD affects the mitral and aortic valves and is either congenital in origin, or acquired as a result of degenerative processes, rheumatic fever, infective endocarditis or ischaemic heart disease. This article overviews practical methodologies which can be used to investigate aortic regurgitation (AR), aortic stenosis (AS) and mitral regurgitation (MR), accompanied by general comments on velocity and flow imaging.
The decision to proceed with medical or surgical treatment is currently typically based on clinical symptoms and an echocardiographic study. Echocardiography is readily available, portable, inexpensive and achieves high temporal and spatial resolution and is therefore well established in the evaluation of VHD. It is particularly well suited to the visualization of small valvular vegetations in endocarditis. It has the disadvantages of limited acoustic windows, poor image quality in obese patients or those with pulmonary disease, difficulties with consistently aligning a Doppler beam along the direction of blood flow and variability due in part to operator dependence. Doppler techniques are able to measure velocity with precision, but this is not always reflected in flow volumes.

The advantages of CMR for the evaluation of VHD include –

- flexibility to acquire flow or anatomical studies in any arbitrary plane,
- high-quality images (without requiring acoustic windows) in virtually all patients,
- accurate and reproducible measurements of velocity and flow, and
- the ability to consistently perform a full valvular study including ventricular volumes, hemodynamic evaluation and anatomical morphology.

The CMR assessment of stenotic, regurgitant or mixed VHD can be divided into three main components:

(1) An assessment of the consequences of the valve lesion on left and right ventricular function and mass (see article on ventricular function) and effect on aortic and atrial size,
(2) haemodynamic evaluation of lesion severity by measurement of stenotic velocities or

regurgitant volumes, and
(3) anatomical imaging including planimetry of the valve orifice, and direct visualization of the valve and leaflet morphology.

Many previous difficulties with valvular MR such as dealing with arrhythmias, difficulty with direct visualization of leaflet morphology and time required to perform quantitative post-processing have improved significantly over the last few years. CMR is now complementary to echocardiography and can offer precise additional important information on regurgitant volume, valve geometry and lesion severity.

Indications for CMR in valvular disease

In 2006 the American College of Cardiology Foundation [1] (in conjunction with other professional bodies including the Society for Cardiovascular Magnetic Resonance) gave CMR an appropriateness rating for "Characterization of native and prosthetic cardiac valves – including planimetry of stenotic disease and quantification of regurgitant disease" and "Patients with technically limited images from echocardiogram or TEE" of 'A' with a score of 8/9. An appropriate imaging study was defined as one "in which the expected incremental information, combined with clinical judgment, exceeded the expected negative consequences (defined as procedural risks, and the impact of false negatives or false positives) by a sufficiently wide margin that the procedure was generally considered acceptable care and a reasonable approach for the indication". CMR therefore plays an important role where echocardiographic windows are poor, there are contraindications to TEE, where a high degree of accuracy is desirable or where the study forms part of a broader investigation already being performed by MR (for example in congenital heart disease). Standard contraindications to MR apply including pacemakers, ventricular assist devices and implanted defibrillators but prosthetic valves are safe in field strengths up to 1.5 Tesla. Although magnetic forces and heating in the valves are not a cause for concern, the presence of metal may unfortunately produce problematic sequence-dependent local image artifacts.

CMR is complementary to echocardiography and offers precise information on regurgitant volume, valve geometry and lesion severity.

Phase contrast imaging

The mainstay of haemodynamic evaluation is phase contrast (PC) imaging. In a standard MR image, each small image element (known as a pixel) contains a single grey-scale value. In a PC study there are two images as each pixel contains two values, one for the signal intensity (magnitude) and the second for the velocity of blood flowing through the image plane (phase). In the velocity image, mid-grey represents stationary tissue, white the maximum velocity in the through-plane direction, and black the maximum velocity in the reverse direction (Figure 1).
This maximum velocity that can be measured is known as the 'Velocity ENCoding' (VENC) value and this may be set by the user depending on the anticipated peak velocity in the vessel of interest. Typical VENC's for normal aortic flow are in the region of 150 cm/sec, increasing to 400 cm/sec or more for aortic stenosis. If the VENC is set too low, a problem known as 'aliasing' occurs where the blood velocity exceeds the VENC. In this case aliased pixels which should appear black, appear white (Figure 2), or vice versa, and this prevents quantitative analysis. Aliasing is typically seen on the systolic

In a phase-contrast study there are two images as each pixel contains two values, one for the signal intensity (magnitude) and the second for the velocity of blood flowing through the image plane (phase).

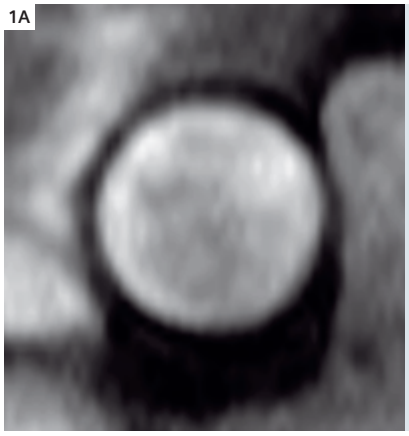

1 **(A)** Standard magnitude image of an aorta, and **(B)** its corresponding velocity or phase image (both at 424 msec after the R-wave). On the phase image, white represents flow through the image plane in one direction and black in the opposite direction. Mid-grey represents stationary tissue. Some diastolic-phase regurgitation is accompanied by forward flow as shown by the presence of black and white regions in the velocity image. "Salt and pepper" or "checker board" noise in the velocity image under the aorta is caused by air in lung tissue where there are insufficient protons to return a reliable signal.

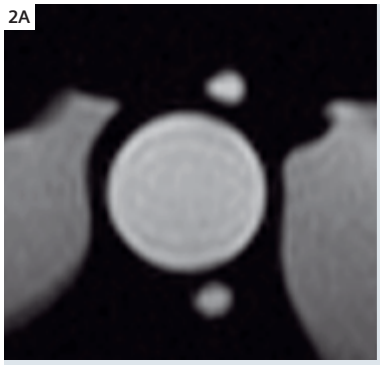

2 **(A)** Magnitude image of water flowing through a pipe, with **(B)** its velocity or phase image showing aliasing due to the VENC being set too low. The peripheral slower moving water is correct, but once the velocity reaches and then exceeds the VENC, there is an abrupt transition from black to white where the velocities are no longer correct.

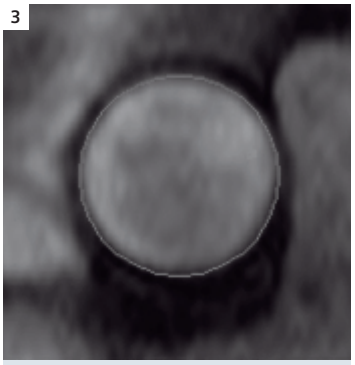

3 Argus contour outlining the region of interest in the aorta. Contouring is performed semi-automatically for each frame through the cardiac cycle cine using both the magnitude and phase images.

The Flow Package contains a Flow Scout which enables fast assessment of up to 5 VENCs.

frame because this contains the highest velocities and if this occurs, the sequence should be repeated. If the VENC is set too high, accuracy and signal-to-noise ratio (SNR) is compromized because only a small subset of the available grey scale is utilized. Where the peak velocity is unknown or difficult to estimate, it may be useful to acquire a few velocity scouts to enable the VENC to be chosen with more certainty. The VENC should be set comfortably above (125–150%) the highest velocity expected to be measured.

The main PC planning issues to be considered are to position the imaging slice at approximately right angles to the vessel of interest (small and even moderate errors in angulation have little or no effect on the flow results but definition of the border of the vessel may be more difficult), choice of the number of frames for the cine (typically 20–30), selection of the VENC, and to select either a breath-hold or free-breathing approach (breath-hold is faster but has lower temporal and spatial resolution).

Once a cine flow series has been acquired, the vessel(s) of interest are outlined semiautomatically on all frames through the cardiac cycle using the Argus Flow analysis software (Figure 3), and the velocity in each pixel within this contour multiplied by its area, and summed to determine the total

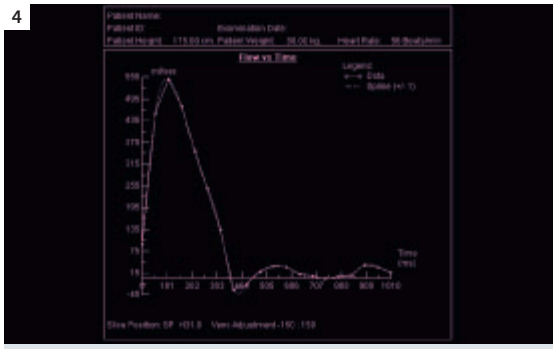

4 Argus flow-versus-time graph for the aorta. The systolic phase with a peak flow rate of 555 ml/s is followed by very low levels of flow in diastole demonstrating normal valvular function.

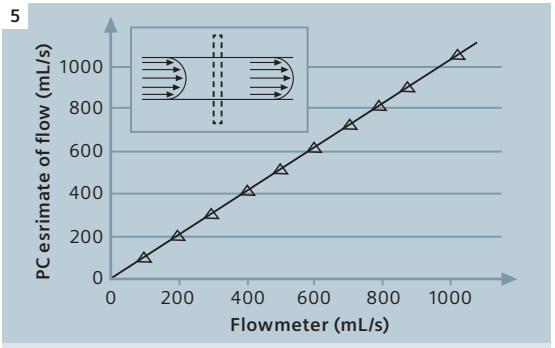

5 Validation of phase contrast on a Siemens MAGNETOM Avanto scanner. Water was pumped through a straight pipe (internal diameter 17 mm) and compared to an electromagnetic flowmeter which acted as the gold standard. The maximum error was 2.9% (average error 1.9 ± 0.7%, r=0.99).

flow for each frame (Figure 4). Peak and average velocities, net flow and other parameters are then calculated automatically.
The high accuracy of PC imaging during non-pulsatile flow of water through a pipe with a diameter equal to the adult aorta on an Siemens MAGNETOM Avanto system is demonstrated in Figure 5.

Aortic regurgitation

Case 1: A 25-year-old man presented with dyspnoea and clinical evidence of aortic regurgitation. An initial trans-thoracic echo reported severe aortic regurgitation but was technically limited for left ventricular (LV) and aortic measurements. CMR was requested to better quantify LV size and function, lesion aetiology and severity, and aortic dilatation.
After establishing a good quality ECG signal, the patient was positioned with the phased-array body coil anteriorly and standard cardiac scouts performed followed by breath-hold short and long axis TrueFISP (SSFP) cines for ventricular function. Three parallel oblique coronal slices were planned along the long axis of the aortic root from an axial scout, and the one showing the best view of the aortic root selected to plan the aortic flow study (Figure 6 shows slice planning in a normal volunteer including a three-chamber view). A PC study was acquired using a segmented k-space breath-hold sequence with 24 frames, VENC=150 cm/s, slice thickness 8 mm, pixel size 1.5 x 1.5 mm, and with an acquisition matrix of 192 x 256.
The analysis produced forward and regurgitant volumes of 223 and 90 ml/s respectively from which a regurgitant fraction of 40% was calculated. With an LV end-diastolic volume of 503 ml and end-systolic volume of 280 ml the LV ejection fraction (EF) was reduced at 44%. The aortic root was assessed using standard aortic imaging techniques and showed maximum dilatation at the level of the aortic sinuses of 5.8 cm.
In order to visualize the leaflet morphology, True FISP cine images were obtained in the long and short axes of the aortic valve. The short axis (Figure 7) demonstrated an unusual congenital quadricuspid aortic valve with four unequal cusps and sinuses instead of the normal three. Interestingly each of the two pairs of leaflets were fused, resulting in a functionally bicuspid valve and there was central AR secondary to the leaflet abnormalities. On the basis of this information and the aortic imaging

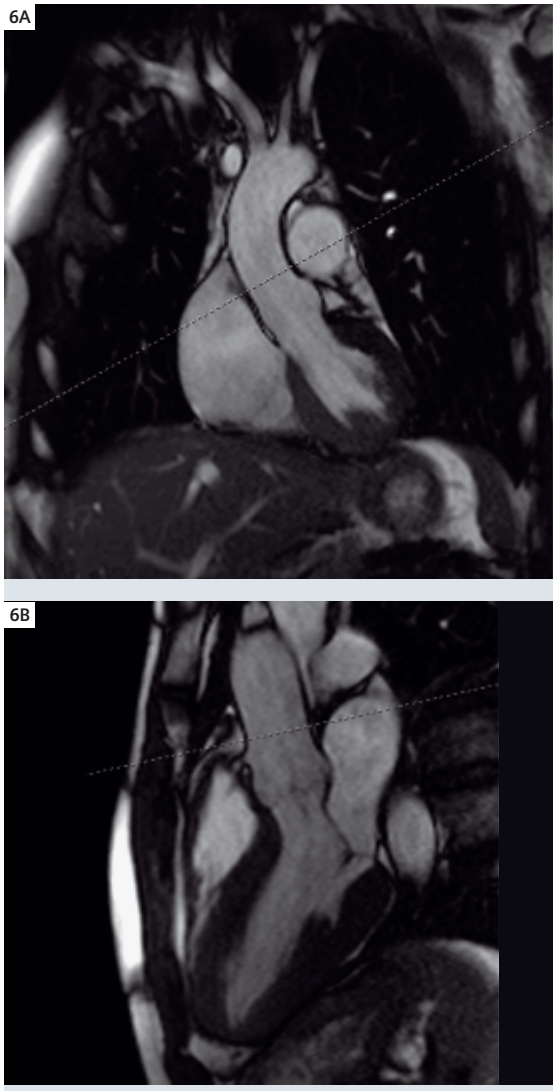

Argus Flow® allows for automatic calculation of peak and average velocities, flow, net flow and other parameters needed for accurate assessment of valvular disease.

6 Planning of an aortic flow study in a normal volunteer using **(A)** an aortic scout and, **(B)** a three-chamber view.

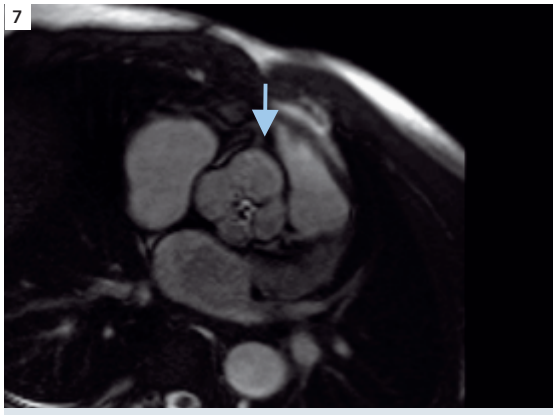

Valvular regurgitant fraction can be assessed accurately using PC CMR. Cine images can be used for the evaluation of leaflet morphology.

7 **Case 1:** Quadricuspid aortic valve (arrowed).

showing a dilated root and proximal ascending aorta, the patient was referred for aortic valve and root replacement.

Background phase correction

MAGNETOM Avanto has siginificantly lower eddy currents than older generation magnets, enabling highly reliable flow measurements.

It is common for eddy currents to be induced in the frame of the magnet by the gradients and these can produce a background phase (and hence velocity) signal in stationary tissue. A 'background phase correction' may be applied in Argus Flow by selecting a region of stationary tissue and subtracting this from the results in the vessel of interest.
Although this may provide some correction, unfortunately the background phase is not always constant across the entire FoV and may vary linearly [2], so that the selection of a region of stationary tissue relatively remote from the vessel of interest may introduce additional errors. More recent magnet designs such as the Siemens MAGNETOM Avanto have significantly lower eddy currents compared to older generation magnets and this has significantly reduced this problem. In the future, automated algorithms that calculate the true background phase distribution in all regions of the image are likely to provide a better solution.

Aortic stenosis

Maximum velocity assessment in stenotic jets can be done using longitudinal in-plane phase-contrast imaging.

Case 2: A 70-year-old man presented with shortness of breath and clinical evidence of aortic stenosis, but had an equivocal echocardiographic study and MRI was requested to image the valve. The peak velocity in the stenotic jet is an important determinant of lesion severity and may be used as part of a calculation of effective valve area. Stenotic jets may be eccentric and the exact position of the maximum velocity may not always be readily apparent. It is possible to acquire multiple PC images transverse to the aortic root and to check each for their maximum velocity, or to acquire a longitudinal view of the aorta using in-plane (as opposed to through-plane) velocity encoding. In this case, three PC slices with a VENC of 400 cm/sec were acquired transverse to the aorta with a peak velocity of 245 cm/sec found in the jet. Valve area was calculated with the continuity equation using PC data obtained from both below the valve in the left ventricular outflow tract and at valve level. Ventricular function was good and in the presence of moderate hypertrophy the criteria for valvular replacement was not met and he was managed medically with regular follow-up.

Accurate assessment of velocity in the jet is essential for reliable diagnosis. Recent data from our laboratory has demonstrated that in the most severe cases of aortic stenosis, where jet velocities can exceed 400 cm/sec with very high levels of turbulence, there can be significant loss of signal due to intra-voxel dephasing and other effects. In order to minimize these effects, it is helpful to keep the TE as short as possible. When signal loss is severe, the PC images may develop evidence of 'salt and pepper' noise (as opposed to aliasing) indicating that the results are likely to be unreliable. When evaluating very high velocity jets, it is important to check the magnitude image in the vessel of interest for dark areas indicative of signal loss and low SNR. The velocity results may be unreliable in these regions, especially if the phase images also contain salt and pepper noise in the same region.
It is common to see flow artifacts in cines which can give a useful subjective impression of any jets or regurgitant flow that may be present.
Although correlation with echocardiography has been shown, some caution must be exercised when attempting to accurately quantify or grade the severity of the lesion based on these subjective impressions. These techniques can be useful to quickly determine if there are likely to be solitary or multiple orifices in the valve as can sometimes be seen in mitral regurgitation.
True-FISP cines in the plane of the aortic valve may be used to visualize and directly planimeter the area of the systolic opening providing a valve area independent of velocity or flow measurements, pressure gradients or formulae. These have been shown to be correlated with catheterization data and reasonably well correlated to echocardiographic results in aortic stenosis [3].

Mitral regurgitation

Case 3: A 55-year-old woman with a history of rheumatic fever had been followed for mitral regurgitation for 15 years. Her clinical status had deteriorated and there was uncertainty as to whether this was due to her rheumatic valvular disease or other significant co-morbities including ischaemic heart disease. She was high risk for surgery and was referred for a detailed quantitative evaluation of her valve as part of a delayed enhancement and ventricular function CMR workup. The mitral valve descends by approximately 12 mm

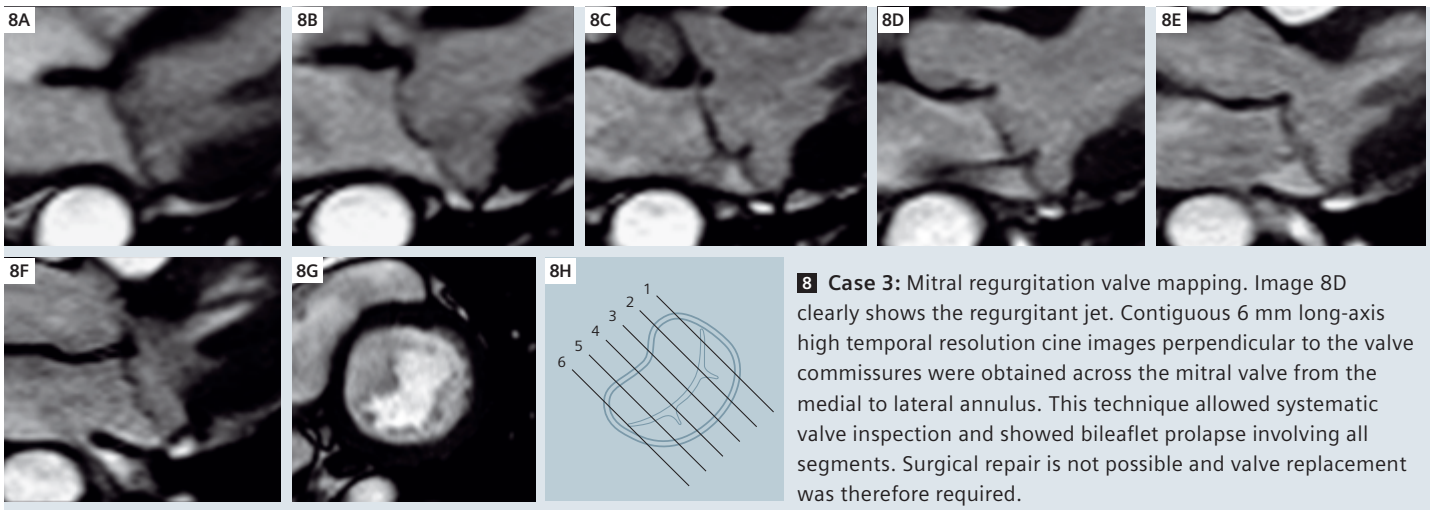

8 Case 3: Mitral regurgitation valve mapping. Image 8D clearly shows the regurgitant jet. Contiguous 6 mm long-axis high temporal resolution cine images perpendicular to the valve commissures were obtained across the mitral valve from the medial to lateral annulus. This technique allowed systematic valve inspection and showed bileaflet prolapse involving all segments. Surgical repair is not possible and valve replacement was therefore required.

during systole, and this movement through a fixed imaging plane makes flow measurement at the mitral annulus challenging. In addition, direct measurement of a regurgitant jet is technically difficult because of jet eccentricity, possible multiple jets, and jet turbulence. It is therefore usual to measure mitral regurgitant volume indirectly by measuring the antegrade flow in the aorta with PC imaging, and comparing this to the ventricular stroke volume calculated from EDV – ESV with the difference representing the mitral regurgitant flow.

The PC flow results from the aorta showed a SV of 65 ml/m^2, and the ventricular function an EDV of 345 ml/m^2, ESV of 197 ml/m^2, SV of 148 ml/m^2, and ejection fraction of 43%. This equated to a regurgitant fraction of 56% (mitral valve regurgitant volume = LV ventricular SV – aortic SV) at the mitral valve in a dilated and de-compensating ventricle and the patient was referred for surgery. The delayed enhancement scan showed no evidence of previous myocardial infarction.

With improvements in hardware and software, it is now possible to acquire high quality images of the mitral valve leaflets in a similar way to those shown for the aortic valve. Generally a thinner slice (5 mm) and increased in-plane and temporal resolution (within the limits of maintaining adequate SNR) are helpful in improving leaflet definition. Leaflets are best appreciated in cine mode, but representative images from across the regurgitant valve are shown in Figure 8. The slices were acquired serially across the valve and are especially useful for mapping leaflet prolapse or defining detailed valve morphology for surgical planning where repair is being contemplated.

Left atrial measurements are an important part of the evaluation and may be made from long axis cine views and volume estimated using standard echocardiographic formulae. If serial short axis slices are acquired through the left atrium, left atrial volume can be measured with more sophisticated software without geometric assumptions.

In order to overcome the issues associated with mitral movement, newer research sequences are able to define the motion of the valve annulus and move the imaging slice with the valve through the cardiac cycle to ensure the acquisition remains aligned with the annulus. This technique may make the direct measurement of mitral regurgitant fraction clinically feasible.

Using CMR, high-resolution images of the mitral valve leaflets can be acquired for defining detailed valve morphology.

Hardware

Most new generation magnets with cardiac gating and post-processing software are capable of performing valvular assessments without additional special equipment. In terms of maintaining flow measurement accuracy, low eddy currents are an important consideration and some older generation magnets with higher eddy currents may not be as well suited to flow studies.

The Flow Package for image acquisition and Argus Flow® for post-processing are available for all 1.5 and 3T systems.

Summary

CMR assessment of valvular disease is an appropriate indication and feasible on current equipment.

References

1 Hendel RC et al. ACCF/ACR/SCCT/SCMR/ASNC/NASCI/SCAI/SIR 2006 Appropriateness criteria for cardiac computed tomography and cardiac magnetic resonance imaging. J Am Coll Cardiol 2006;48:1475–97.

2 Lankhaar J et al. Correction of phase offset errors in main pulmonary artery flow quantification. J Mag Res Img 2005;22:73–79.

3 Friedrich MG. Quantification of valvular aortic stenosis by magnetic resonance imaging. Am Heart J 2002;144(2):329–34.

Contact
Associate Professor
Brett Cowan
Centre for Advanced MRI
c/o University of Auckland
Private Bag 92019
Auckland, New Zealand
b.cowan@auckland.ac.nz

Evaluation of Cardiac Masses by CMR

Oliver Bruder, M.D.; Markus Jochims, M.D.; Christoph Jensen, M.D.; Georg V. Sabin, M.D.

Department of Cardiology and Angiology, Elisabeth Hospital Essen, Germany

Introduction

The prevalence of primary tumors of the heart is less than 0.3%, making them a relatively rare cardiac disease compared to other cardiovascular disease entities [1].
Secondary cardiac tumors are approximately 20 times more common according to post mortem studies [2]. Secondary tumors are the result of local invasion of cancer or metastatic involvement of the myocardium and/or pericardium.
Although cardiac tumors are rare, the clinical relevance is high as primary tumors can be malignant, and therefore lethal if left untreated, but curable if excised in time.
Ventricular thrombi are an important differential diagnosis of cardiac masses. Thrombi are in most cases related to prior myocardial infarction with extensive left ventricular aneurysm formation, and carry a high risk of embolic complications.
Apart from thrombi, there is a wide variety of diseases that can be confused with primary cardiac tumors such as:

- vegetations,
- atypical focal variants of hypertrophic cardiomyopathies,
- abscesses,
- anatomic variants,
- pericardial cysts, or
- juxtacardiac findings such as diaphragmatic hernia.

Cardiac tumors can be classified by histopathology (malignant, benign), location (pericardial, intracavitary, paracardial, intramyocardial), morphology (sessile, pedunculated, or by the effect on blood flow (obstructive, non-obstructive).
In pre–MRI times diagnosis of cardiac tumors was, due to insufficient imaging techniques, mainly confined to autopsy, leaving the majority of tumors undiagnosed during life time.
With the rapid development of CMR, cardiac tumors are diagnosed more frequently.

With the rapid development of CMR cardiac tumors are diagnosed more frequently. Secondary cardiac tumors are twenty times more common than primary tumors.

Benign cardiac tumors

75% of all primary tumors of the heart are benign, including myxomas, rhabdomyomas, fibromas, papillary fibroelastomas, lipomas, hemangiomas and teratomas.
Myxomas account for 50% of all cardiac tumors. They are typically located within the left atrium, although left ventricular, or right atrial involvement occurs. The morphology is rather polypoid than round-shaped, and they are often pedunculated-prolapsing into the mitral valve apparatus or even the left ventricle during diastole [3].
On CMR, myxomas are diagnosed by the typical location close to the interatrial septum, high signal intensity on T2-weighted spin-echo sequences, and heterogeneous enhancement following contrast administration [4]. Myxomas can grow rather large, and may be complicated by mitral valve obstruction, endocarditis or thrombotic embolism.
Rhabdomyomas present as several small tumors in the interventricular septum myocardium. Rhabdomyomas are most frequently found in young children.
Fibroelastomas are very small, mobile tumors that are fixed to the aortic or mitral valve leaflets.

Malignant cardiac tumors

25% of all primary cardiac tumors exhibit local tissue invasion and metastasize, and are therefore classified as malignant.

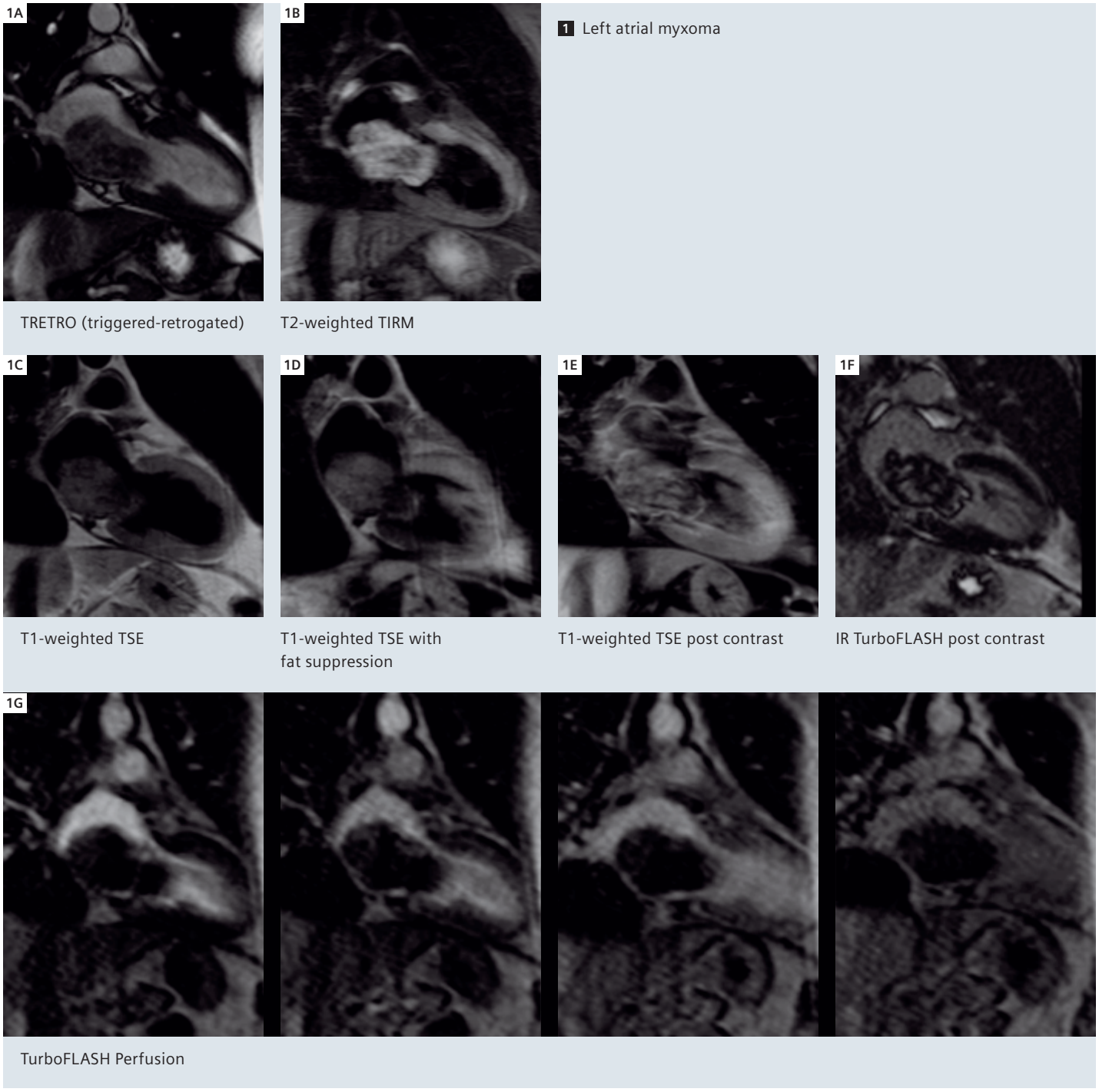

1 Left atrial myxoma

TRETRO (triggered-retrogated)

T2-weighted TIRM

T1-weighted TSE

T1-weighted TSE with fat suppression

T1-weighted TSE post contrast

IR TurboFLASH post contrast

TurboFLASH Perfusion

Sarcomas constitute the majority of malignant primary cardiac tumors (95%) including – in order of descending frequency – angiosarcomas (50%), leiomyosarcomas, rhabdomyosarcomas, and liposarcomas [5].

On CMR, malignant tumors are characterized by heterogeneous tissue characterization on T1-weighted, T2-weighted, and contrast-enhanced pulse sequences, a sessile morphology with broad invasive attachment to the myocardium, large size, central necrosis, and invasion into more than one cardiac chamber [6]. They are often, especially with angiosarcomas, complicated by cardiac tamponade and tend to metastasize into the spine.

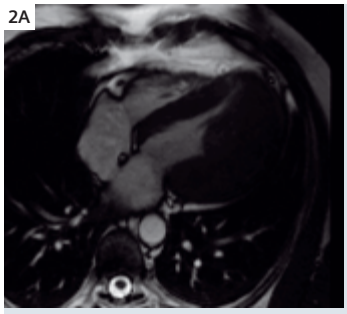

TRETRO (triggered-retrogated)

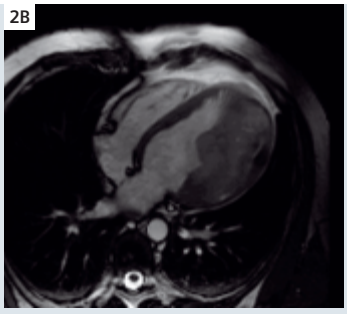

TRETRO post contrast

2 Left ventricular sarcoma.

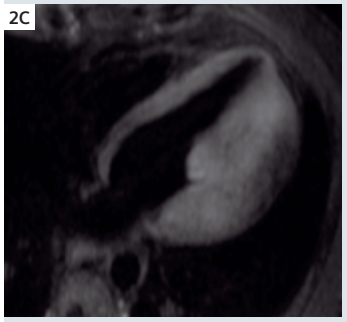

T2-weighted TIRM

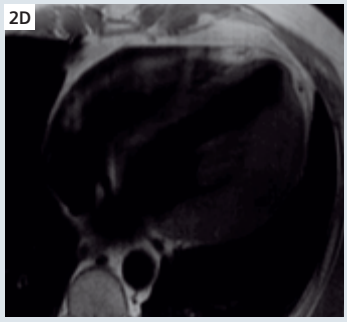

T1-weighted TSE

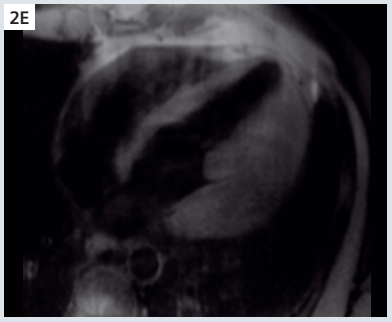

T1-weighted TSE with fat suppression

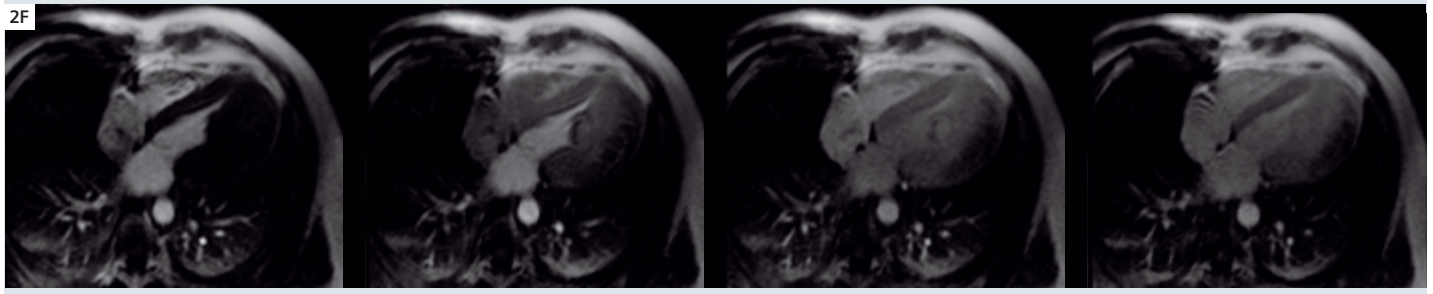

Perfusion

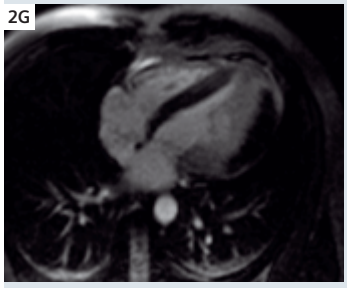

TI Scout TT 227 ms

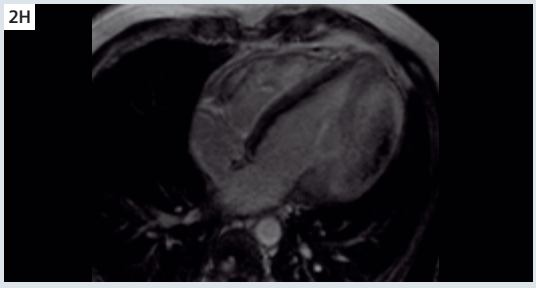

T1-weighted 3D IR TurboFLASH post contrast, TI 300

CMR protocol for cardiac tumors

A typical protocol consists of anatomic images in sagittal, coronal and axial orientation (e.g. fast low-angle shot gradient echo, FLASH), cine-imaging for function (steady-state free precession, TrueFISP), tissue characterization with various T1-weighted and T2-weighted spin-echo sequences with and without fat suppression, and finally contrast-enhanced T1-weighted imaging for vascularisation. Apart from those general recommendations CMR protocols for cardiac tumors should be adapted to the specific needs of the individual patient.

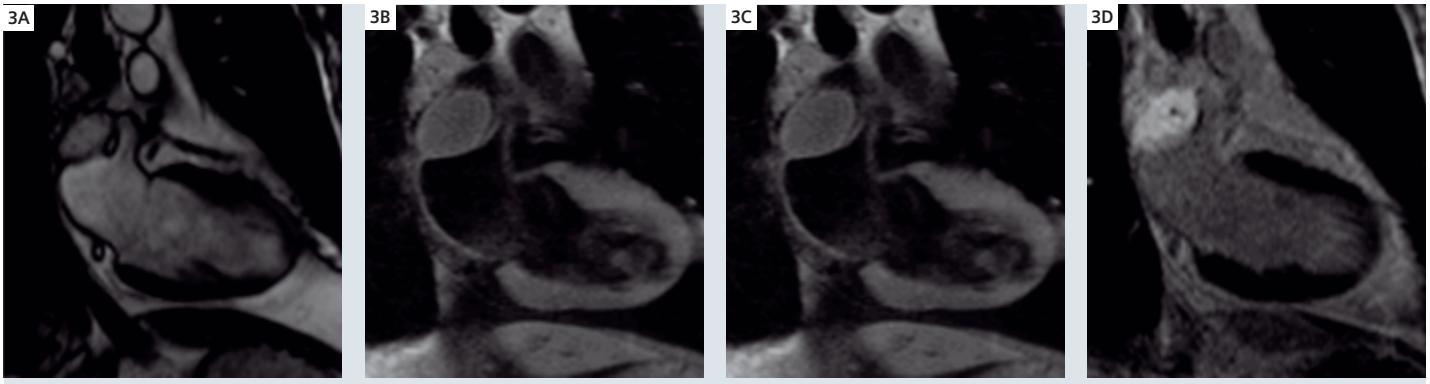

TRETRO (triggered-retrogated)

T1-weighted TSE

T1-weighted TSE with fat suppression

T1-weighted IR TurboFLASH post contrast

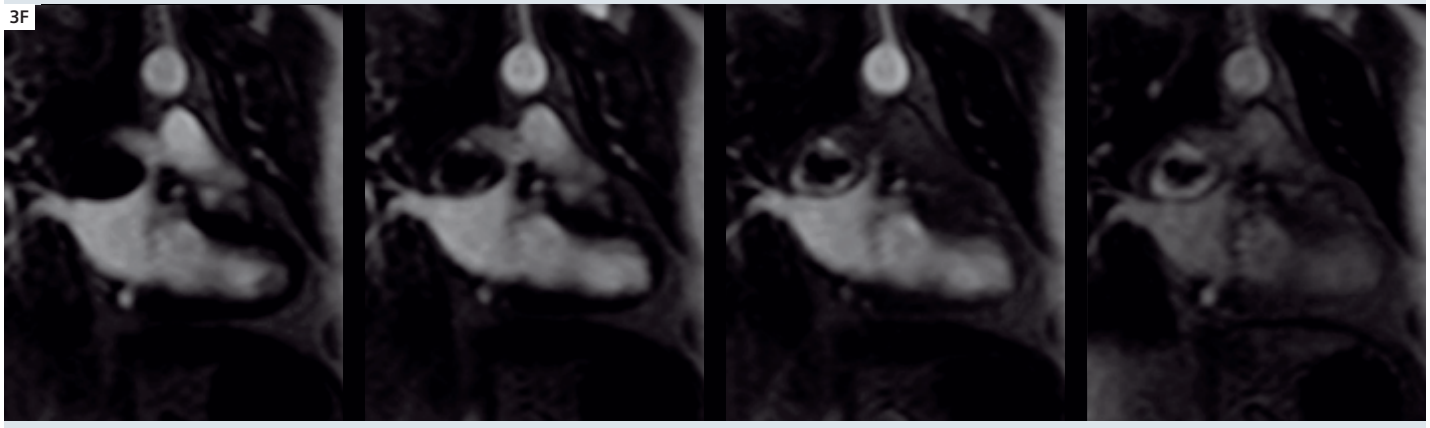

Perfusion series

3 Hemangiopericytoma

Cardiac thrombi

Left ventricular thrombus formation is a frequent complication following myocardial infarction in approximately 15% of patients [7]. Patients with left ventricular thrombi are treated with oral anticoagulation to reduce the risk of embolization. In clinical practice LV thrombi are diagnosed by transthoracic echocardiography. The diagnosis of thrombi by echocardiography, however, is challenging due to insufficient acoustic windows, problematic apical segment imaging, and reduced endocardial border delineation. With contrast-enhanced CMR, LV function and LV tissue characterization are combined in one examination with a single imaging modality. Steady-state cine imaging further improves delineation of endocardial borders compared to ultrasound, allowing for a superior differentiation of thrombus and ventricular myocardium. In most cases thrombi are located at the side of myocardial infarction, and are closely related to the extent of myocardial damage and impairment of segmental and global LV function. With the rare exception of large, old, and extensively vascularized thrombi, cardiac thrombi do not show enhancement following contrast application. On contrast-enhanced CMR using segmented gradient-echo sequences with an inversion-recovery prepulse (e.g. IR TurboFLASH) thrombi are visualized as dark areas between enhanced left ventricular cavity and infarct delayed enhancement. A 3D gradient echo sequence with a short inversion time early after contrast administration further improves cavity-to-thrombus contrast [8]. The "optimal TI" of a thrombus is different than the one for optimal myocardial suppression in delayed enhancement. Therefore, a brighter appearance of a thrombus when visualizing the myocardium for delayed enhancement imaging should not be

Contrast-enhanced CMR detects more thrombi than echocardiography in chronic myocardial infarction.

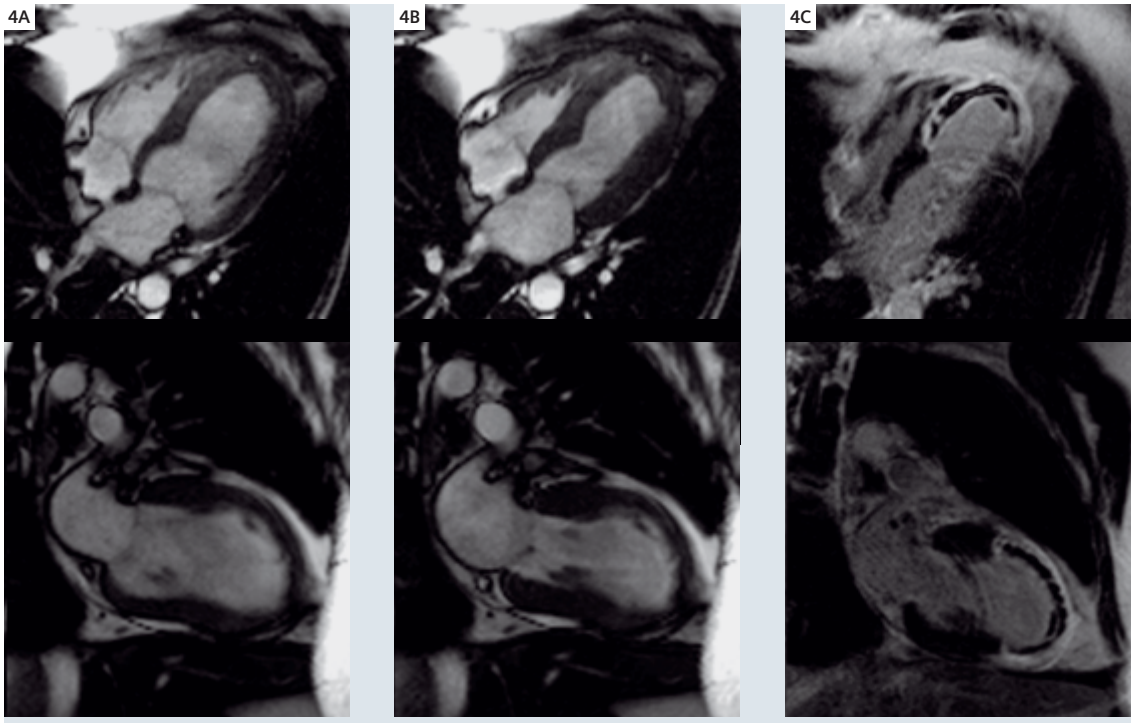

4 CMR in a patient with acute myocardial infarction. Note the black (nulled) subendocardial zone surrounded by delayed enhancement. This corresponds to a no-reflow zone. Additionally, a small apical thrombus can be seen in DE imaging.

In a pulmonary embolism protocol, MRA of the pulmonary arteries can be combined with cine and DE imaging of the right ventricle to detect RV thrombi.

mixed with a vascularisation of the thrombus. Not surprisingly, contrast-enhanced CMR detects more thrombi than echocardiography in chronic myocardial infarction [9]. In the setting of acute myocardial infarction, however, it can be difficult to differentiate thrombus and no-reflow zones, since microvascular obstruction (no-reflow) is predominantly located in the subendocardial layer of the left ventricular myocardium with no, or a very small rim of signal enhancement separating cavity from infarct no-reflow.

In pulmonary embolism right ventricular thrombi are frequently missed by echocardiography. In this setting MR angiography of the pulmonary arteries can be easily combined with delayed enhancement and cine imaging of the right ventricle [10].

Contact
Oliver Bruder, M.D.
Department of Cardiology and Angiology
Elisabeth Hospital
Klara-Kopp-Weg 1
45138 Essen
Germany
o.bruder@elisabeth-essen.de

References

1 Reynen K. Frequency of primary tumors of the heart. Am J Cardiol 1996;77(1):107.
2 Hanfling SM. Metastatic cancer to the heart. Review of the literature and report of 127 cases. Circulation 1960;22: 474–83.
3 Reynen K. Cardiac myxomas. N Engl J Med 1995;333(24): 1610–7.
4 Grebenc ML, et al. Cardiac myxoma: imaging features in 83 patients. Radiographics 2002;22(3):673–89.
5 Herrmann MA, et al. Primary cardiac angiosarcoma: a clinicopathologic study of six cases. J Thorac Cardiovasc Surg 1992; 103(4):655–64.
6 Siripornpitak S, Higgins CB. MRI of primary malignant cardiovascular tumors. J Comput Assist Tomogr 1997;21(3): p. 462–6.
7 Greaves SC, et al. Incidence and natural history of left ventricular thrombus following anterior wall acute myocardial infarction. Am J Cardiol 1997;80(4):442–8.
8 Bruder O, et al. [Detection and characterization of left ventricular thrombi by MRI compared to transthoracic echocardiography]. Rofo 2005;177(3):344–9.
9 Mollet NR, et al. Visualization of ventricular thrombi with contrast-enhanced magnetic resonance imaging in patients with ischemic heart disease. Circulation 2002;106(23): 2873–6.
10 Barkhausen J, et al. Detection and characterization of intracardiac thrombi on MR imaging. AJR Am J Roentgenol 2002; 179(6):1539–44.

Clinical Application of 3D/4D MR Angiography in Cardiovascular Diseases

Jörg Barkhausen, M.D.; Florian M. Vogt, M.D.; Stefan Maderwald, MSc; Harald H. Quick, Ph.D.

Department of Diagnostic and Interventional Radiology and Neuroradiology
University Hospital Essen, Germany

Introduction

Less than a decade following its first description, contrast-enhanced MR angiography (MRA) has replaced invasive catheter angiography as the diagnostic procedure of first choice for most vascular diseases. MRA provides high-spatial resolution 3D data sets with excellent image contrast and allows visualization of almost all vascular territories. Motivated by the clinical success of MRA, the technical developments have even gained speed within the last years. Latest hardware and software developments aim to move from static imaging of a single vascular territory towards dynamic data acquisition schemes.

For a standard MRA examination 10 to 30 ml of a Gadolinium-based contrast agent followed by a saline bolus are typically injected into the antecubital vein with a flow rate of 1 to 3 ml/s. The transit time is defined using a test bolus or care bolus technique and during peak arterial enhancement in the vascular territory of interest a 3D data set is collected within 10 to 30 seconds. This technique provides a stack of 60 to more than 100 cross-sectional images of the contrast filled arteries which can be post processed using maximum intensity projection (MIP), multi-planar reformats (MPR) or volume rendering. However, compared to DSA standard MRA techniques only provide morphologic information, whereas digital subtraction angiography as the standard of reference collects several images during the first-pass of the contrast agent providing additional information on flow dynamics. The lack of functional information has been considered one of the major limitations of MRA by some clinicians familiarized with DSA examinations. The recently introduced ***syngo* TWIST** dynamic MRA application provides **sub-millimeter 3D data sets** with a high temporal resolution of about 1 to 5 seconds depending on the sequence parameters and the spatial resolution. Incorporating parallel acquisition techniques (iPAT) even a **subsecond temporal resolution** can be obtained while maintaining a reasonable spatial resolution. Additionally, MRA with perfect arterial enhancement can be performed **without bolus-timing**, and only **very low doses of contrast** are required for excellent arterial enhancement using TWIST.

syngo TWIST: dynamic MRA with subsecond temporal or submillimeter spatial resolution in all body regions.

Another exciting recent development is ***syngo* TimCT**, a technique for continuous moving table data acquisition providing seamless volume coverage for large body parts. The craniocaudal field-of-view (FoV) for a conventional single station MRA examination is limited to typically 40–50 cm. Therefore, MRA examinations of the run-off system covering the abdominal aorta down to the pedal arteries have to be performed using multi-station protocols. Following a single contrast bolus the different vascular territories are covered step by step in rapid succession using three to four 3D-data sets. This approach results in several steps which have to be performed by the technician at the right time and in the correct order, making peripheral MRA examinations difficult to perform for inexperienced staff. TimCT (Continuous Table move acquisitions using Tim – Total imaging matrix – coils) introduces a completely new approach since a single high-resolution large-FoV 3D data set covering the entire run-off system can be collected "on the move".

syngo TimCT Angiography allows MRA image acquisition „on the move".

High-quality MRA requires a 1.5 or 3 Tesla MR scanner equipped with high-performance gradients, dedicated surface coils that can cover the different regions of interest and an automatic injector for the contrast agent. The typical in-room time for an MRA examination is about 15 to 20 minutes, however additional sequences for functional information or parenchymal imaging may

need some extra time. In this article we would like to give an overview of techniques, scan protocols and the impact on patient management for five of the most common indications for MRA with regard to cardiovascular diseases.

Carotid artery stenosis

MRA is the diagnostic test of first choice for a comprehensive evaluation of the carotid arteries and the brain.

Background: Arterial steno-occlusive disease of the carotid arteries can frequently be found in elderly patients with the potential risk of ischemic cerebral infarctions and fatal stroke.
MRA versus other imaging modalities: Imaging of the carotid arteries is feasible using several different imaging modalities including ultrasound (US), computed tomography angiography (CTA), digital subtraction angiography (DSA) and magnetic resonance imaging (MRI). Ultrasound can easily be performed as a bed-side test and allows reliable measurements of wall thickness and the degree of stenoses especially in the carotid bifurcation. However, the ability to provide information on vascular morphology from the aortic arch up to the small intracranial arteries combined with information on parenchymal brain lesion related to carotid artery stenoses and microvascular diseases is a unique feature of magnetic resonance imaging.
Protocol recommendation: The basic protocol should include a diffusion-weighted sequence for the detection of acute ischemic lesions, a T2*-weighted sequence for the detection of intraparenchymal hemorrhage and a FLAIR / DarkFluid sequence for the morphologic evaluation of brain lesions. The MRA should preferably be performed using the care-bolus technique for timing of the data acquisition. The voxel size should be below 1 mm^3 and the scan time should not exceed 20 seconds to avoid venous overlay (Figure 1).
Conclusion: MRA is the diagnostic test of first choice for a comprehensive evaluation of the carotid arteries and the brain.

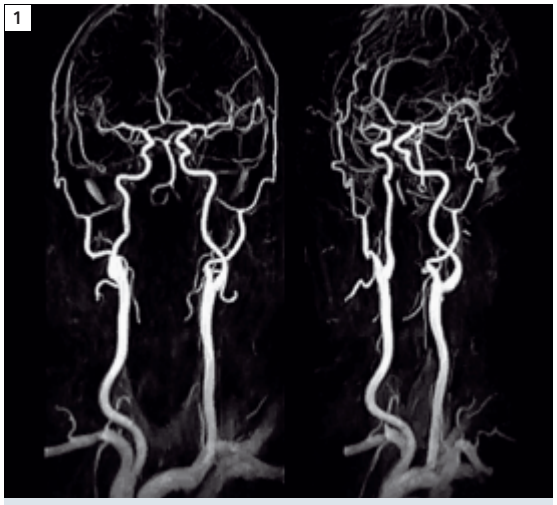

1 High-resolution MRA of the carotid arteries.

Congenital heart disease and vascular variants

Background: The most frequent congenital heart diseases (CHD) are frequently associated with vascular variants and malformations. Therefore in patients with known or suspected CHD cardiac MRI examinations including dark-blood TSE sequences, steady-state free precession sequences (e.g. True-FISP) for the assessment of right and left ventricular function and phase velocity encoded cine MRI for flow measurements are typically combined with an MRA examination of the thoracic vessels. This comprehensive protocol provides all clinically relevant information on morphology and function that cannot be obtained with any other single imaging modality.
MRA versus other imaging modalities: Echocardiography, which is typically the first diagnostic test in CHD patients cannot visualize the entire vascular system and is of limited value for the assessment of right ventricular function. Additionally, a poor acoustic window may hamper a comprehensive cardiac exam especially in grown-up patients with CHD. ECG-triggered computed tomography (CT) provides excellent information on cardiac and vascular morphology but lacks functional information, e.g. quantification of shunt volumes and flow. Additionally, due to the need of routine follow-up examinations and the fact that mainly children and young adults are affected, radiation exposure must be considered a major limitation. Compared to all other imaging modalities catheter angiography still provides an unbeaten spatial and temporal resolution, however the lack of 3D information inherent to a projection technique and the invasiveness have to be taken into account.
Protocol recommendation: For a comprehensive assessment of cardiac and vascular abnormalities in CHD patients we perform a time-resolved 3D (= 4D) MRA with subsecond temporal resolution using *syngo* TWIST and a small amount of contrast (5–8 ml) injected at a high flow rate (≥ 3 ml/s)

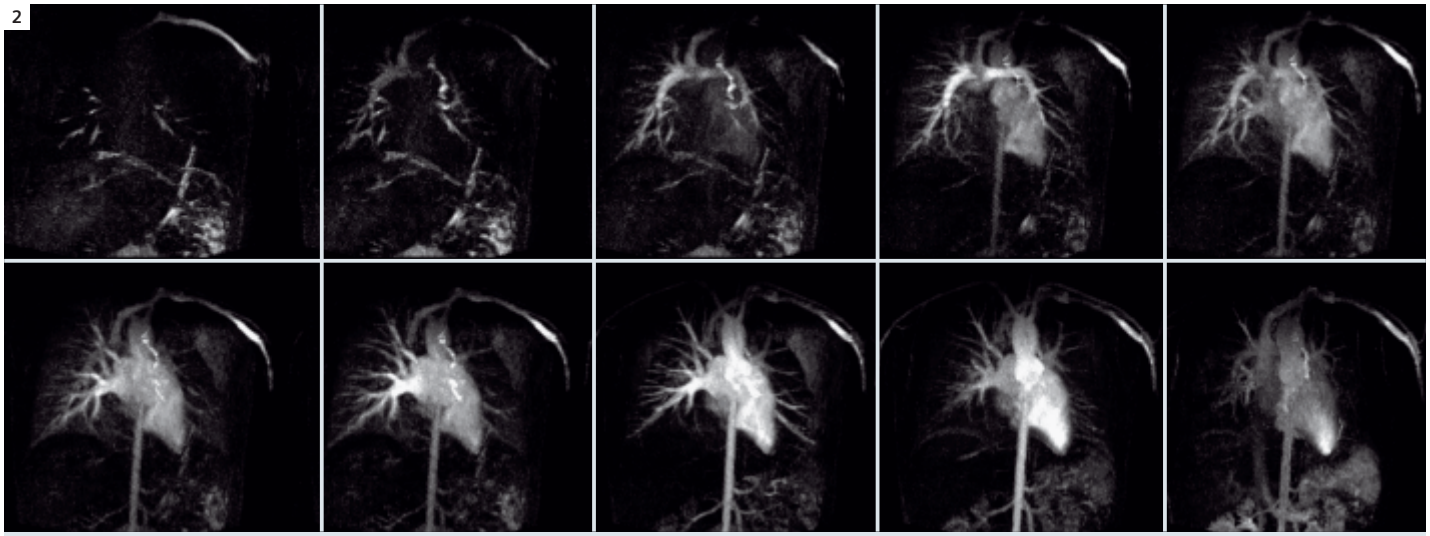

2 Subsecond 4D MRA using *syngo* TWIST in a patient with cavopulmonary anastomosis and hypoperfusion of the left lung.

(Figure 2). Due to the very high temporal resolution required for the assessment of shunts, spatial resolution has to be sacrificed to some degree. Therefore, the dynamic MRA is combined with a standard high-resolution MRA. The dynamic information from the TWIST sequence can be used for bolus timing and according to our experience the injected contrast does not reduce the image quality of the high resolution scan even if performed immediately following the dynamic MRA scan.
Conclusion: The combination of time-resolved and high-resolution MRA allows a comprehensive and fast evaluation of vascular abnormalities and shunts in patients with known or suspected congenital heart disease.

Aortic diseases

Background: Acute aortic syndromes are an important differential diagnosis in chest pain patients which are frequently missed or delayed diagnosed. Especially in Type A dissections this may have fatal consequences due to the high mortality rate if left untreated.
MRA versus other modalities: In patients with suspected acute aortic syndrome transesophageal echocardiography (TEE) is a fast and reliable bedside test that can be performed in the emergency room or the intensive care unit. However, TEE cannot display entire aorta including the side branches. Therefore, additional cross-sectional imaging is routinely performed prior to treatment. Due to the short scan time and the excellent patient access during the examination computed tomography is the imaging modality of first choice in case of an emergency. However, in stable patients, for follow-up examinations or for treatment planning MRA is an attractive alternative. Major advantages of MRA compared to CTA include the additional functional information (flow direction, tissue perfusion) that can be obtained from time-resolved MRA and the higher sensitivity of MRA for the detection of slow filling endoleaks after interventional treatment. Due to the invasive nature, the low sensitivity for the detection of small penetrating atherosclerotic ulcer, and the inability to detect intramural hemorrhage, catheter angiography can no longer be considered as a first line diagnostic test in patients with acute aortic syndromes.
Protocol recommendations: Our standard protocol comprises a timeresolved MRA in patients with suspicion of aortic syndromes. *syngo* TWIST combined with Parallel Acquisition Techniques (iPAT) provides a temporal resolution of about 2 seconds allowing the assessment of flow dynamics and organ perfusion combined with a sufficient spatial resolution for the assessment of vascular morphology (Figure 3). The time-resolved MRA allows a reliable detection and exclusion of aortic dissections and aneurysms. For the detection of intramural hemorrhage and small penetrating atherosclerotic ulcer, however, additional morphologic sequences (dark-blood turbo spin echo, steady-state free precession cine) and a high resolution stan-

syngo TWIST as a 4D MRA solution can be used either as a standalone technique or in addition to 3D MRA.

Time-resolved MRA with *syngo* TWIST allows reliable detection and exclusion of aortic dissections and aneurysms.

3

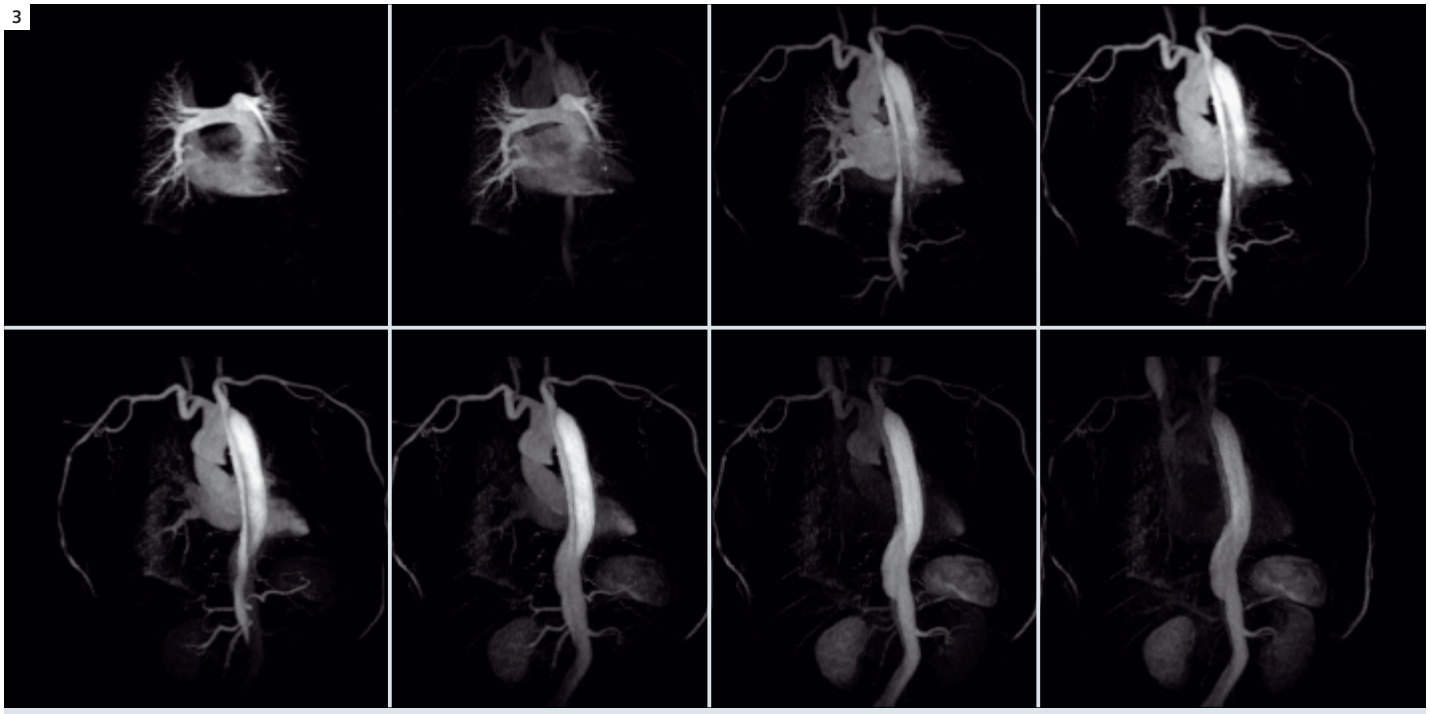

3 4D MRA using *syngo* TWIST in a patient with acute aortic dissection and delayed perfusion of the left kidney, which is supplied by the false lumen.

dard MRA sequence may be added to the protocol. **Conclusion:** MRA allows a complete evaluation of acute aortic syndromes in clinically stable patients and for follow-up examinations. Due to the limited patient access during the examination and the longer scan time, multi-slice CT should preferably be used in emergency patients.

Renal artery stenosis

Background: Arterial hypertension is a common clinical finding and must be considered an important risk factor for several potentially fatal events including stroke and myocardial infarction. Although arterial hypertension is only rarely caused by renal artery stenoses it has to be excluded to avoid missing of treatment options e.g. stent placement.

MRA can be combined with flow and tissue perfusion measurements providing additional functional information in renal artery stenosis.

MRA versus other modalities: Digital subtraction angiography is still considered the standard of reference for detecting renal artery stenosis. However, DSA has several important disadvantages including risk of death, arterial dissection and renal failure. Therefore non-invasive imaging techniques such as ultrasound, CTA and MRA have been introduced for the diagnostic work-up of renal artery stenosis. Ultrasound of the renal arteries is challenging especially in obese patients and the results strongly depend on the experience of the investigator. MRA and CTA developed rapidly within the last five years and both modalities provide a high negative predictive value in patients with suspected atherosclerotic renal artery stenosis, whereas the diagnosis of fibromuscular dysplasia is more challenging. However, MRA can be combined with flow measurements and measurements of tissue perfusion providing additional functional information (Figure 4) which must be considered an important advantage of MRA compared to CTA.

Protocol recommendation: For the visualization of the renal arteries spatial resolution is crucial. We perform a multiphase standard MRA examination using the test bolus or care bolus approach for the timing of the data acquisition. The scan duration must be adapted to breath-hold capabilities of the patients to avoid motion artifacts. Most patients can hold their breath for about 20 seconds and within that scan time a spatial resolution below 1 mm^3 can be obtained. To assess the hemodynamic significance of stenoses and to detect concomitant renoparenchymal disorders, flow measurements using the phase-contrast technique and first-pass perfusion mea-